MSRI
Mathematical Sciences Research Institute

17 Gauss Way Berkeley, CA 94720-5070 p: 510.642.0143 f: 510.642.8609 www.msri.org

# NOTETAKER CHECKLIST FORM

**(Complete one for each talk.)**

**Name:** Jeffrey Heninger **Email/Phone:** jeffrey.heninger@yahoo.com

**Speaker's Name:** Ibere Caldas

**Talk Title:** Shearless Invariant Curves in Confined Plasmas

**Date:** 11 / 26 / 2018 **Time:** 11 : 00 **am / pm (circle one)**

**Please summarize the lecture in 5 or fewer sentences:** When perturbing a map which does not satisfy the twist condition, the shearless curve is the last invariant to break. The destruction of the shearless curve can be calculated using either Greene's method or Slater's Criterion. Shearless curves can exist in plasma devices such as tokamaks. Creating a shearless curve decreases transport, improving the confinement of the plasma.

# CHECK LIST

(This is **NOT** optional, we will **not pay** for **incomplete** forms)

- ☑ Introduce yourself to the speaker prior to the talk. Tell them that you will be the note taker, and that you will need to make copies of their notes and materials, if any.
- ☑ Obtain ALL presentation materials from speaker. This can be done before the talk is to begin or after the talk; please make arrangements with the speaker as to when you can do this. You may scan and send materials as a .pdf to yourself using the scanner on the 3rd floor.
  - **Computer Presentations**: Obtain a copy of their presentation
  - **Overhead**: Obtain a copy or use the originals and scan them
  - **Blackboard**: Take blackboard notes in black or blue **PEN**. We will **NOT** accept notes in pencil or in colored ink other than black or blue.
  - **Handouts**: Obtain copies of and scan all handouts
- ☑ For each talk, all materials must be saved in a single .pdf and named according to the naming convention on the "Materials Received" check list. To do this, compile all materials for a specific talk into one stack with this completed sheet on top and insert face up into the tray on the top of the scanner. Proceed to scan and email the file to yourself. Do this for the materials from each talk.
- ☑ When you have emailed all files to yourself, please save and re-name each file according to the naming convention listed below the talk title on the "Materials Received" check list. (*YYYY.MM.DD.TIME.SpeakerLastName*)
- ☑ Email the re-named files to notes@msri.org with the workshop name and your name in the subject line.

# *Shearless Invariant Curves In Confined Plasmas*

Iberê L. Caldas
Institute of Physics, University of São Paulo
Brazil

MSRI, Berkeley, November 26 , 2018

# Collaborators (Theory)

University of São Paulo: C. Abud, J. Fonseca, R. Ferro, F. A. Marcus

Brazil

ITA/CTA: M. Roberto, K. Rosalem, C. Martins, F. A. Marcus

Federal University of Paraná (Curitiba): R. L. Viana, S. Lopes

State University of Ponta Grossa: J. D. Szezech Jr., A. Batista, M. Santos, M. Mugnaine

National University of Brasília: A. Schelin

Other Countries

University of Texas (Austin, USA): P. Morrison

National Laboratory (Oak Ridge, USA): D. Del-Castillo-Negrete

Humboldt University (Germany, Berlin): I. Sokolov

Aix-Marseille University (France): S. Benkadda, Y. Elskens

Aberdeen University (Scotland): M. Baptista

# Collaborators (Experiment)

- USP: Z. Guimarães-Filho, F. Pereira
- Federal Inst. of Education (São Paulo, Brazil): D. Toufen
- University of Texas (Austin): K. Gentle

# Outline

I- Shearless  Invariant Curves in the Non Twist Standard Map

II- Shearless  Invariants in Magnetic Field Lines Transport.
Experimental Evidences

III-Shearless Invariants in Plasma Particles Transport.
Experimental Evidences

# I- Shearless invariant curves in the Standard Nontwist Map

Standard nontwist map:

- Del-Castillo-Negrete, Morrison, Phys. Fluids 1993

Shearless transport barriers in the standard nontwist map:

- Del-Castillo-Negrete, Greene, Morrison, Physica D 1996
- Corso, Rizzato, Physical Review E 1998
- Fuchs, Wurm, Apte, Morrison, Chaos 2006
- Szezech Jr., Caldas, Lopes, Viana, Morrison, Chaos 2009

# Non Twist Sympectic Maps

- Shearless invariants appear in several models, due to non monotonic profiles or due to bifurcations.

- From these models, maps derived as local analytical approximations of Poincaré sections in phase space of Hamiltonian systems.

- Most known map: **standard nontwist map**

# NonTwist Standard Map

$$y_{n+1} = y_n + a\left(1 - x_{n+1}^2\right)$$

$$x_{n+1} = x_n - b\sin\left(2\pi y_n\right)$$

$\det(J) = 1 \Rightarrow$ Symplectic Map

**Two control parameters:**

***a***: Equilibrium shear

***b***: Perturbation amplitude

# Non Twist Standard Map / Rotation Number

$$y_{n+1} = y_n + a(1 - x_{n+1}^2) \qquad \bmod 1$$
$$x_{n+1} = x_n - b\sin(2\pi\, y_n)$$

$$\omega = \lim_{n\to\infty} \frac{x_{n+1} - x_0}{n}$$

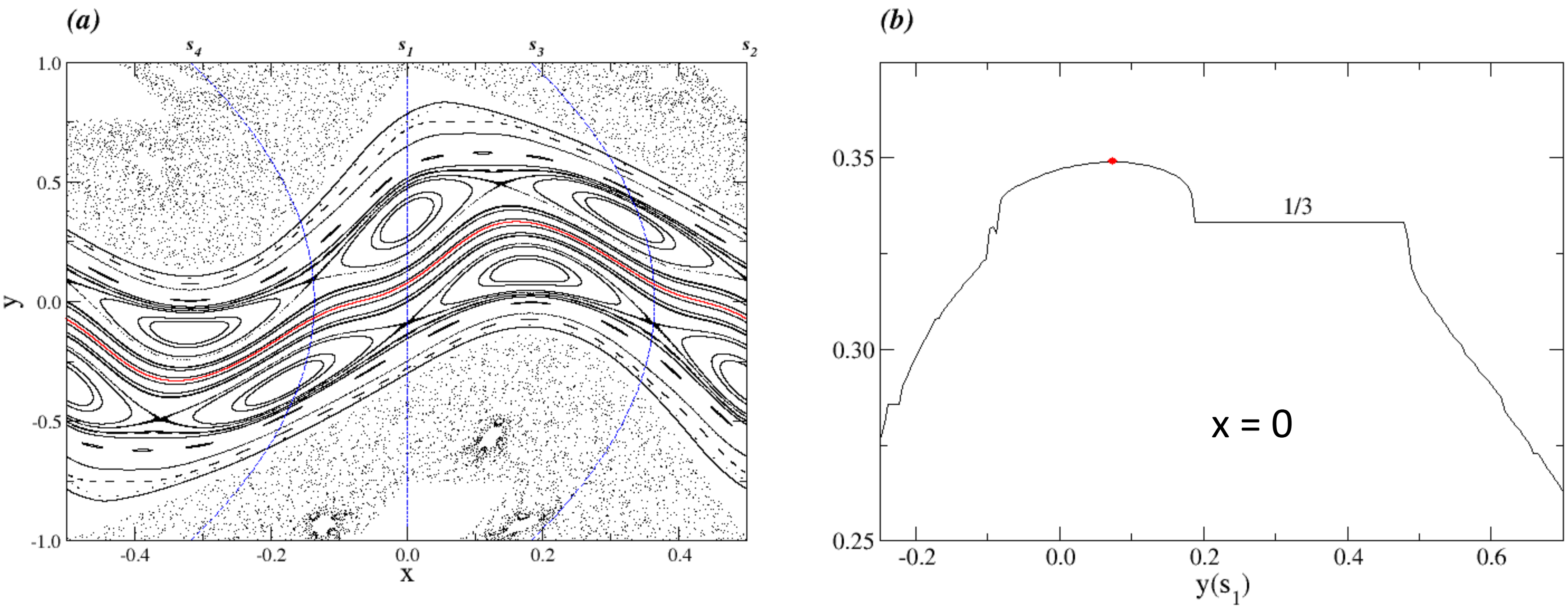


# Twin Islands

*a=0.3640; b=0.5232*

# Shearless Invariant Break Up

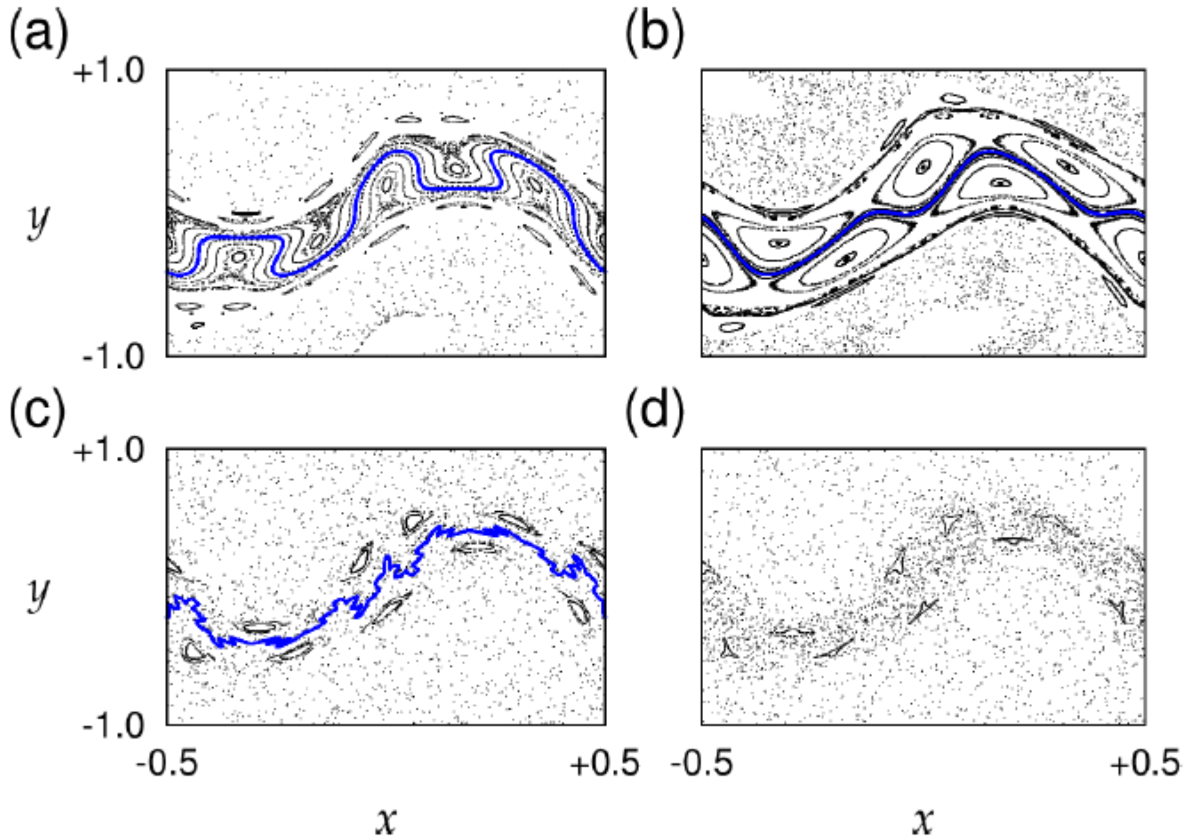


FIG. 1. Phase space of the SNM for (a) $a = 0.354$ and $b = 0.6$, (b) $a = 0.364$ and $b = 0.6$, (c) $a = 0.455$ and $b = 0.8$, and (d) $a = 0.455$ and $b = 0.847$. The blue line represents the shearless curve obtained by the evolution of the IP (1/4,b/2) as the initial condition in Eqs. (1).

Santos, Chaos 2018

# Before Barrier Break

Basin of Scape

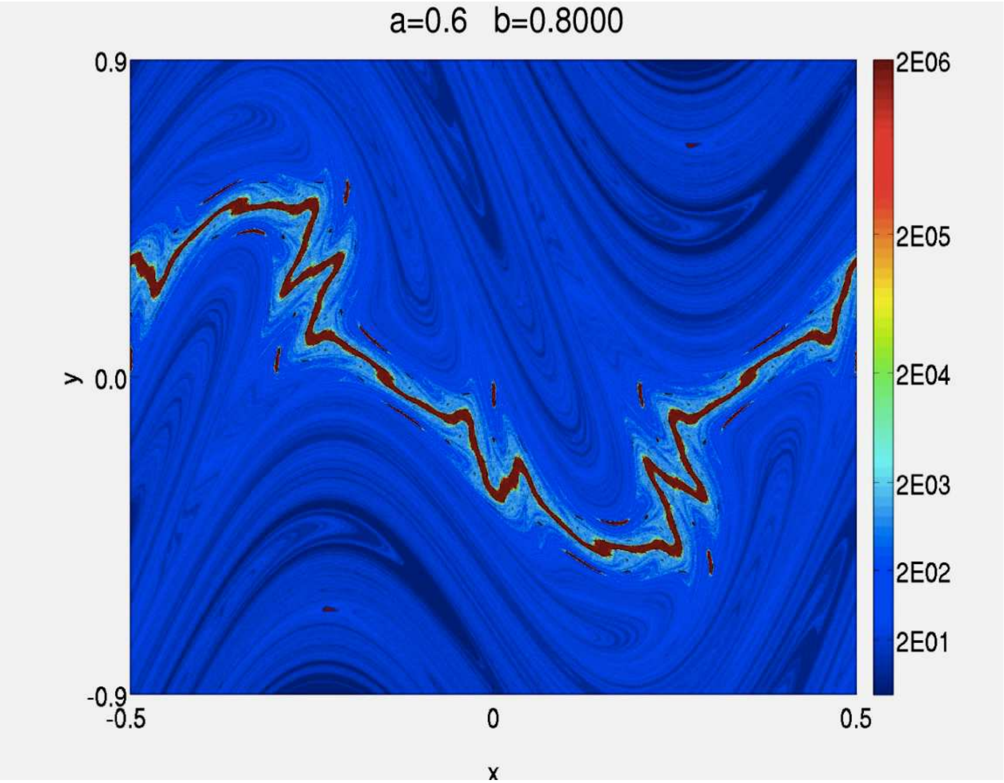


Phase Space

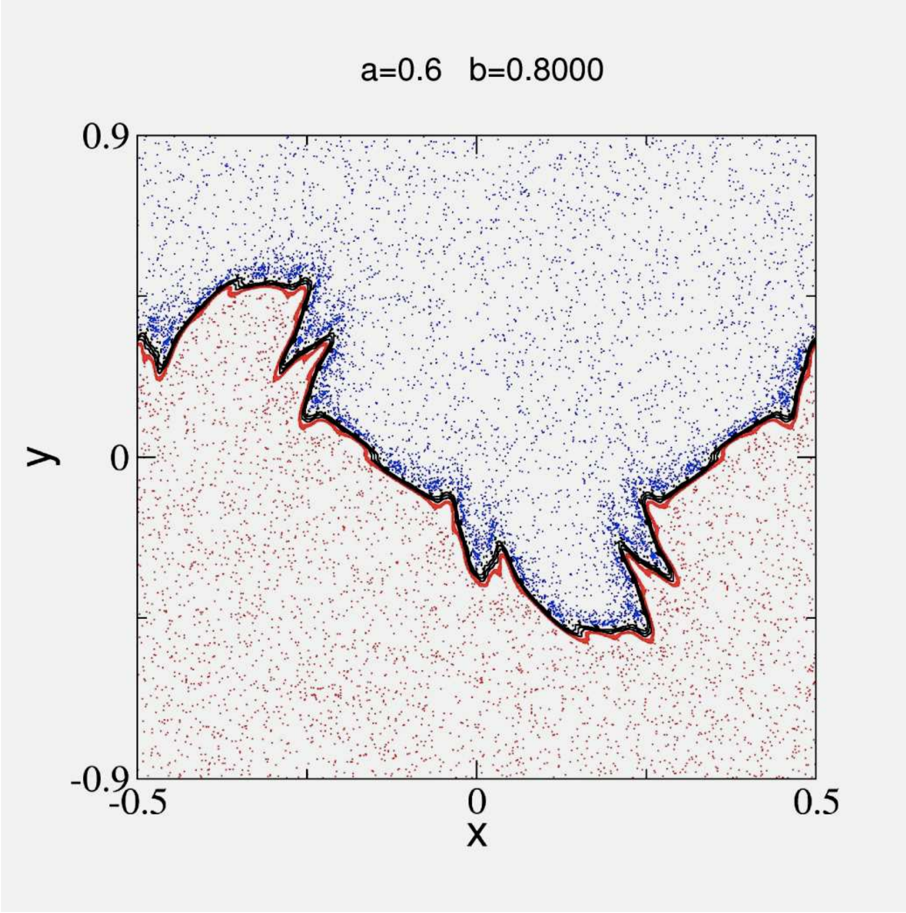

# Break up of the barrier

Phase space for before and after the break up of the last invariant (Meander). The blue trajectories represent a initial condition starting in lower phase space region, and the red in the upper phase space region.

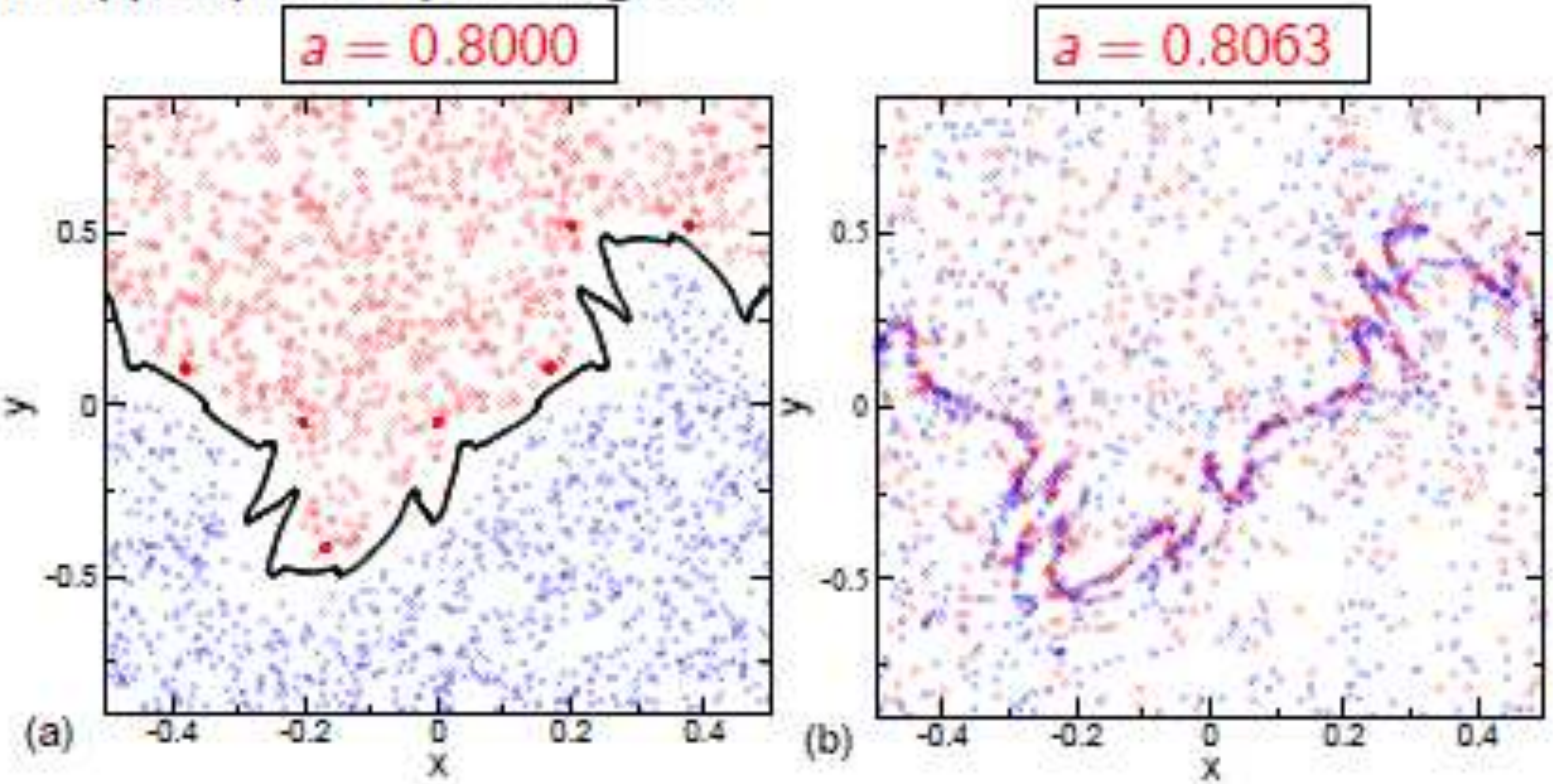

# Phase Space for the two cases

High transmissivity

$\boxed{a = 0.80552}$

Persistent Barrier

$\boxed{a = 0.80630}$

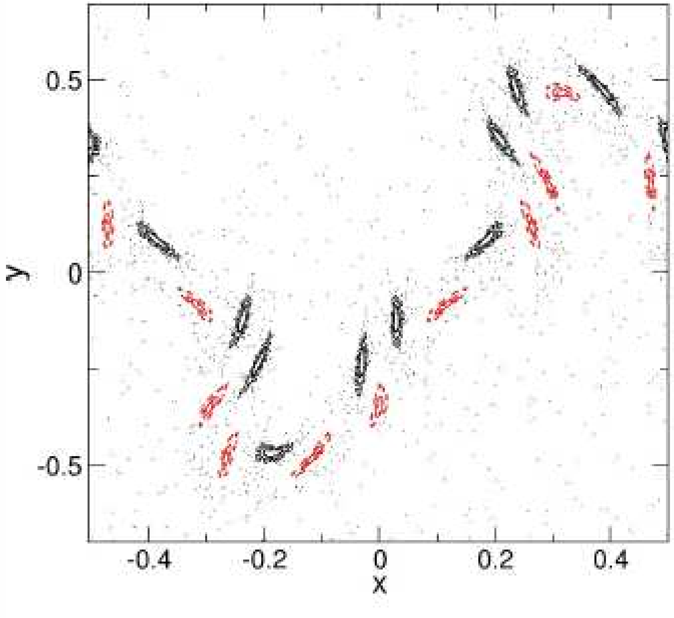


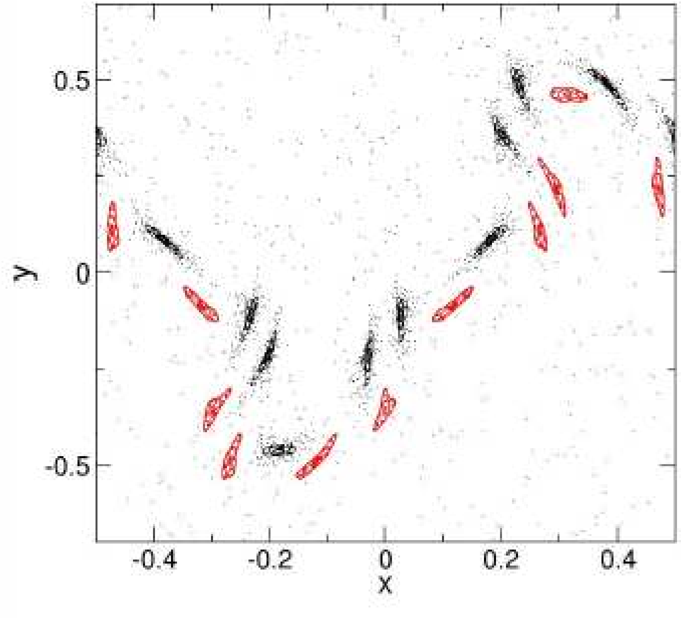

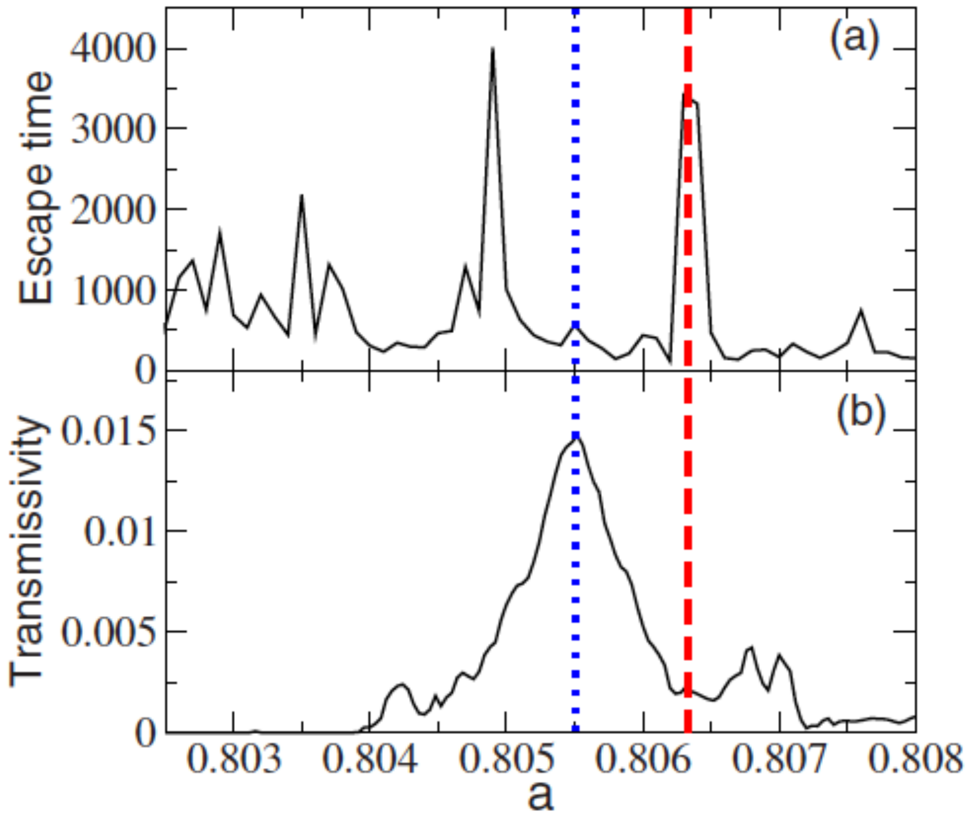


FIG. 3. (Color online) (a) Mean escape time and (b) transmissivity of the SNM with $b=0.6$ and variable $a$. The blue dotted line indicates an $a$-value of fast escape and large transmissivity, while the red dashed line indicates an $a$-value with an effective barrier in that the escape time is long and the transmissivity is low.

Szezech, Chaos 2009

# Escape time for diferent initial conditions

High transmissivity

$\boxed{a = 0.80552}$

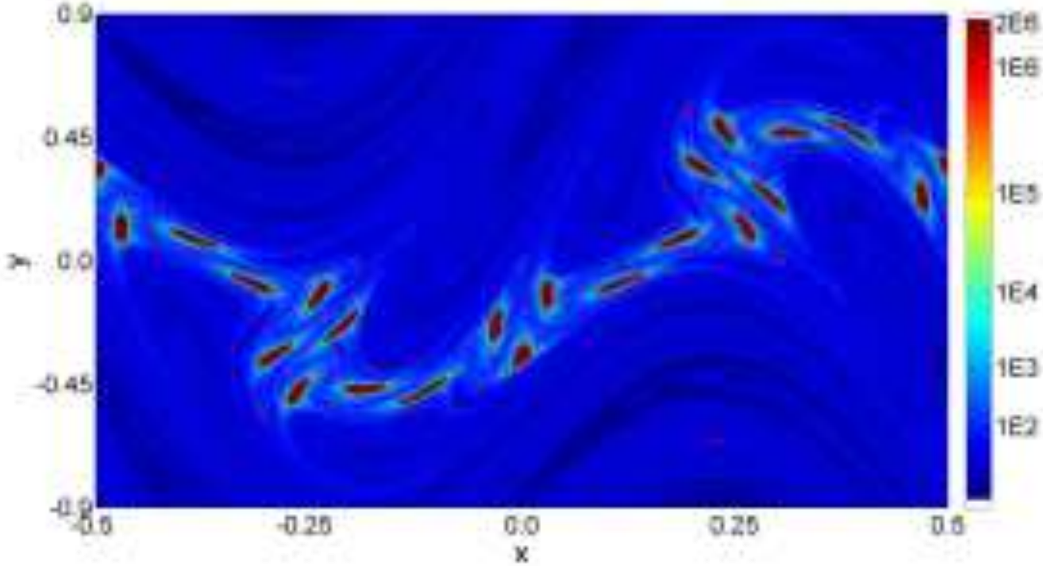


Persistent Barrier

$\boxed{a = 0.80630}$

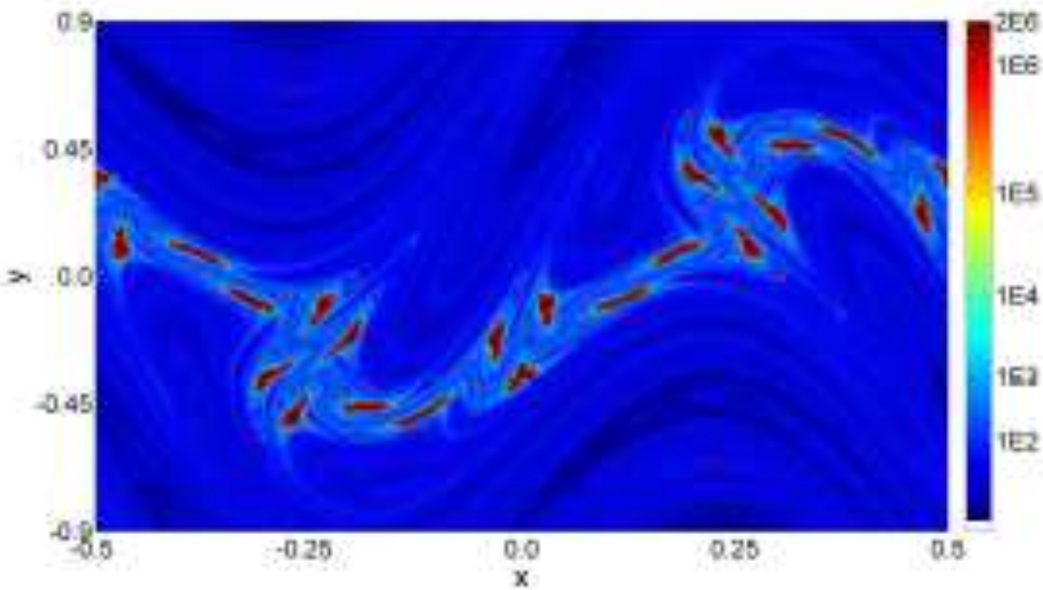

# Amplification of the escape time for diferent initial conditions

High transmissivity

$\boxed{a = 0.80552}$

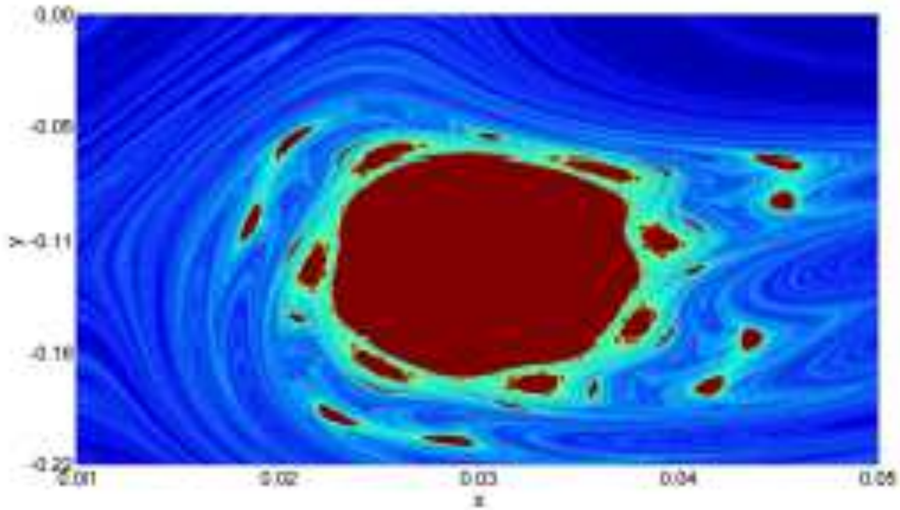


Persistent Barrier

$\boxed{a = 0.80630}$

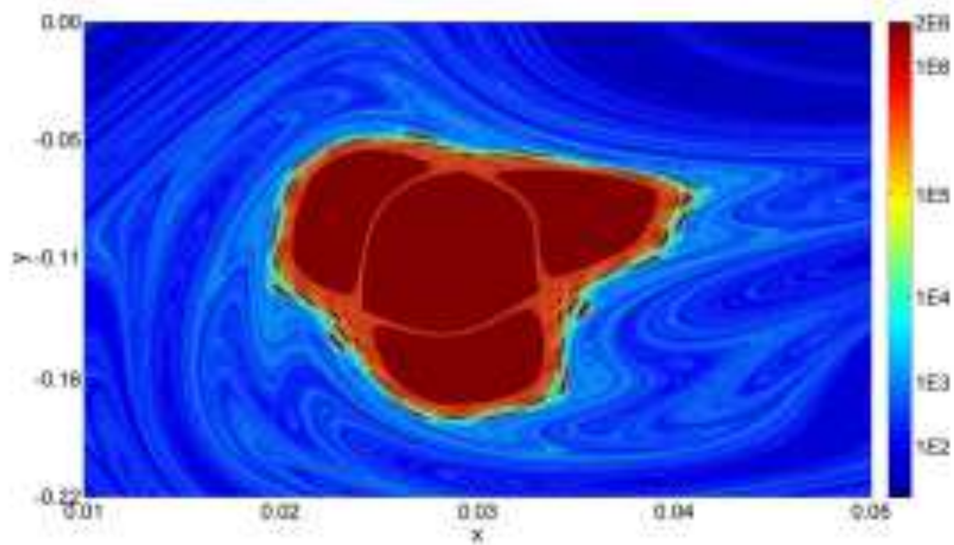

# Finite Time Lyapunov Exponent (FTLE)

A typical trajectory of a initial condition starting inside the trapping domain. The figure of left is the phase space and the figure of right is the FTLE temporal series.

$$\boxed{a = 0.80630}$$

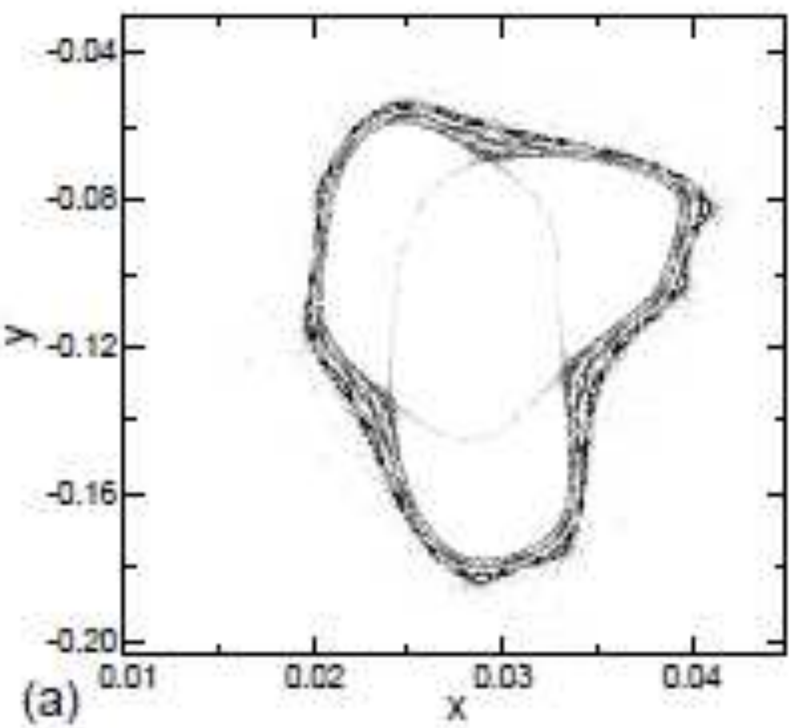


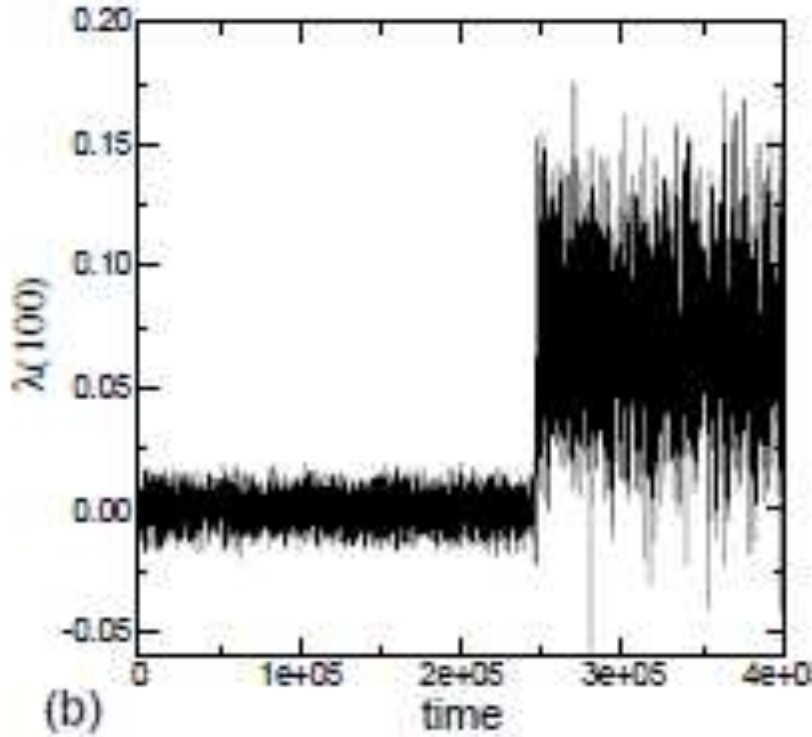

# Schematic description of the channels

G.Corso, F.B. Rizzato, PRE(1998)

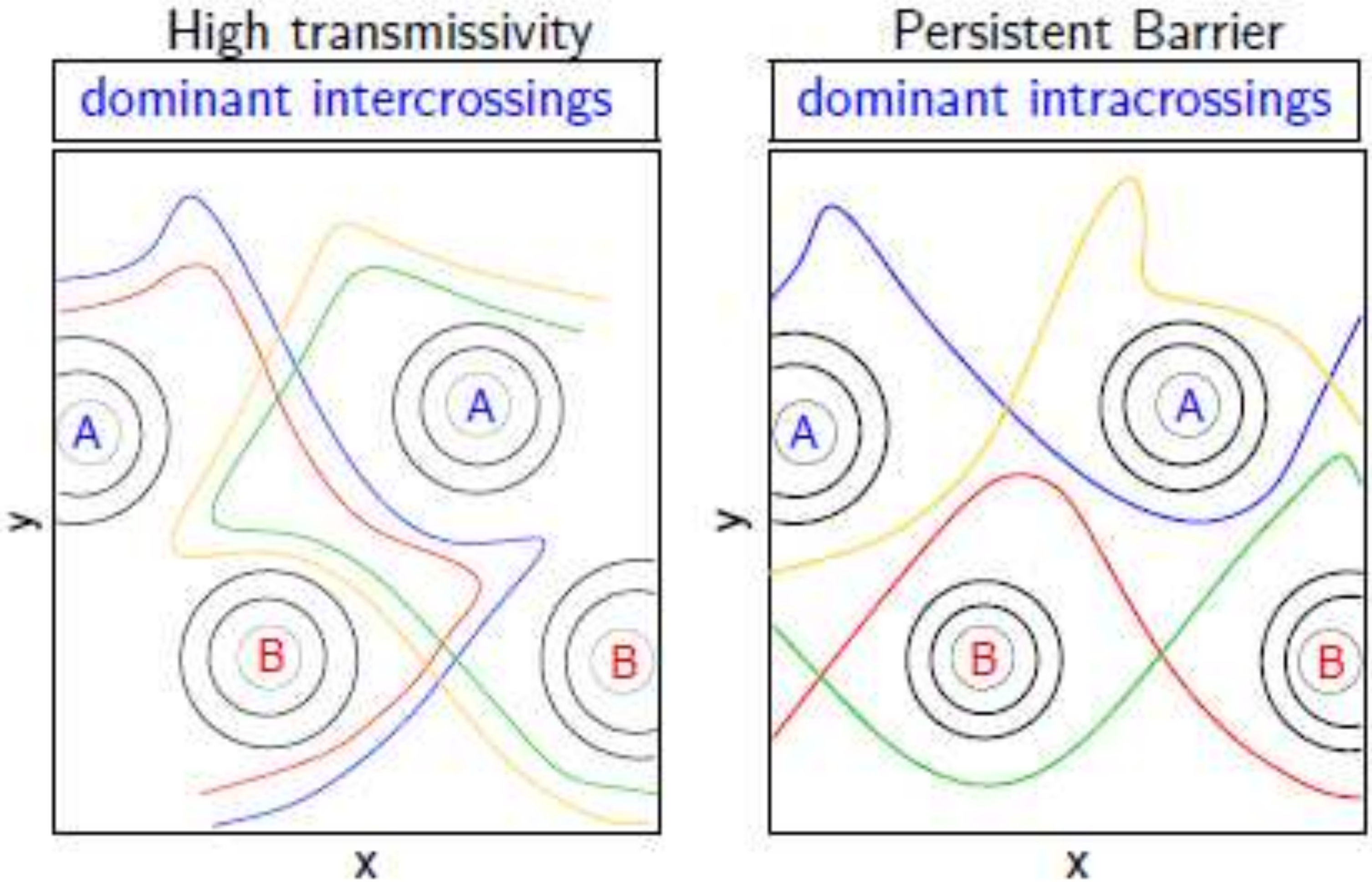

# Amplification of the Phase Space for the two cases and his respectives manifolds

High transmissivity

$\boxed{a = 0.80552}$

Persistent Barrier

$\boxed{a = 0.80630}$

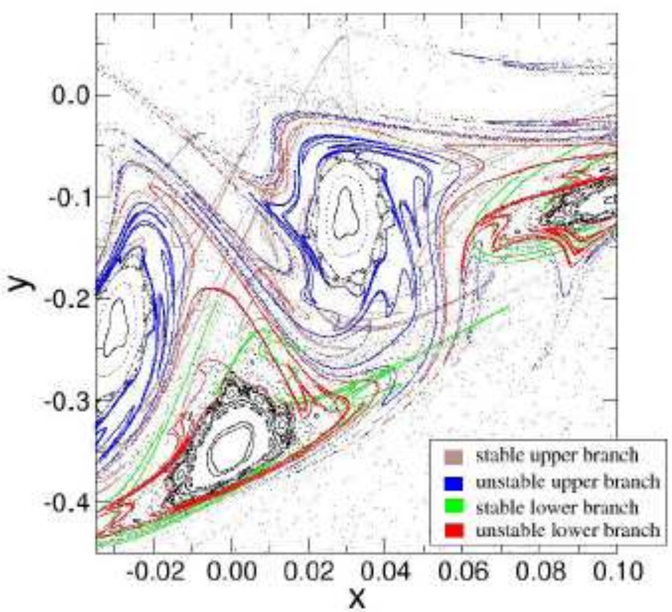


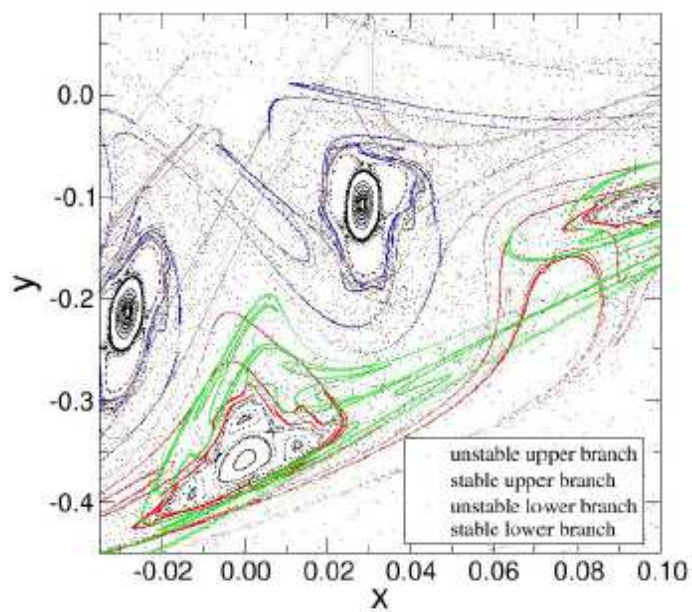

# Transmissivity of Shearless Transport Barrier

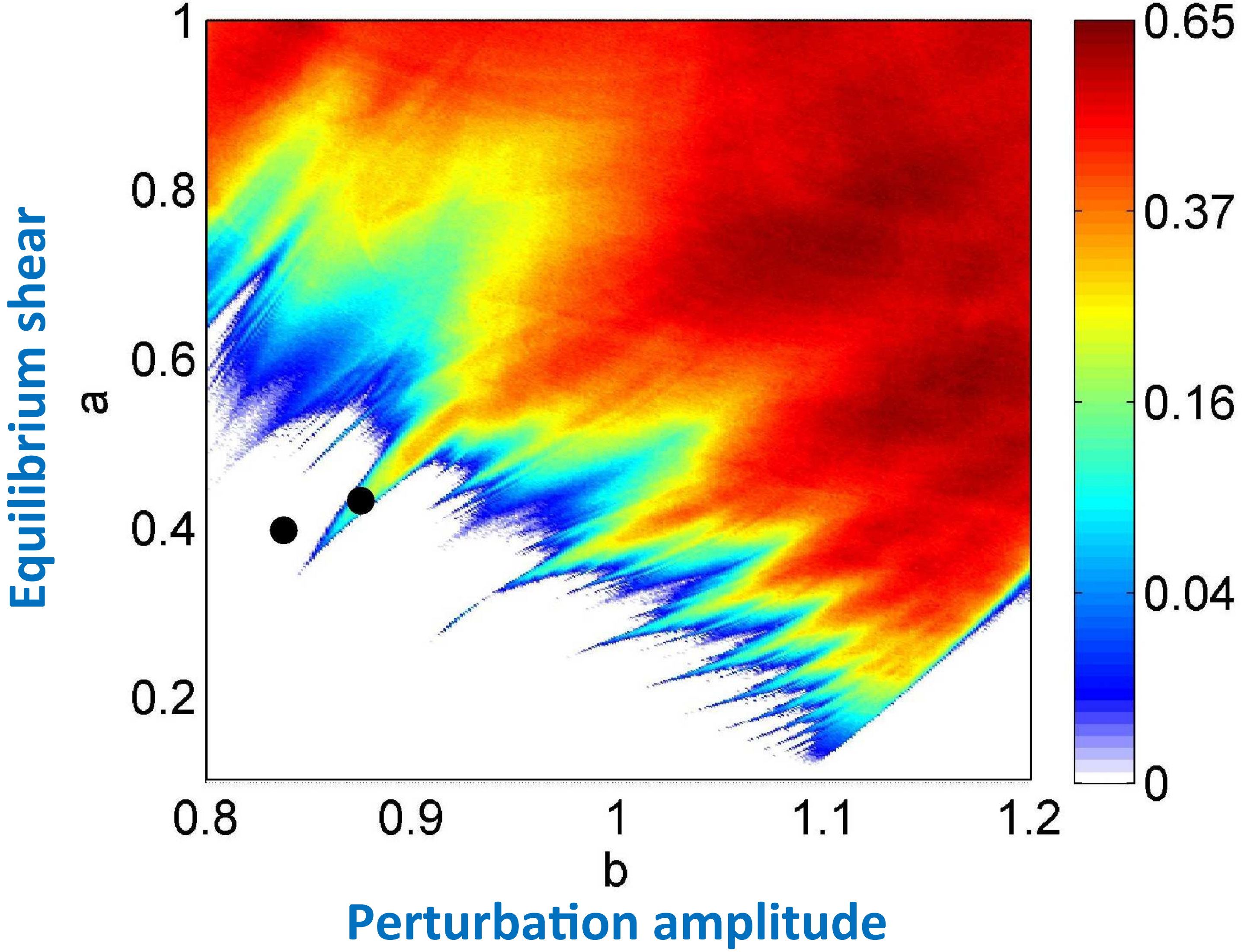

# A method for determining a stochastic transition

John M. Greene

*Plasma Physics Laboratory, Princeton, New Jersey 08544*
(Received 6 November 1978)

A number of problems in physics can be reduced to the study of a measure-preserving mapping of a plane onto itself. One example is a Hamiltonian system with two degrees of freedom, i.e., two coupled nonlinear oscillators. These are among the simplest deterministic systems that can have chaotic solutions. According to a theorem of Kolmogorov, Arnol'd, and Moser, these systems may also have more ordered orbits lying on curves that divide the plane. The existence of each of these orbit types depends sensitively on both the parameters of the problem,, and on the initial conditions. The problem addressed in this paper is that of finding when given KAM orbits exist. The guiding hypothesis is that the disappearance of a KAM surface is associated with a sudden change from stability to instability of nearby periodic orbits. The relation between KAM surfaces and periodic orbits has been explored extensively here by the numerical computation of a particular mapping. An important part of this procedure is the introduction of two quantities, the residue and the mean residue, that permit the stability of many orbits to be estimated from the extrapolation of results obtained for a few orbits. The results are distilled into a series of assertions. These are consistent with all that is previously known, strongly supported by numerical results, and lead to a method for deciding the existence of any given KAM surface computationally.

 0022-2488/79/061183-19$01.00  

ELSEVIER

Physica D 91 (1996) 1–23

PHYSICA D

# Area preserving nontwist maps: periodic orbits and transition to chaos

D. del-Castillo-Negrete [1], J.M. Greene [2], P.J. Morrison

*Department of Physics and Institute for Fusion Studies, The University of Texas at Austin, Austin, TX 78712, USA*

Received 27 February 1995; revised 6 August 1995; accepted 24 August 1995
Communicated by J.D. Meiss

**Abstract**

Area preserving nontwist maps, i.e. maps that violate the twist condition, are considered. A representative example, the *standard nontwist map* that violates the twist condition along a curve called the shearless curve, is studied in detail. Using symmetry lines and involutions, periodic orbits are computed and two bifurcations analyzed: periodic orbit collisions and separatrix reconnection. The transition to chaos due to the destruction of the shearless curve is studied. This problem is outside the applicability of the standard KAM (Kolmogorov-Arnold-Moser) theory. Using the residue criterion we compute the critical parameter values for the destruction of the shearless curve with rotation number equal to the inverse golden mean. The results indicate that the destruction of this curve is fundamentally different from the destruction of the inverse golden mean curve in twist maps. It is shown that the residues converge to a six-cycle at criticality.

Sudden change from stability to instability of scads of nearby periodic Orbits indicates the breakup of invariant tori

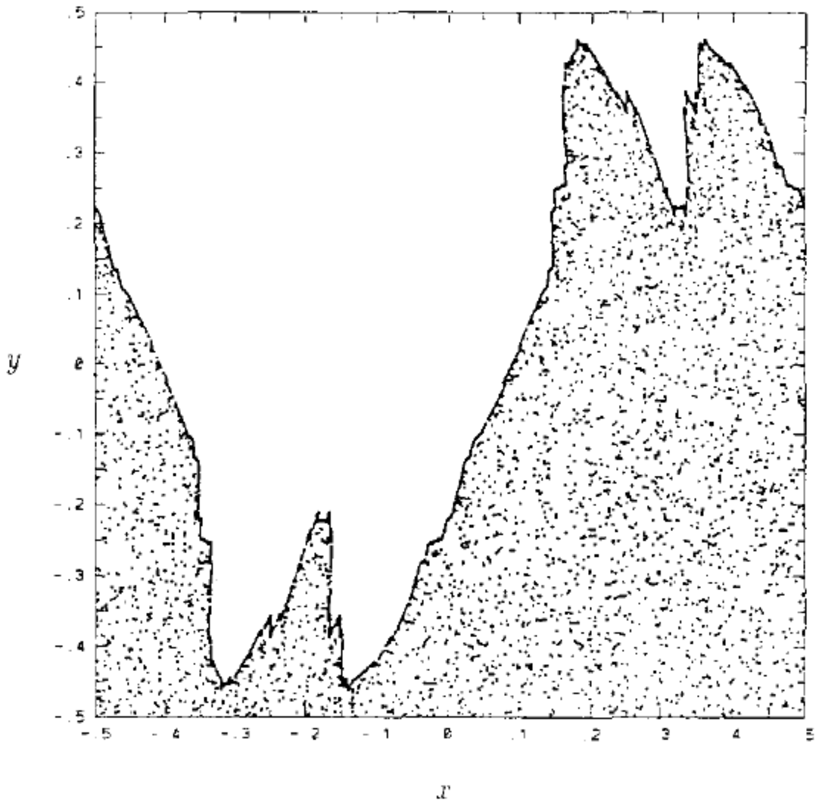


Fig. 13. The standard nontwist map at the critical parameter values, $(a_c, b_c) = (0.686049, 0.742493131039)$ for destruction of the $1/\gamma$ shearless orbit.

Residue criterion relates the existence of an invariant torus to a family of periodic orbits nearby

Castillo-Negrete, Greene, Morrison, Phisica D, 1996

# High accuracy

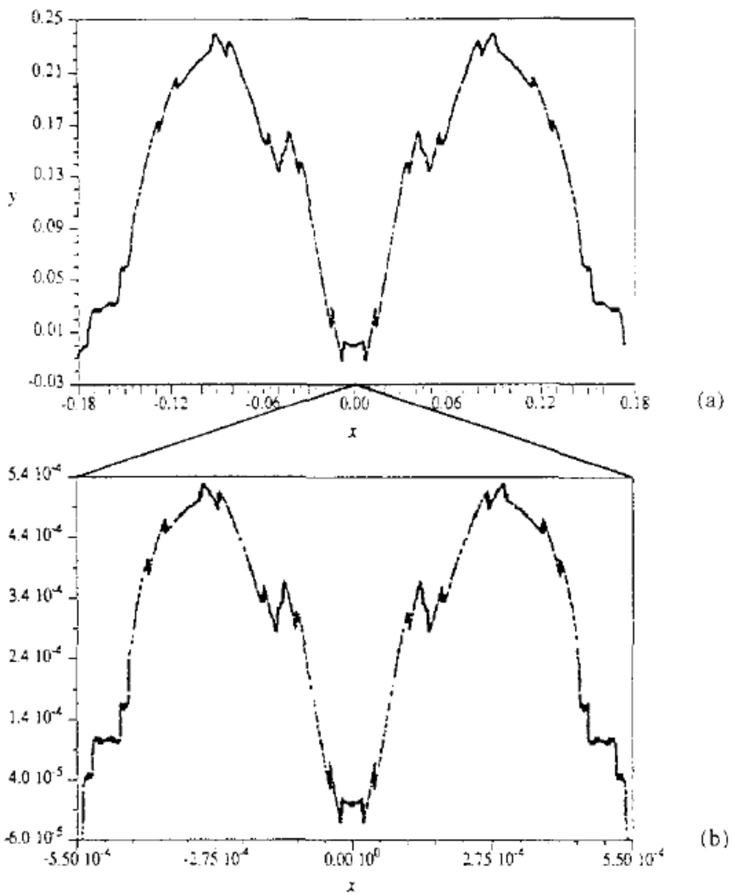


Fig. 15. Self-similar structure of the $1/\gamma$ shearless curves at criticality. In case (a) the shearless curve has been plotted in symmetry-line coordinates. Case (b) is a magnification of (a) by a factor of 321.92 in the $x$-direction and 463.82 in the $y$-direction.

Castillo-Negrete, Greene, Morrison, Phisica D, 1996

Physica D 308 (2015) 34–39

Contents lists available at ScienceDirect

Physica D

journal homepage: www.elsevier.com/locate/physd

# On Slater's criterion for the breakup of invariant curves

C.V. Abud *, I.L. Caldas

*Instituto de Física, Universidade de São Paulo, São Paulo, 05315-970 São Paulo, Brazil*

## HIGHLIGHTS

- We investigate Slater's theorem in the context of area-preserving maps.
- The breakup diagram of the nontwist map was obtained using Slater's criterion.
- Slater's criterion can be implemented to determine the last invariant curve.
- To the standard map our heuristic Slater's criterion was $K_c = 0.9716394$.
- Our result is very close to the widely accepted Greene's result, $K_c = 0.971635$.

## ARTICLE INFO

*Article history:*
Received 6 October 2014
Received in revised form
13 June 2015
Accepted 17 June 2015
Available online 24 June 2015
Communicated by I. Melbourne

## ABSTRACT

We numerically explore Slater's theorem in the context of dynamical systems to study the breakup of invariant curves. Slater's theorem states that an irrational translation over a circle returns to an arbitrary interval in at most three different recurrence times expressible by the continued fraction expansion of the related irrational number. The hypothesis considered in this paper is that Slater's theorem can be also verified in the dynamics of invariant curves. Hence, we use Slater's theorem to develop a qualitative and quantitative numerical approach to determine the breakup of invariant curves in the phase space of area-preserving maps.

# The Slater's Theorem

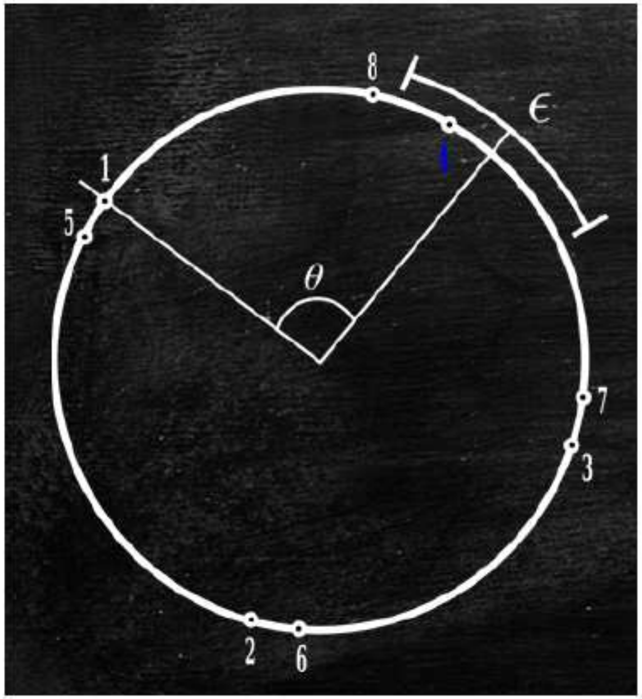


An irrational translation, θ, over an unity circle can take <u>at most three</u> different recurrence times to a connected interval of size $\epsilon < 1$.

$\sigma_1$ $\sigma_2$ $\sigma_3$

Irrational: continued fraction expansion

$$\sigma_i = [a_1, a_2, a_3, \dots, a_s, \dots] = \cfrac{1}{a_1 + \cfrac{1}{a_2 + \cfrac{1}{\dots + \cfrac{1}{a_s}}}} = \frac{P_s}{Q_s}$$

According to Slater the three recurrences are:

$\sigma_1 = Q_{s-1}$

$\sigma_2 = Q_s - nQ_{s-1}$

$\sigma_3 = Q_s - (n+1)Q_{s-1}$

$\varepsilon = (n+1)\eta_s + \eta_{s+1} + \psi \qquad (0 < \psi \leq \eta_s)$

$\eta_s = (-1)^{s-1}(\theta Q_{s-1} - P_{s-1})$

N. B. Slater , *The Distribution of the integers N for which* $\{N\theta\} < \varepsilon$. Proc. Camb. Phil. Soc. 46 (1949) 525.

## Invariant curves in phase space of dynamical systems

- Irrational rotation
- Can be parameterized to a circle map

$F = I \cdot I_1$

$I_0$: $(x, y) = (-x,\quad y - b\sin(2\pi x))$

$I_1$: $(x, y) = (x + a(1 - y'^2),\quad y)$

Symmetry: $S(x, y) = (x + \frac{1}{2}, y)$ $\quad F \cdot S = S \cdot F$

Reversible: $I_{0,1} \cdot F = F^{-1} \cdot I_{0,1}$

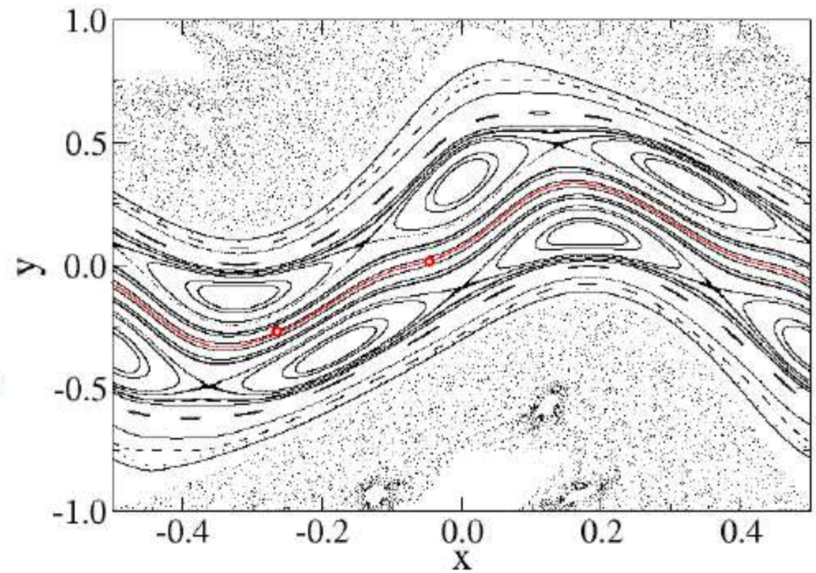


Indicator Points:

$$(\frac{n}{2} - \frac{1}{4}, (-1)^{n+1}\frac{b}{2})$$

$$(\frac{a}{2} + \frac{n}{2} - \frac{1}{4}, 0).$$

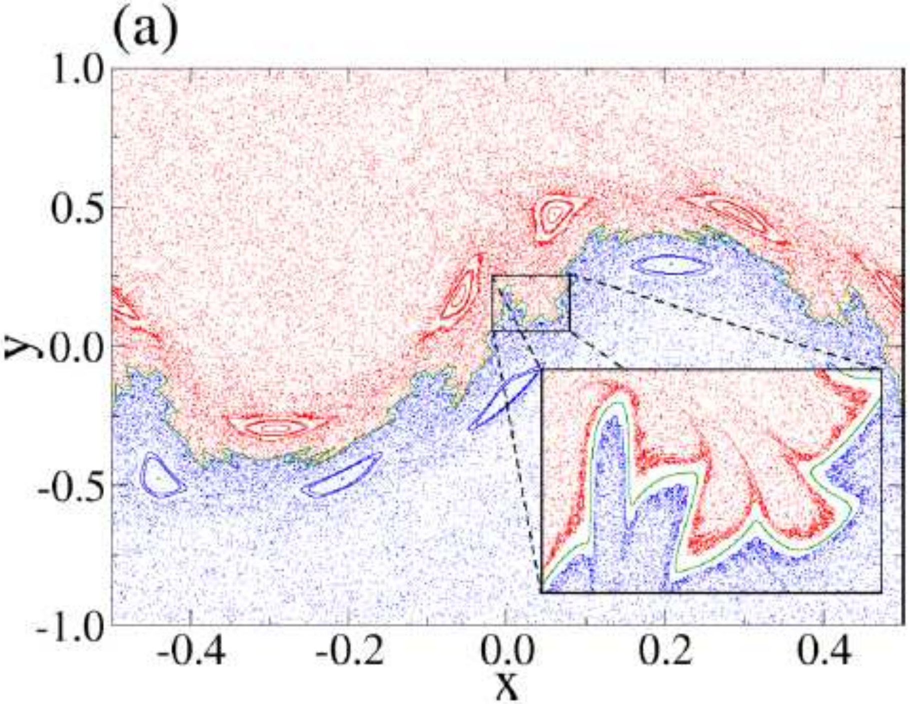


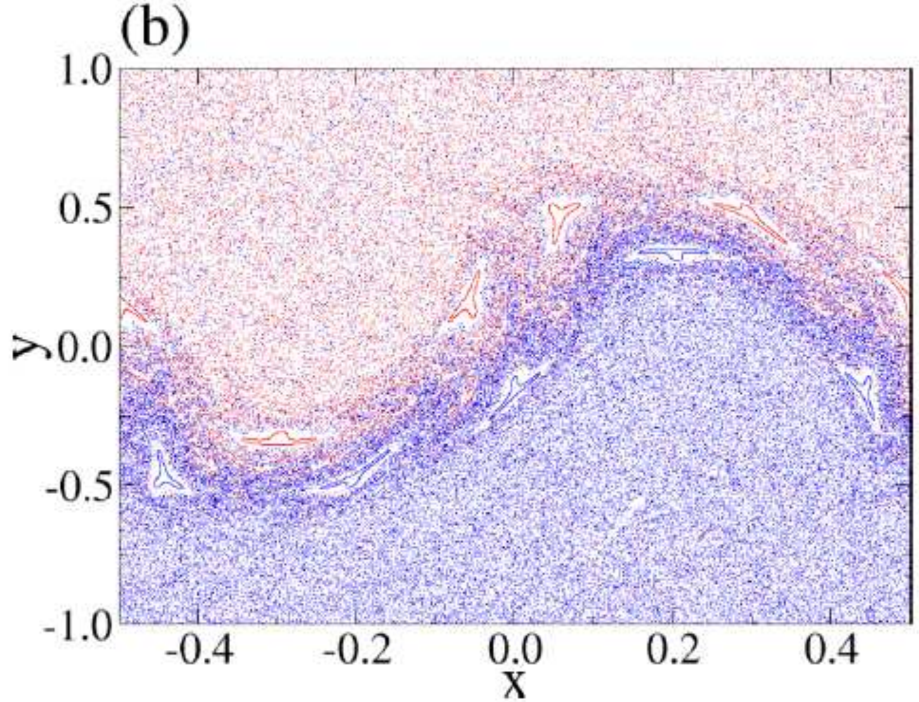


a = 0.455; b = 0.800

a = 0.455; b = 0.847

ε = 0.001

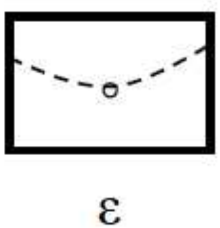


- Indicator Point: (1/4; b/2)

# Parameter Space
# Fractal Critical Curve

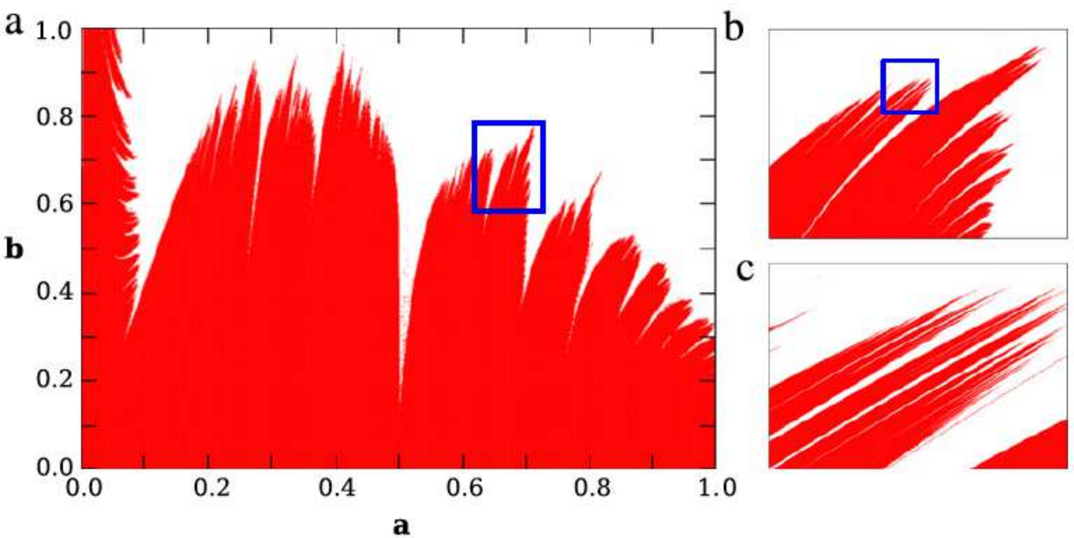


**Fig. 2.** Parameter space of SNM showing the breakup boundary for the central shearless curve. The red color indicates the set of parameters $(a, b)$ in which the shearless curve exists in the phase space. (For interpretation of the references to color in this figure legend, the reader is referred to the web version of this article.)

Suited for large parameters set

# Conclusions

- Invariant shearless barrier could appear for non monotonic profile.
- Transition to global chaos. A typical scenario to breakup the shearless invariant curve.
- Persistent barriers for non twist maps, J. D. Szezech Jr. et. al , Chaos (2009)

# Bifurcations: Onset of Shearless Invariant Curves

# Non Twist Bifurcations

Nonlinearity **13** (2000) 203–224. Printed in the UK PII: S0951-7715(00)01342-6

## Generic twistless bifurcations

H R Dullin†‡, J D Meiss† and D Sterling†

CHAOS **22**, 033142 (2012)

## Secondary nontwist phenomena in area-preserving maps

C. Vieira Abud[a] and I. L. Caldas[b]
*Instituto de Física, Universidade de São Paulo, São Paulo, 05315-970 São Paulo, Brazil*

# Non Twist Bifurcations

*Birkhoff normal form* → *expansion around an eliptic point*

$$J_{n+1} = J_n$$

$$\theta_{n+1} = \theta_n + 2\pi\,\Omega(J)$$

$$\Omega(J) = \omega + \gamma_0 + \gamma_1 J$$

*Birkhoff coefficients*

Our procedure

*Internal rotation number*

$$\omega_{in} = \lim_{n\to\infty} \frac{1}{2\pi\, n} \sum_{n=1}^{\infty} P_n(x,y)\,\hat{\theta}\,P_{n+1}(x,y)$$

# (Twist) Standard Map

$$y_{n+1} = y_n + x_{n+1}$$

$$x_{n+1} = x_n - K\sin\left(2\pi y_n\right)$$

# Triple Bifurcation in Standard Map

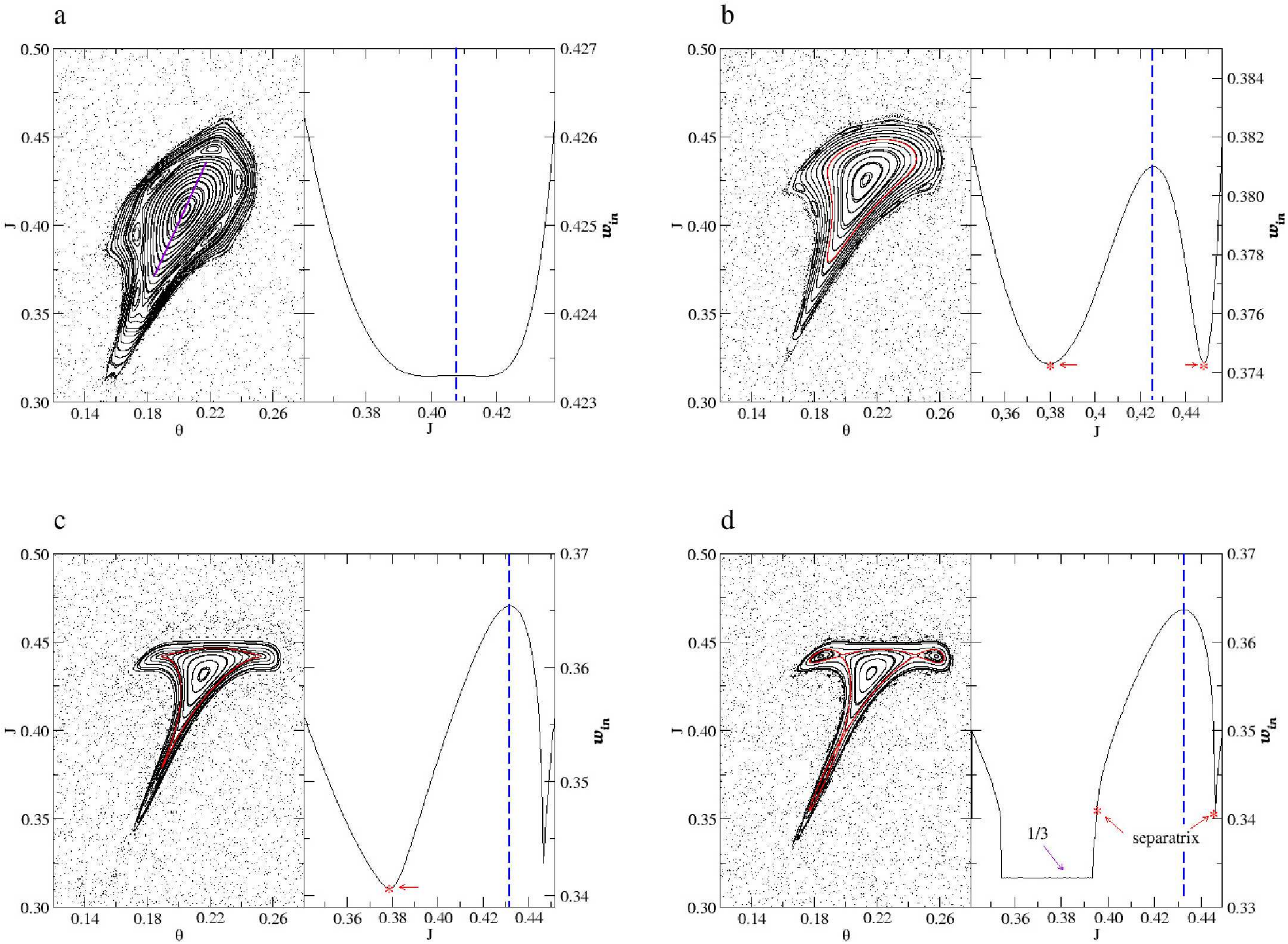


*(a) K=5.35; (b) K=5.50; (c) K=5.554; (d) K=5.56.*

# Triple Bifurcation in Non Twist Standard Map

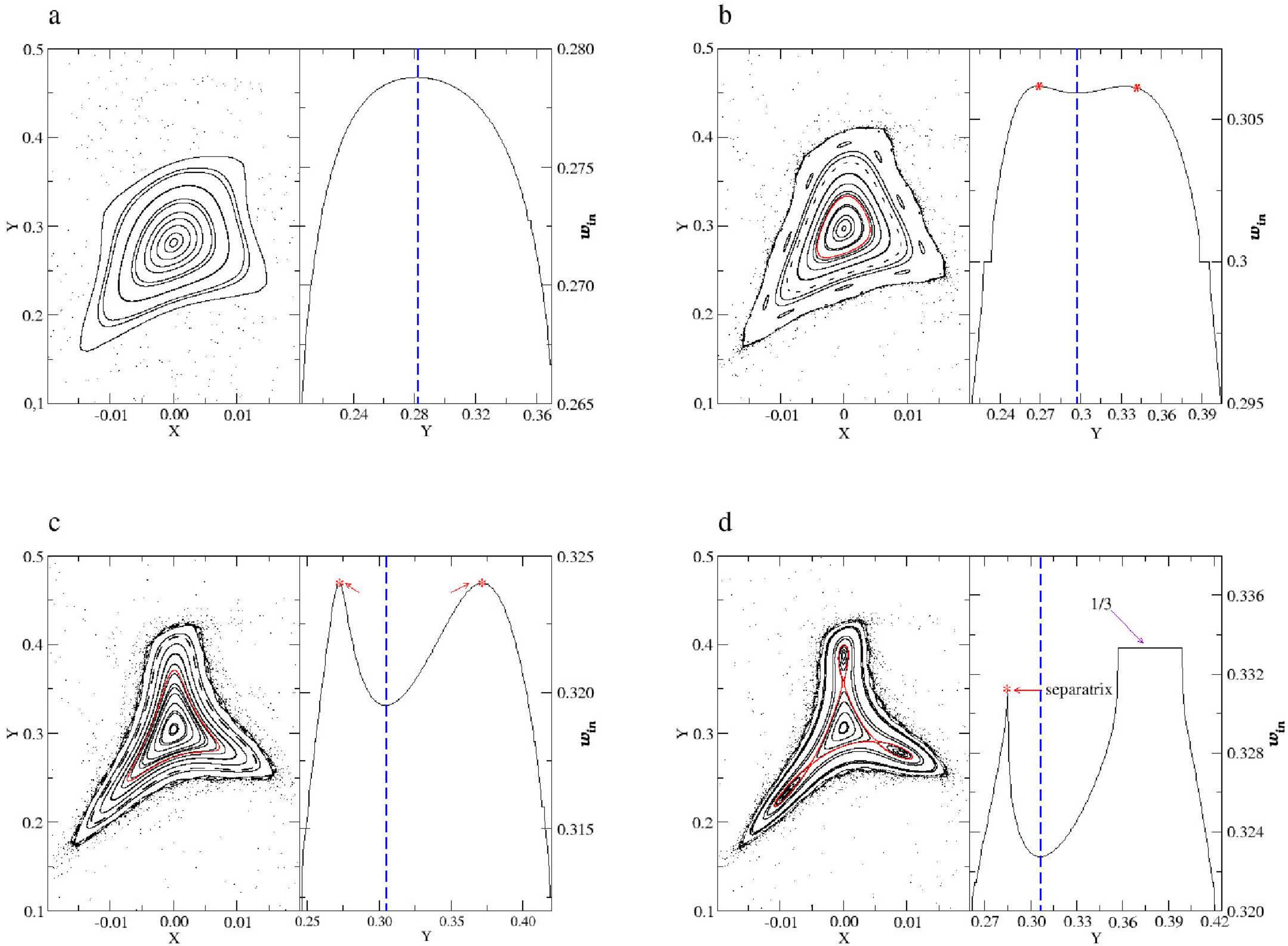


*b=0.8; (a) a=0.543; (b) a= 0.5485; (c) a=0.551; (d) a=0.5517.*

# II- Shearless Invariants in Magnetic Fields

Magnetic Surfaces in Tokamaks

# Tokamak

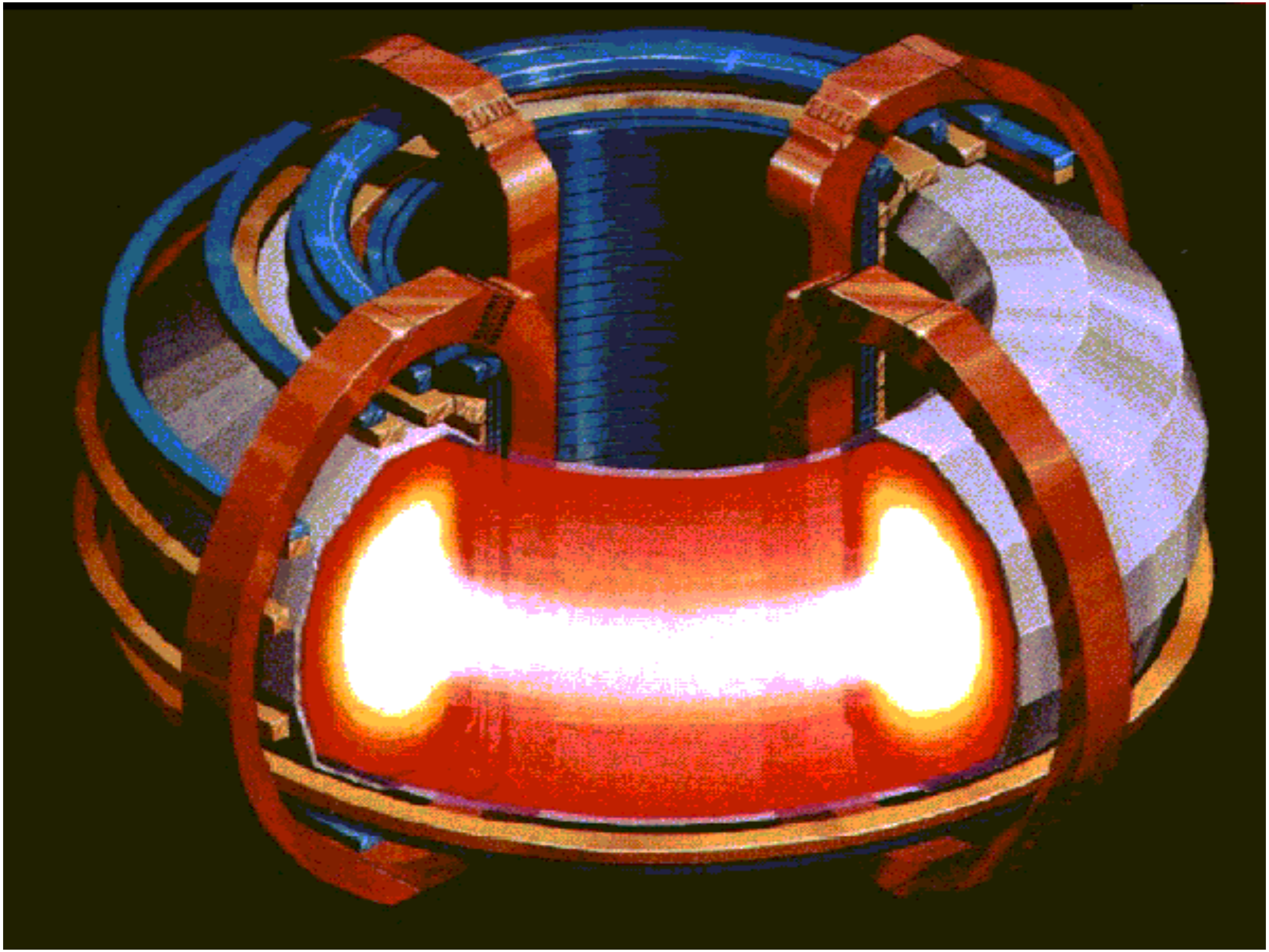

# Plasma Confined in Tokamaks

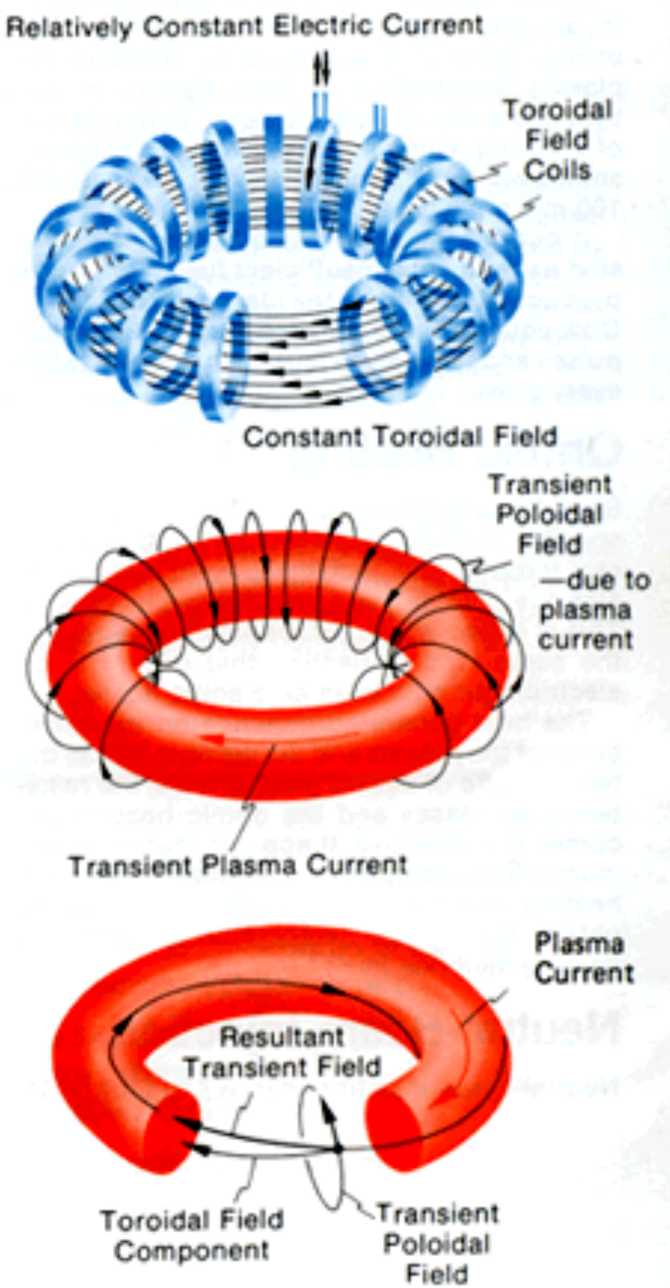


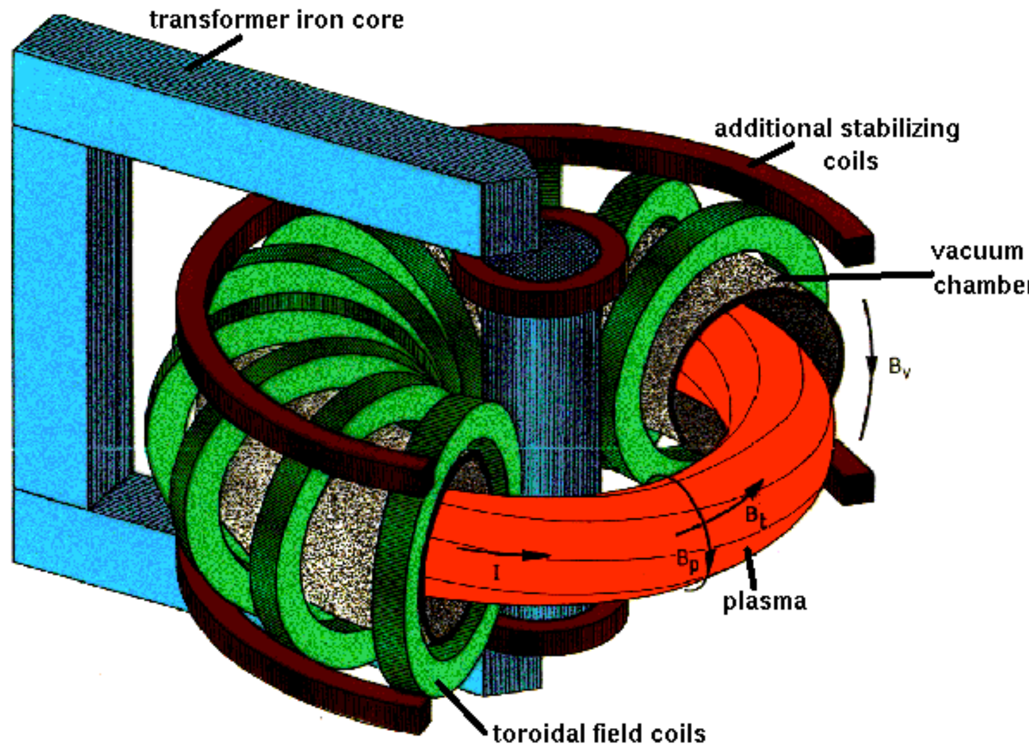


FORSCHUNGSZENTRUM JÜLICH GmbH KFA

# MHD Equilibrium

Equations

$$\nabla p = \vec{j} \times \vec{B}$$

$$\nabla \times \vec{B} = \mu_0 \vec{j}$$

P : plasma pressure

$\vec{j}$ : plasma electric current d

$\vec{B}$ : plasma magnetic field

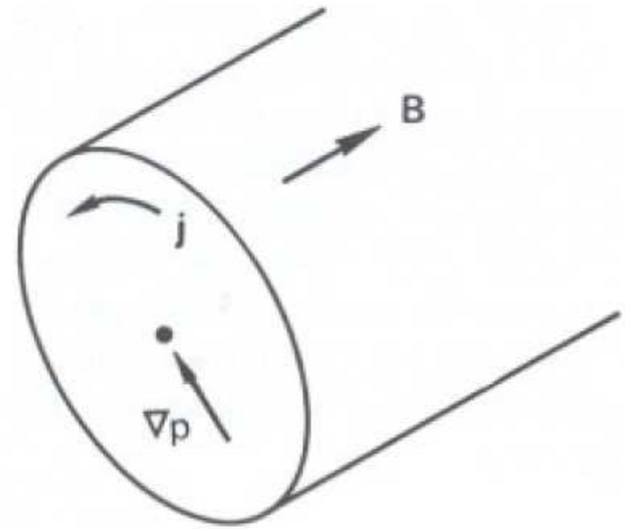


FIGURE 6-2 The j × B force of the diamagnetic current balances the pressure-gradient force in steady state.

# Magnetic Surfaces

Field Lines on surfaces with constant pressure (isobarics)

$$\vec{B} \cdot \nabla p = 0$$

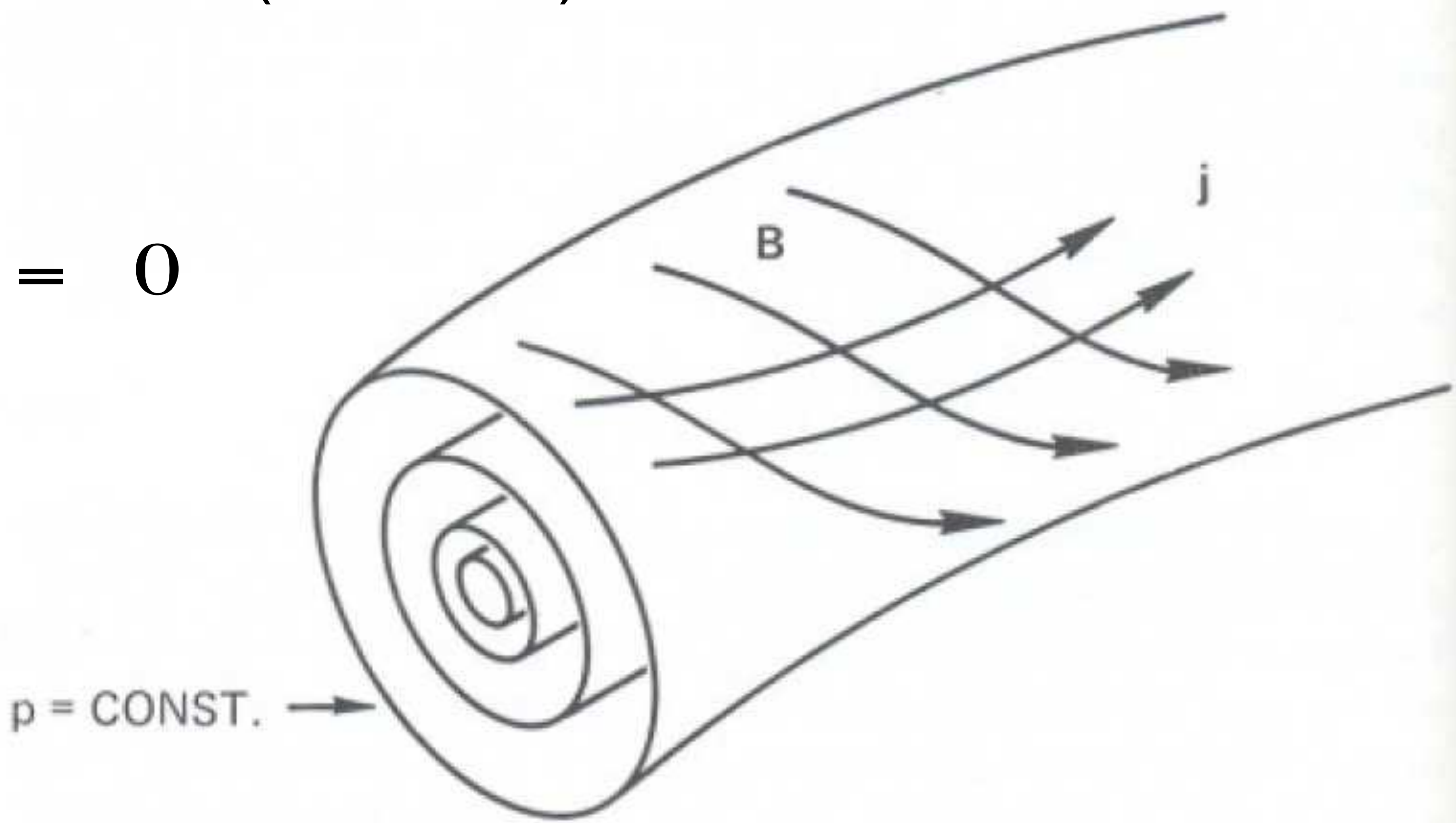


**FIGURE 6-3** Both the j and B vectors lie on constant-pressure surfaces.

# Helicoidal magnetic field lines on toroidal surfaces

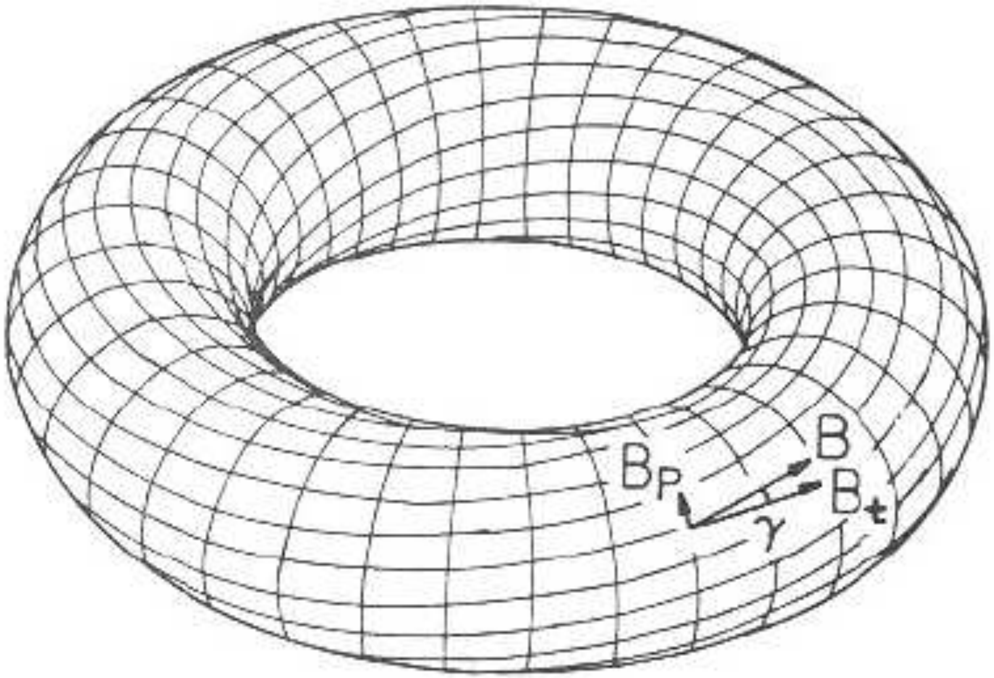


*Linhas e Superfície de Campo Magnético Toroidal.*

# Equilibrium Magnetic Field in Tokamaks

Field lines describe toroidal ($\phi$) and poloidal ($\theta$) angles , on toroidal magnetic surfaces.

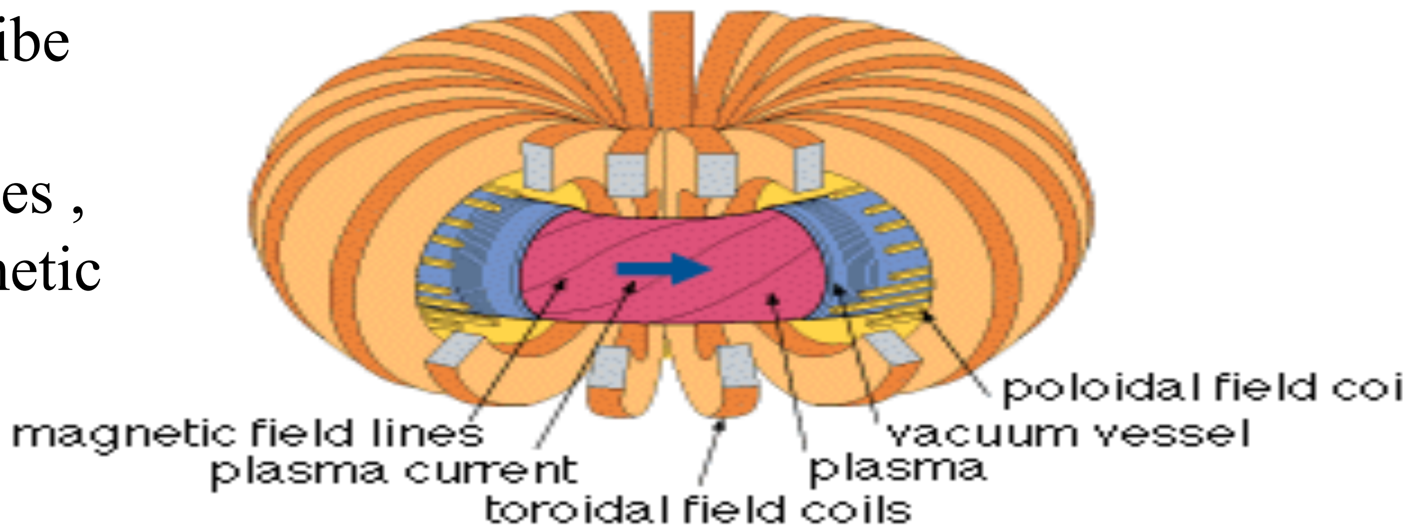


Field line equation

Integrable Field

$$\vec{B}_0 \times d\vec{l} = 0 \quad \rightarrow \quad \dot{\vartheta} = \frac{\partial \mathrm{H}_0(\mathrm{J})}{\partial \mathrm{J}}, \quad \dot{\mathrm{J}} = -\frac{\partial H_0(J)}{\partial \vartheta}$$

t (canonical time) $\equiv \phi$ (toroidal angle)

Frequency $\omega(\mathrm{J}) = \dfrac{\partial \mathrm{H}_0}{\partial \mathrm{J}}$

# Lagrangian Caos

Symmetry $\Rightarrow$ integrable system

$\mathrm{H}=\mathrm{H}_0(J) \Rightarrow \quad J = J_0 \;, \vartheta=\omega\ \mathrm{t}+\vartheta_0$

$(J,\vartheta)$ action/angle de $\mathrm{H}_0$

Helicoidal perturbation $(\varepsilon \neq 0) \Rightarrow$ *symmetry broken*

$\mathrm{H}=\mathrm{H}_0(J) + \varepsilon \mathrm{H}_1(J,\vartheta)$

$\varepsilon<<1 \Leftrightarrow$ quasi-integrabel system

# Ergodic (Chaotic) Magnetic Limiter
## Ressonant perturbations in magnetic surfaces

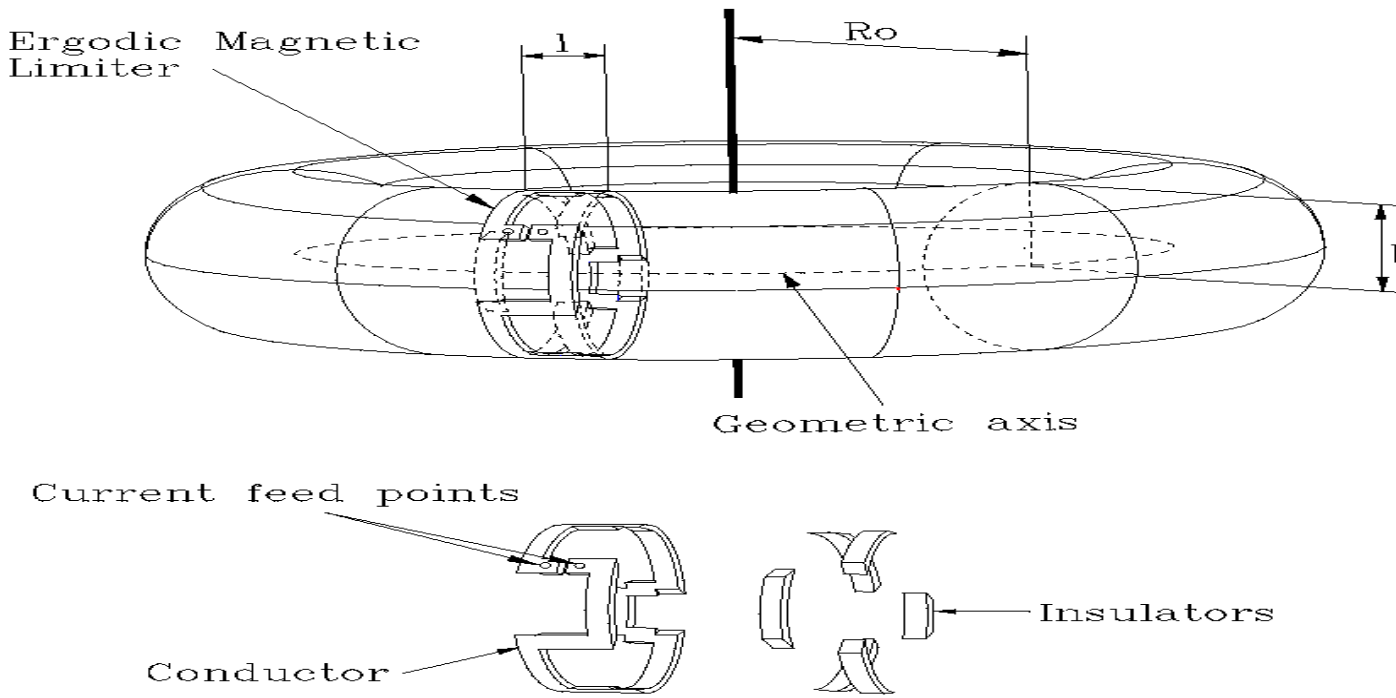


Ressonant perturbation: m/n.

Control parameter: limiter current $I_h$ .

# Toroidal MHD Equilibrium

## Magnetic Surfaces

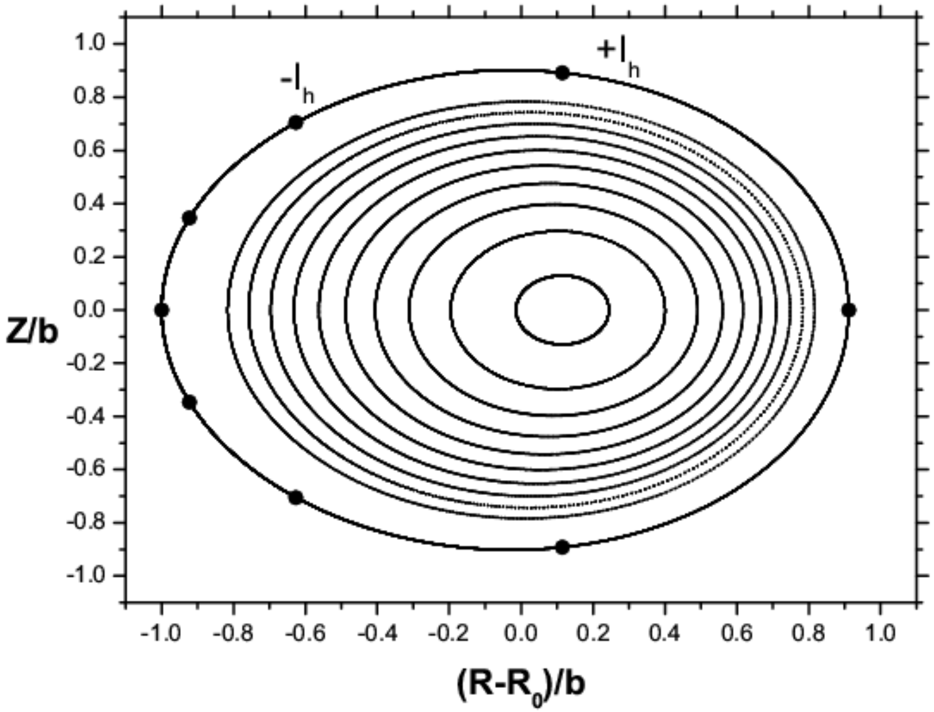


$I_h/I_p = 0$

Normalized distances in polar coordinates

# Field line hamiltonian for a tokamak with EML

- non-integrable hamiltonian in action-angle variables $(\mathcal{J}, \theta)$

$$H_L(\mathcal{J}, \theta, t) = H_0(\mathcal{J}) + \frac{\ell}{R_0'} H_1(\mathcal{J}, \theta, t) \sum_{k=-\infty}^{+\infty} \delta\left(t - k\frac{2\pi}{N_r}\right)$$

  where $R_0'$ is the major radius and $N_r$ is the number of limiters with length $\ell$

- plasma equilibrium: integrable part

$$H_0(\mathcal{J}) = \frac{1}{B_T R_0'^2} \Psi_{p0}(\mathcal{J})$$

  where $\Psi_{p0}$ is the poloidal flux function (Grad-Shafranov eq.)

- resonant perturbation [mode numbers $(m, n)$]

$$H_1(\mathcal{J}, \theta, t) = \frac{1}{B_T R_0'^2} a(\mathcal{J}) \cos\left(m\theta - n\frac{t}{R_0'}\right)$$

# Magnetic field line map

- section at constant azimuthal angle
- $(\mathcal{J}, \theta)$ action-angle field line coordinates at the Poincaré section
- we integrate the canonical equations

$$\frac{d\mathcal{J}}{dt} = -\frac{\partial H}{\partial \theta}, \qquad \frac{d\theta}{dt} = \frac{\partial H}{\partial \mathcal{J}}.$$

- obtaining a field line map $(\mathcal{J}_{n+1}, \theta_{n+1}) = \mathbf{F}(\mathcal{J}_n, \theta_n)$

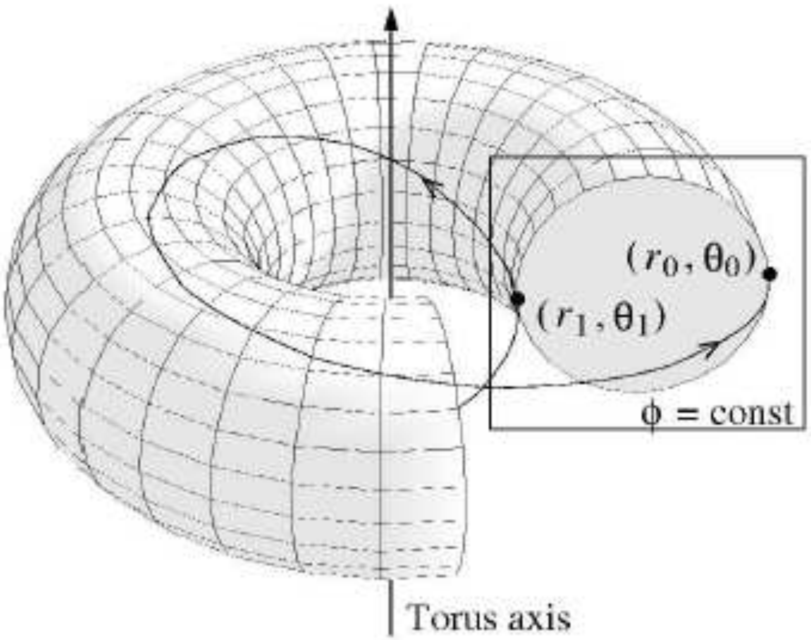

# Non monotonic plasma current density

Stability of Multihelical Tearing Modes in Shaped

Tokamaks

W. Kerner and H. Tasso, Phys. Rev. Lett. **49**, 654 (1982)

Dimerized Islands

G. Oda, Caldas, CSF (1995)

G. Corso, G. Oda, I. Caldas, CSF (1997)

# Toroidal MHD Equilibrium

## Magnetic Surfaces

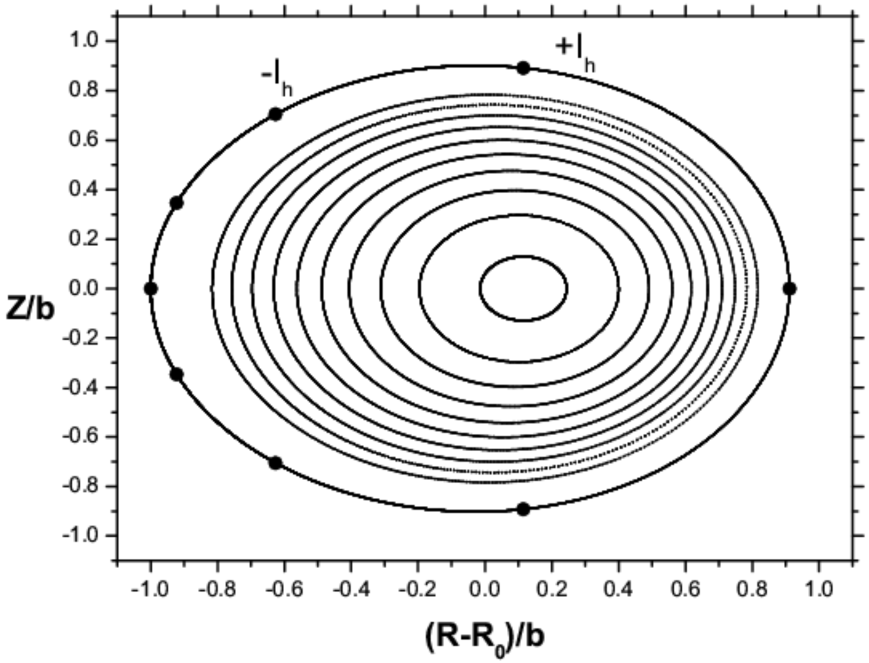


Normalized distances
in polar coordinates

## Nonmonotonic Radial Profile

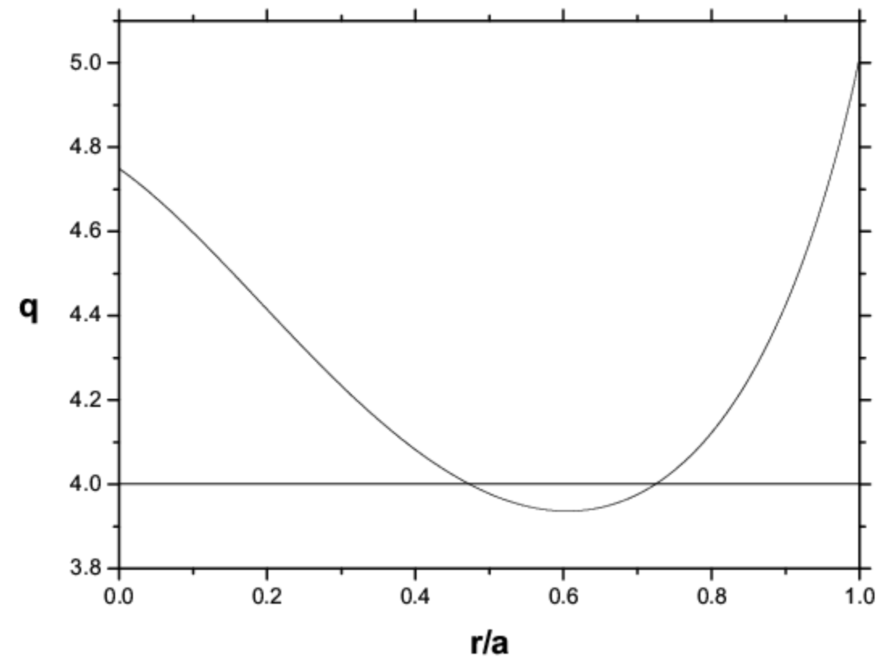


Safety factor x normalized
radial coordinate

# Tokamak with Chaotic Limiter (toroidal geometry)

$m/n = 4/1 \quad \beta = 3.00 \quad \gamma = 0.78$

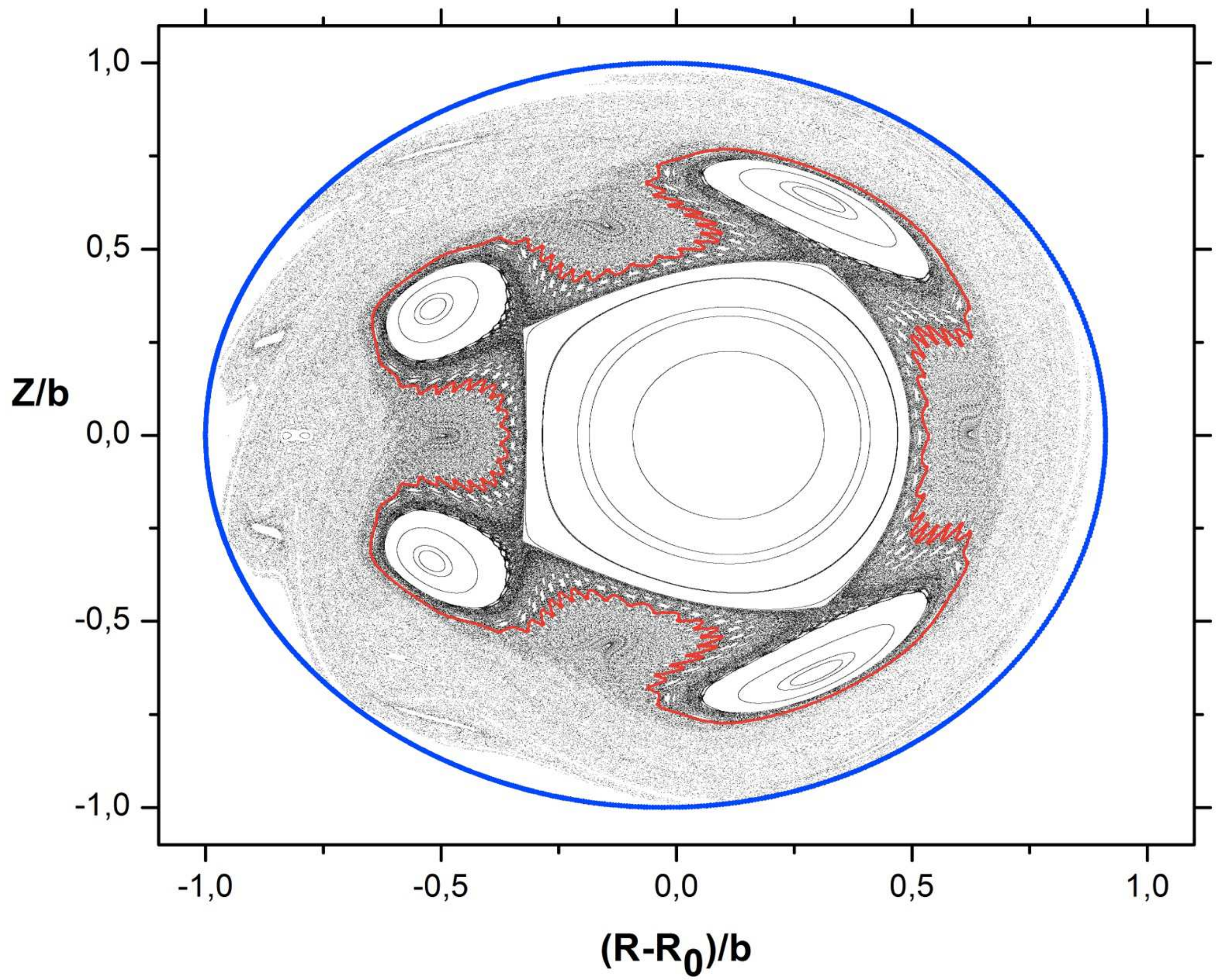


Kroetz et al.
PoP 2008

VOLUME 75, NUMBER 24 PHYSICAL REVIEW LETTERS 11 DECEMBER 1995

# Improved Confinement with Reversed Magnetic Shear in TFTR

F. M. Levinton,[1] M. C. Zarnstorff,[2] S. H. Batha,[1] M. Bell,[2] R. E. Bell,[2] R. V. Budny,[2] C. Bush,[3] Z. Chang,[2] E. Fredrickson,[2] A. Janos,[2] J. Manickam,[2] A. Ramsey,[2] S. A. Sabbagh,[4] G. L. Schmidt,[2] E. J. Synakowski,[2] and G. Taylor[2]

[1]*Fusion Physics and Technology, Torrance, California 90503*
[2]*Princeton Plasma Physics Laboratory, Princeton, New Jersey 08543*
[3]*Oak Ridge National Laboratory, Oak Ridge, Tennessee 37831*
[4]*Columbia University, New York, New York 10027*
(Received 23 May 1995)

Strait et al, PRL 1995

# A new tokamak confinement regime on TFTR
# Enhanced reverse shear confinement (Levinton, PRL 1995)

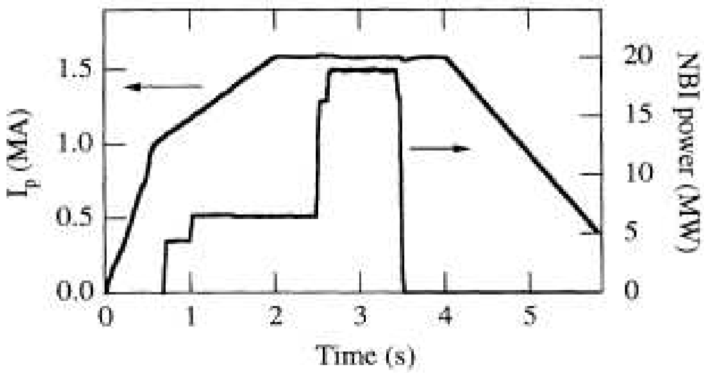


FIG. 1. The plasma current and neutral beam power evolution for a reversed shear startup.

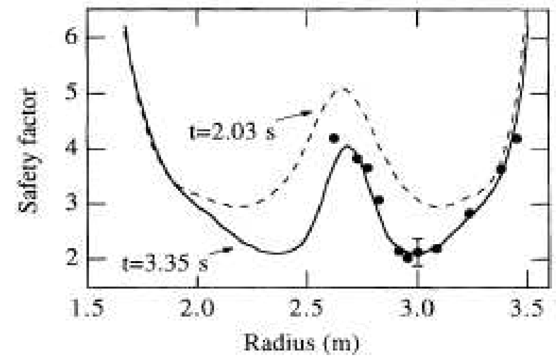


FIG. 2. The $q$ profiles at the beginning of the current flattop at $t = 2$ s (dashed line), and near the end of the heating phase at $t = 3.35$ s (solid line).

# Evidences of transport barriers

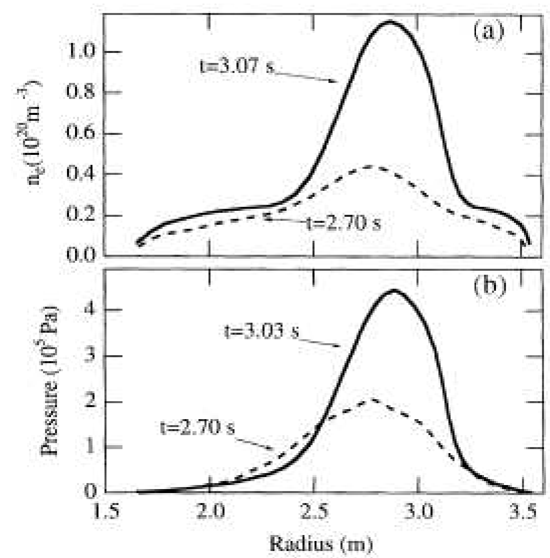


FIG. 3. The (a) density and (b) pressure profile before the transition to the ERS mode (dashed line) and at the time of peak density and pressure (solid line).

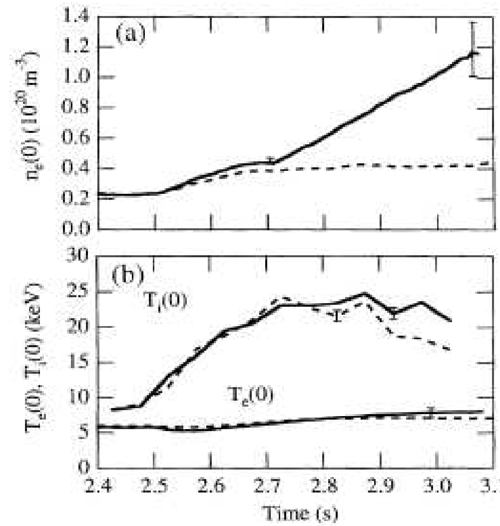


FIG. 4. The evolution of the electron density (a) and temperatures (b) at the magnetic axis for a discharge that makes a transition into the ERS mode at 2.715 s (solid line) and a similar reversed shear discharge at lower NBI power that does not (dashed line).

# MHD Equilibrium

Magnetic Surfaces

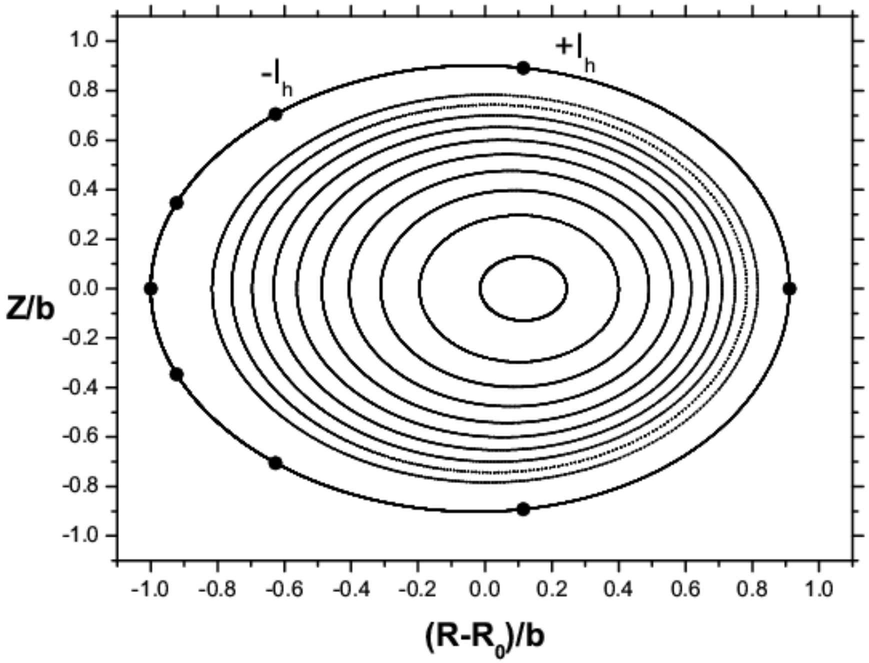


Normalized distances
in polar coordinates

Nonmonotonic Radial Profile

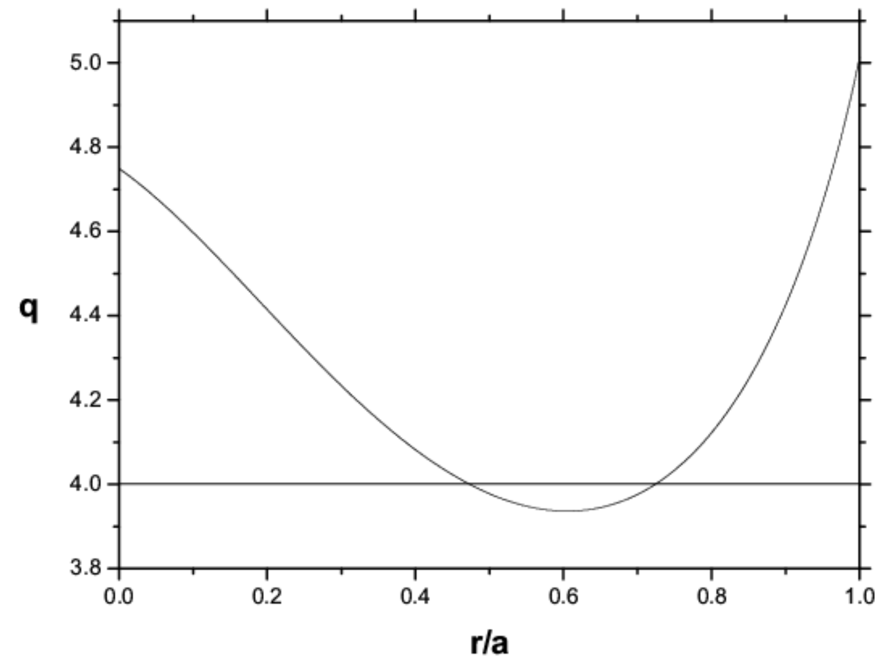


Safety factor x normalized
radial coordinate

# Chaotic Limiter to Improve Confinement
## Resonant perturbations on magnetic surfaces

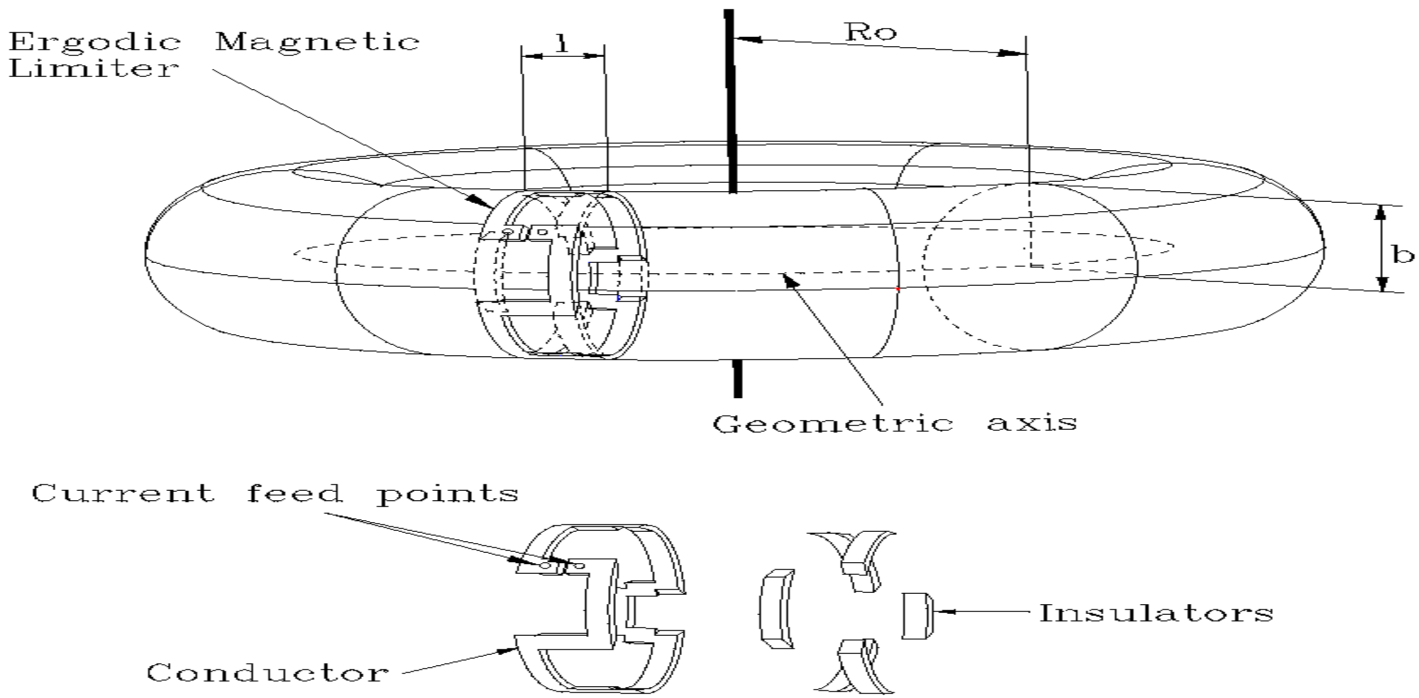


Dominant m/n resonant perturbation in toroidal geometry.
Control parameter: coil current $I_h$ .

Silva et al., IEEE Trans. Plasma Science (2001)

# Poincaré Surfaces

## m/n = 4/1 dominant mode

Laboratory coordinates

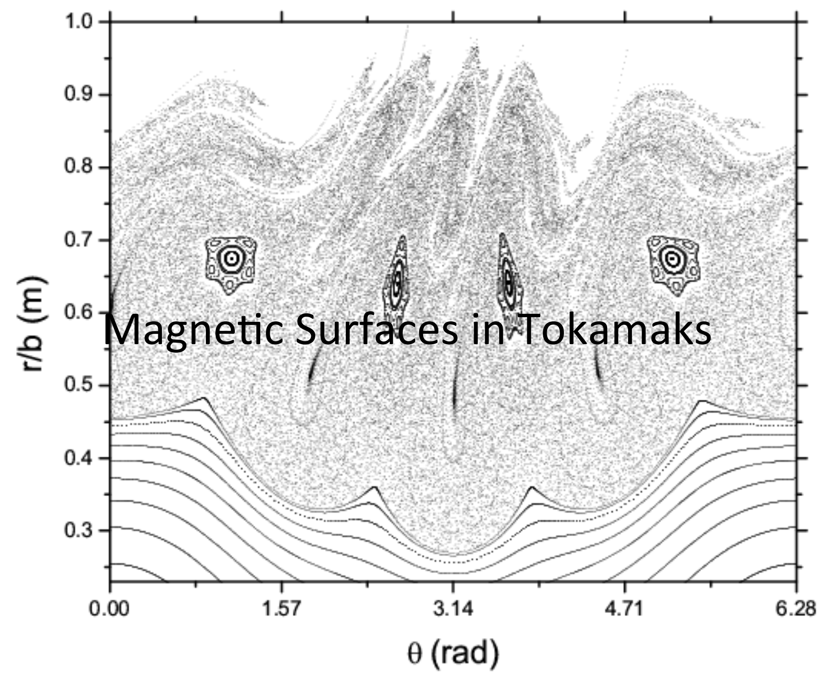


Magnetic Surfaces in Tokamaks

Plasma edge

Center

Normalized radius x poloidal angle

# Conection Lengths for Field Lines

4/1 mode

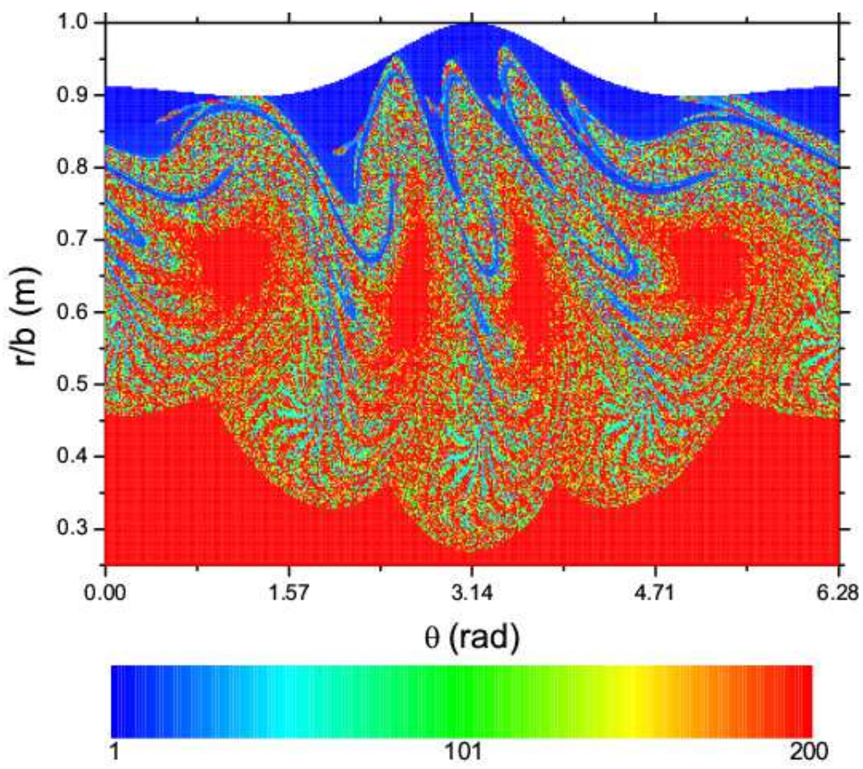


Normalized radius coordinate x poloidal angle

Scales in the range [1, 200]
(number of toroidal turns, for a line, from (r, θ) to the wall)

4/1 Mode

Stable and unstable manifolds

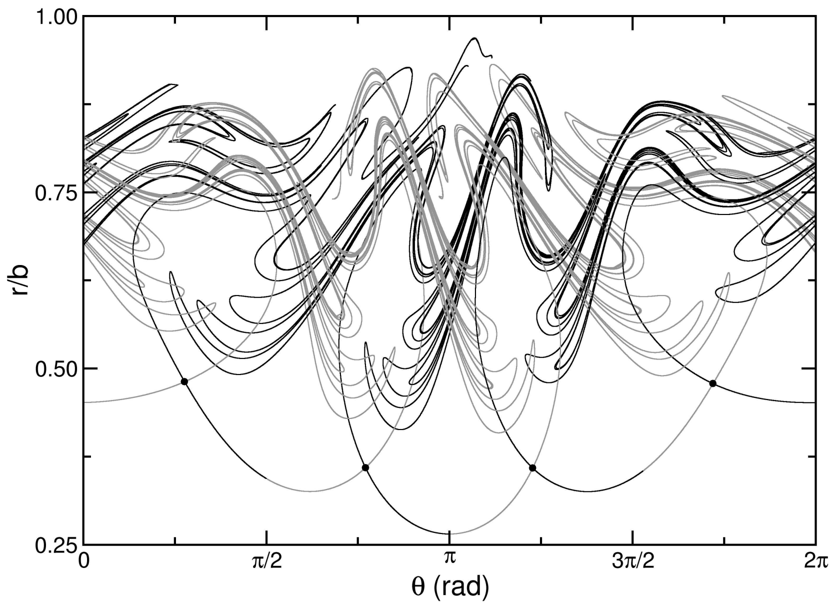


Heteroclinic tangle

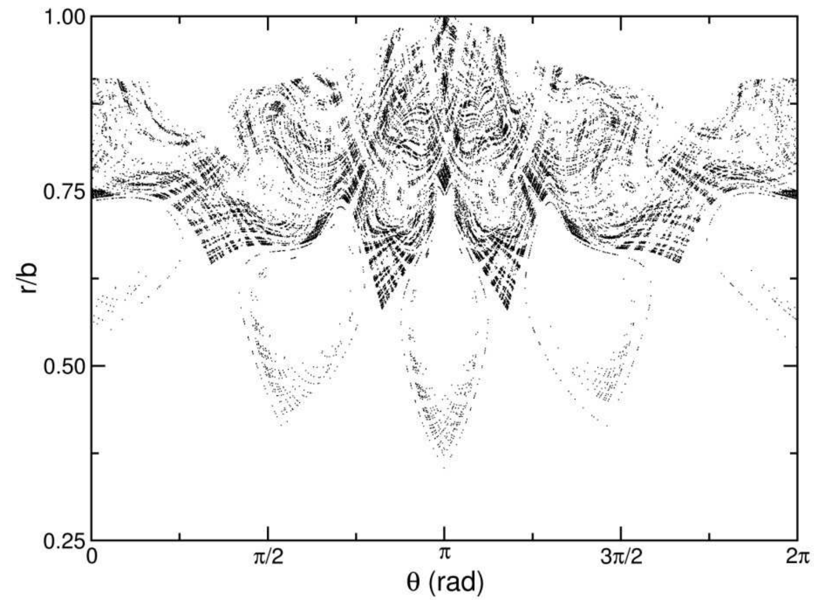


Normalized radius x poloidal angle

# Conection Lengths for Field Lines

4/1 mode

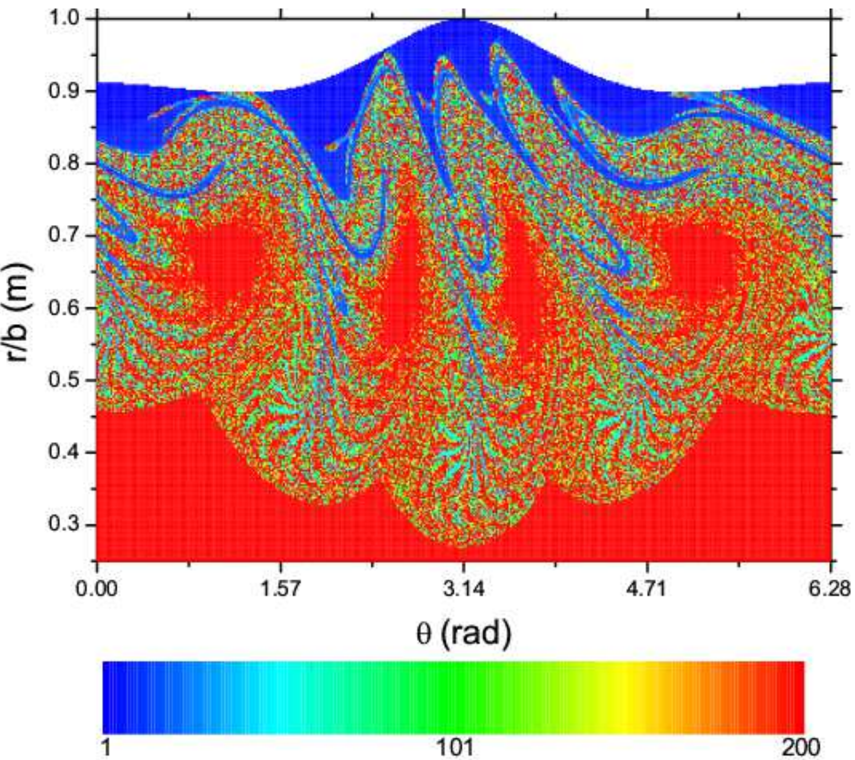


Heteroclinic tangle

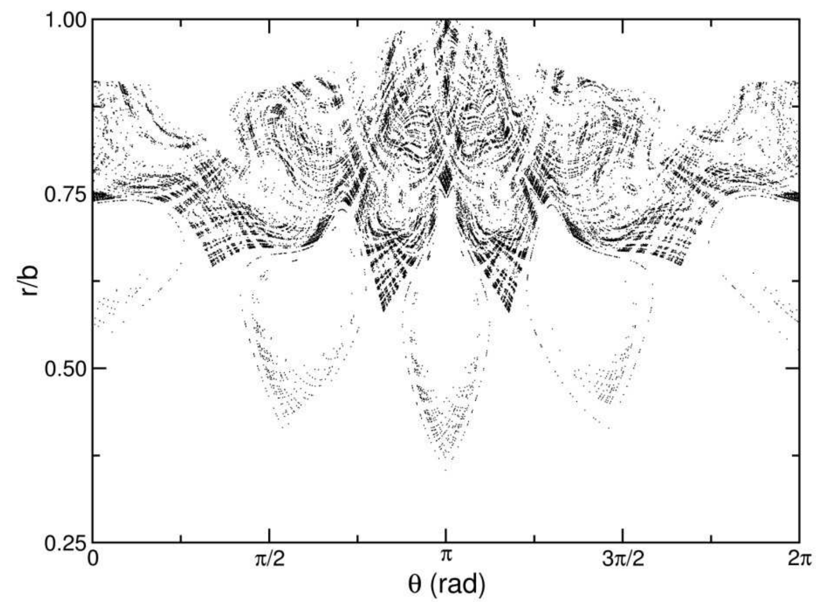


Normalized radiusxPoloidal angle

Normalized radius coordinate x poloidal angle

Scales in the range [1, 200]
(number of toroidal turns, for a line, from (r, θ)
to the wall)

Kroetz et al., Physics of Plasmas 2008

# Wings

Resonant character of field lines escape to the wall

4/1 mode

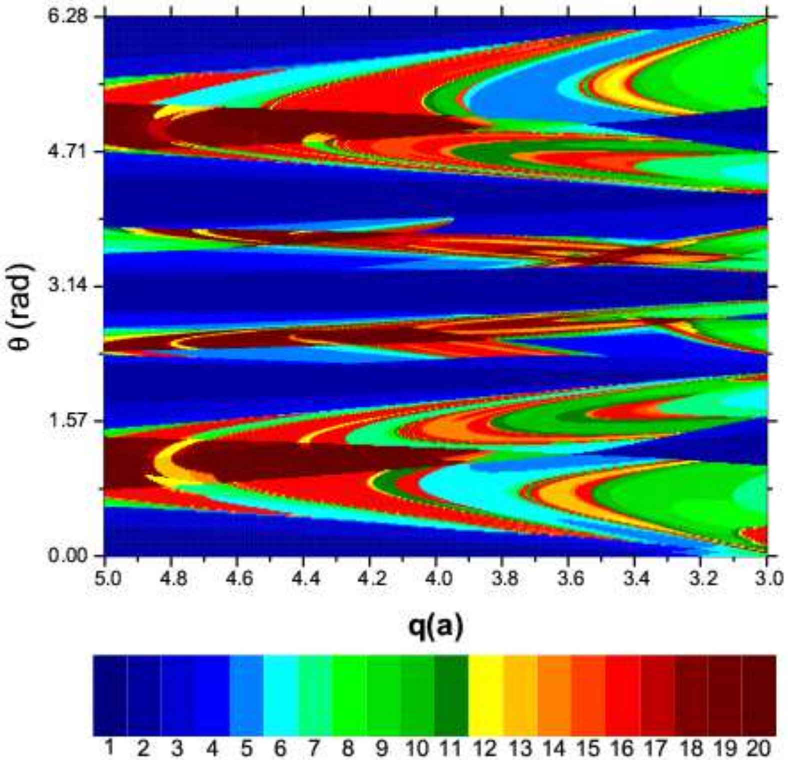


Blow Up of the Wings

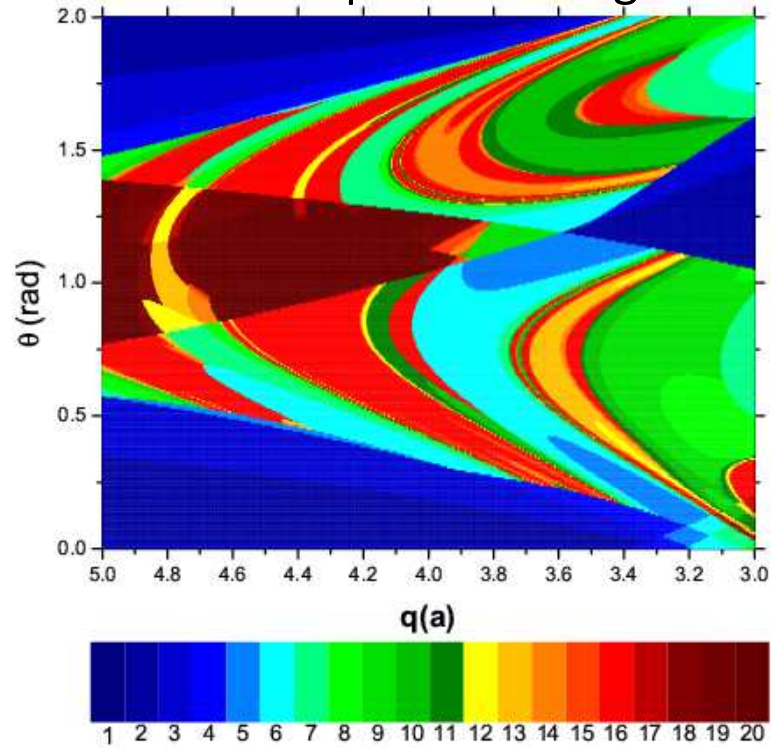


Escape lengths in the range [1, 20] at the wall

Poloidal angle at the wall x safety factor at the edge

# Conclusions

- Perturbed magnetic configuration described by ***maps***.
- Escape of field lines determined by homoclinic tangle.
- For some high amplitude resonances, magnetic lines with long correlation lengths reach the wall in concentrated footprints.

Available online at www.sciencedirect.com

ScienceDirect

Journal of Nuclear Materials 363–365 (2007) 371–376

journal of nuclear materials

www.elsevier.com/locate/jnucmat

# Observation of the heteroclinic tangles in the heat flux pattern of the ergodic divertor at TEXTOR

M.W. Jakubowski [a,*], A. Wingen [b], S.S. Abdullaev [a], K.H. Finken [a], M. Lehnen [a], K.H. Spatschek [b], R.C. Wolf [a], The TEXTOR Team

[a] Institut für Plasmaphysik, Forschungszentrum Juelich GmbH, Association EURATOM-FZJ, D-52425, Trilateral Euregio Cluster, 52425 Jülich, Germany

[b] Institut für Theoretische Physik I, Heinrich-Heine-Universität Düsseldorf, D-40225 Düsseldorf, Germany

# Temperature Distribution at Target Plates
# Experimental Evidences

Textor

Jakubowski
J. Nuclear
Materials
(2007)

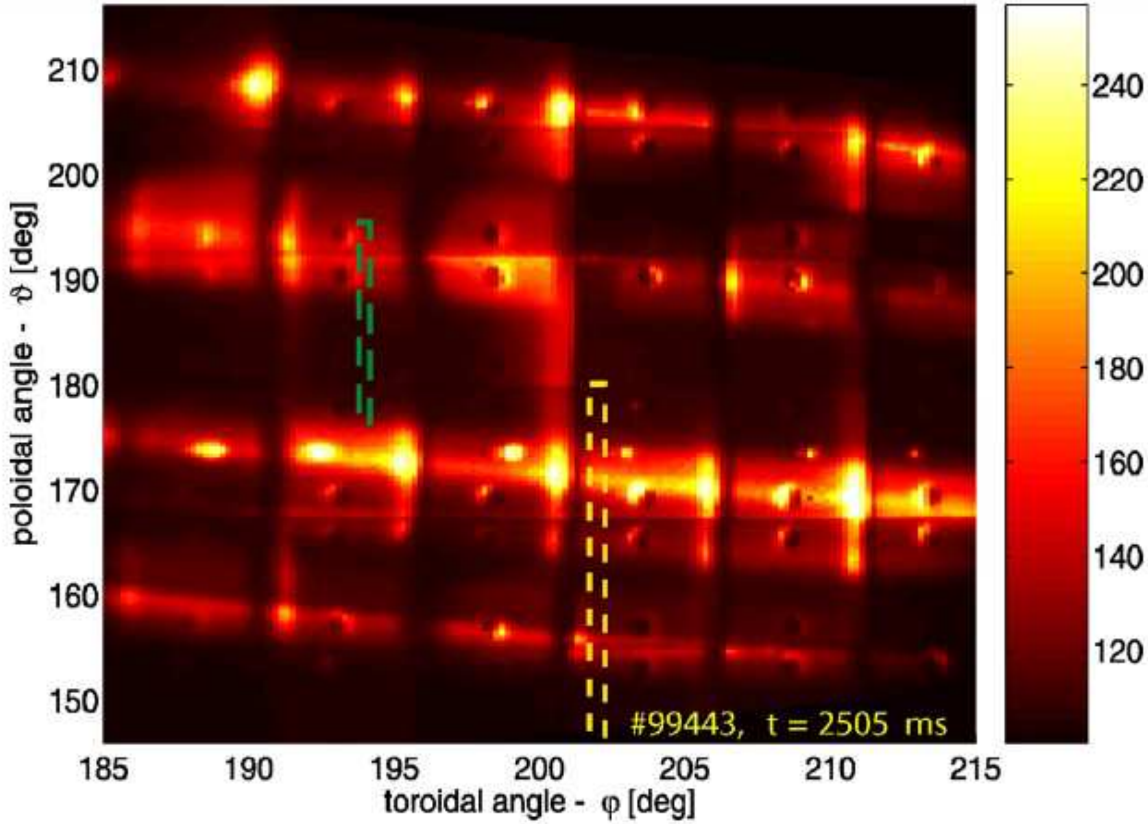


Celsius
centigrade

Fig. 1. The temperature distribution over the DED target plates in Celsius centigrade. The image of the curved and oblique surface is corrected with LEOPOLD [12], such that the tiles form a regular pattern. The yellow ($m/n = 6/2$) and green ($m/n = 12/4$) rectangles indicate the areas, where the heat flux density is evaluated with the THEODOR code.

These measurements give evaluation of heat flux

Textor

Jakubowski
J. Nuclear Materials
(2007)

# Resonant Character of Heat Flux

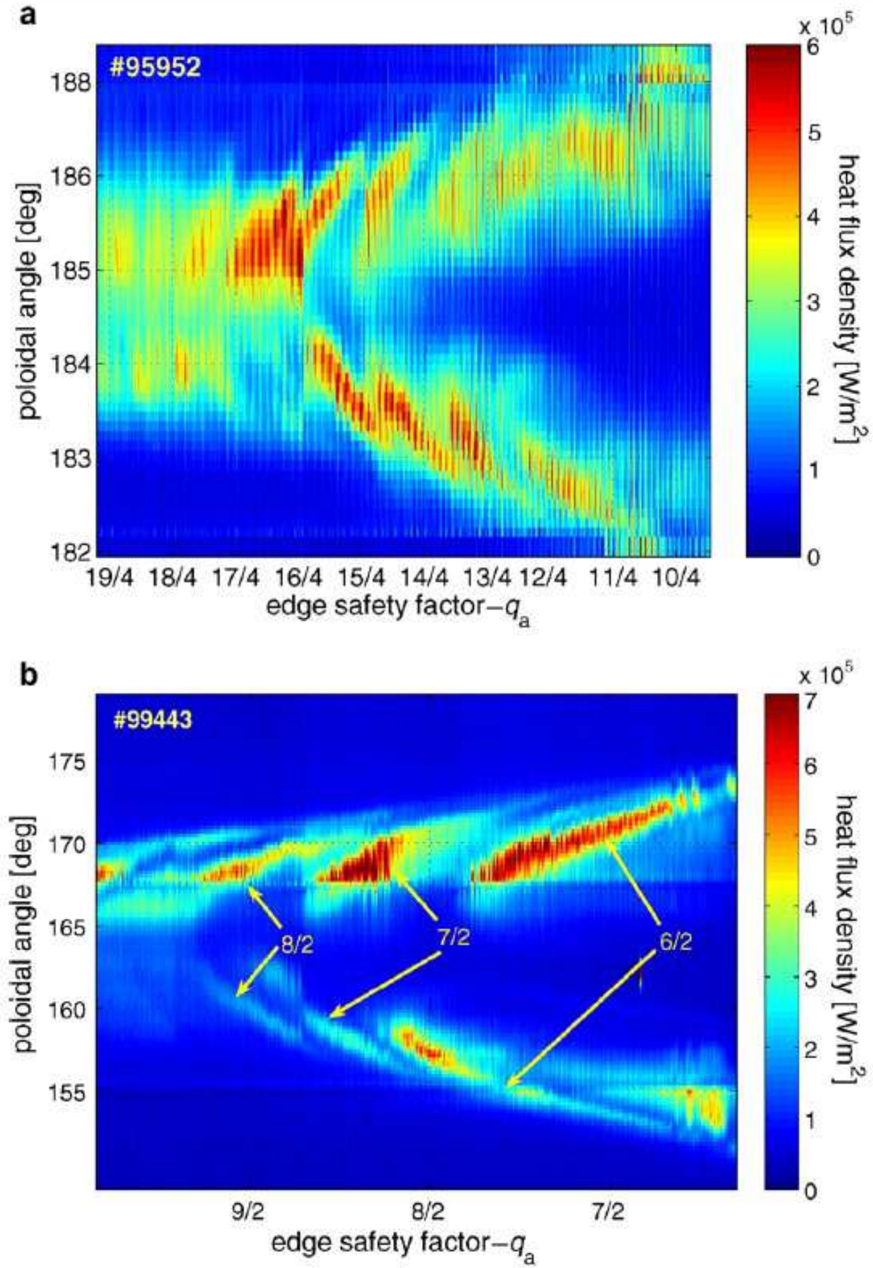


ig. 2. Heat flux to the divertor target plates as a function of the edge safety factor and the poloidal angle: (a) in the 12/4 mode; (b) in the

Evaluated Heat Flux to Target Plates

as a function of edge safety factor and poloidal angle at the wall

Blow up of the previous figure

# Ullman Map / Nontwist Symplectic Map

- Non integrable magnetic field line of tokamaks with reversed magnetic shear.
- Resonant perturbations created by an ergodic magnetic limiter.

Map with local behavior similar to the standard nontwist map.

Ulmann, Caldas, CSF 2000

Portela, Caldas, Viana, Morrison, IJBC 2007

Portela, Viana, Caldas, EPJ ST 2008

# Tokamak with Ergodic Limiter / Periodic Cylinder

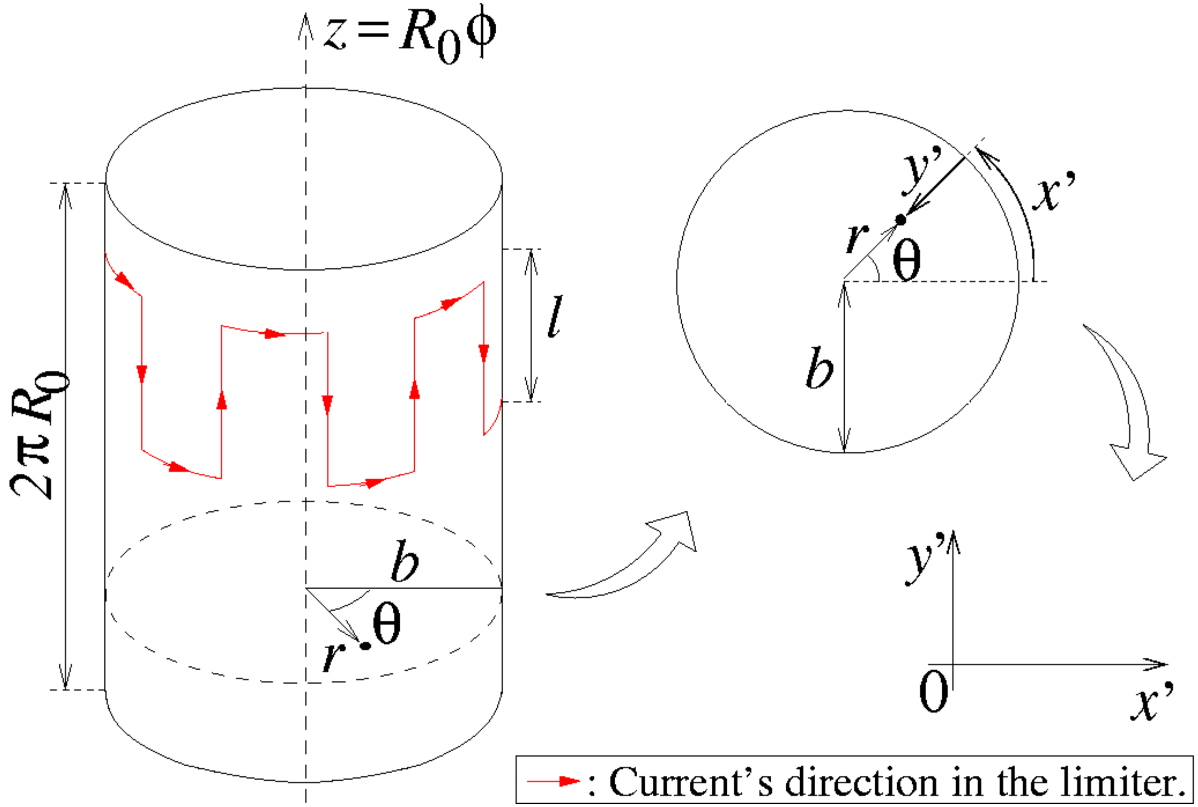


$$x' = b\theta$$

$$y' = b - r$$

Plasma current in z direction
Perturbing current in red

z (Rϕ): toroidal direction
θ: poloidal direction

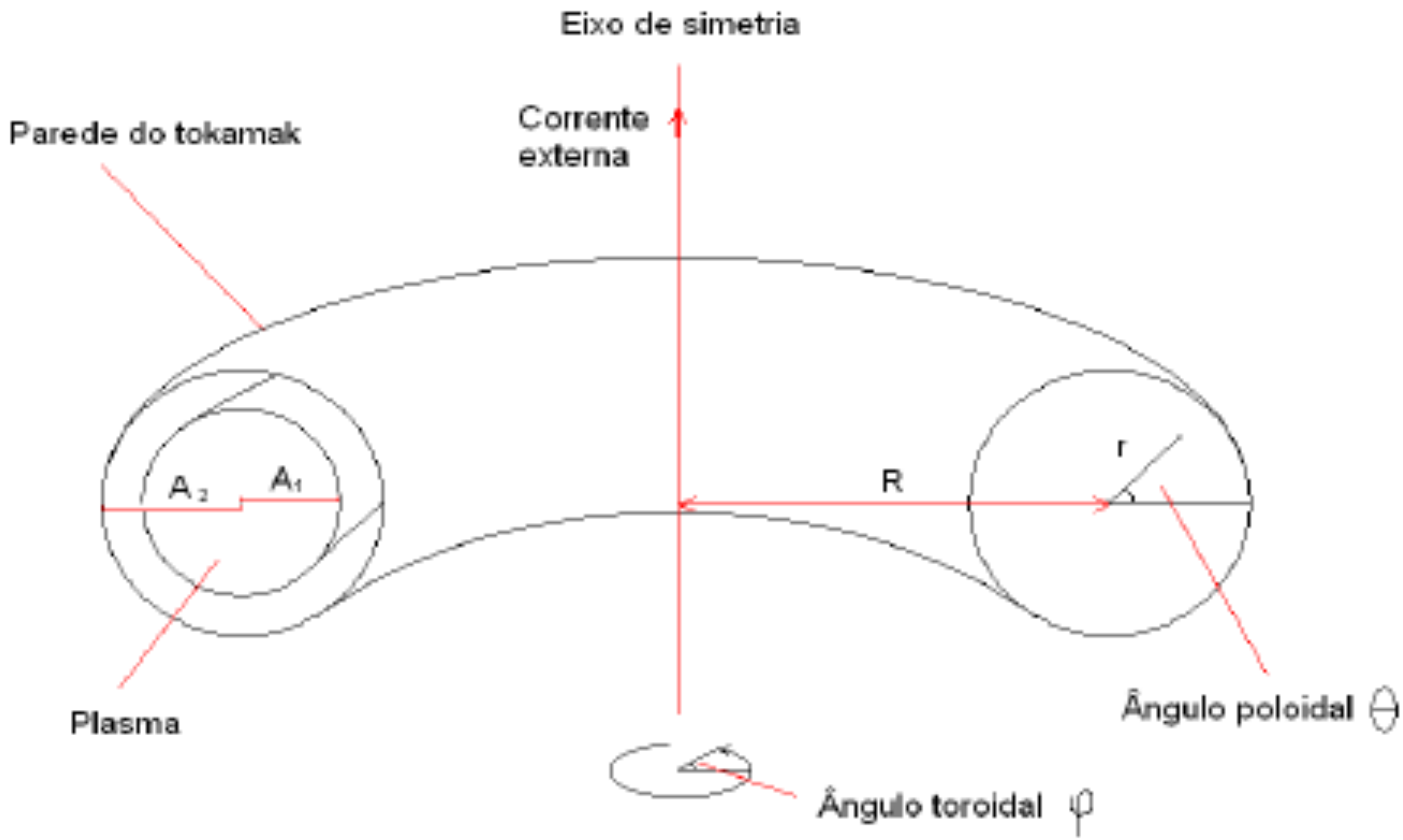


Correspondência com coordenadas da seção toroidal: x → $r$, y → $\theta$.

Safety factor profile used in this work.
Inset amplifies the reversed shear region.

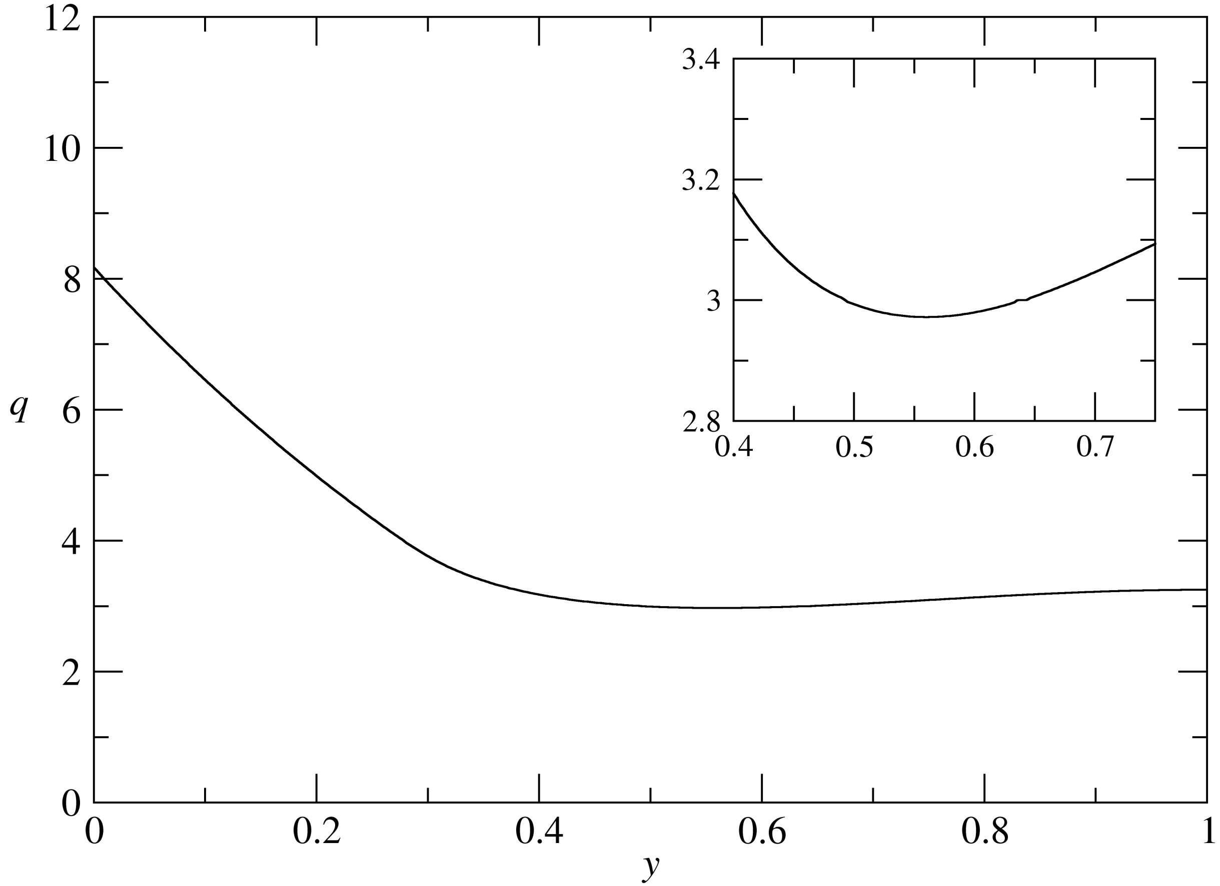

Equilibrium described by the map

$$r_{n+1} = \frac{r_n}{1 - a_1 \sin\theta_n} ,$$

$$\theta_{n+1} = \theta_n + \frac{2\pi}{q_{\mathrm{eq}}(r_{n+1})} + a_1 \cos\theta_n \mod 2\pi$$

# Perturbative map due to chaotic magnetic limiter:

$$r_n = r_{n+1} + \frac{mC\epsilon b}{m-1}\left(\frac{r_{n+1}}{b}\right)^{m-1}\sin(m\theta_n)\ ,$$

$$\theta_{n+1} = \theta_n - C\epsilon\left(\frac{r_{n+1}}{b}\right)^{m-2}\cos(m\theta_n)\ ,$$

where $C = (2mla^2 I_l)/(R_0 q_a b^2 I_p)$ represents the perturbation strength

# Addition of Randon Noise in the Ullman Map
*Shearless barriers are robust*

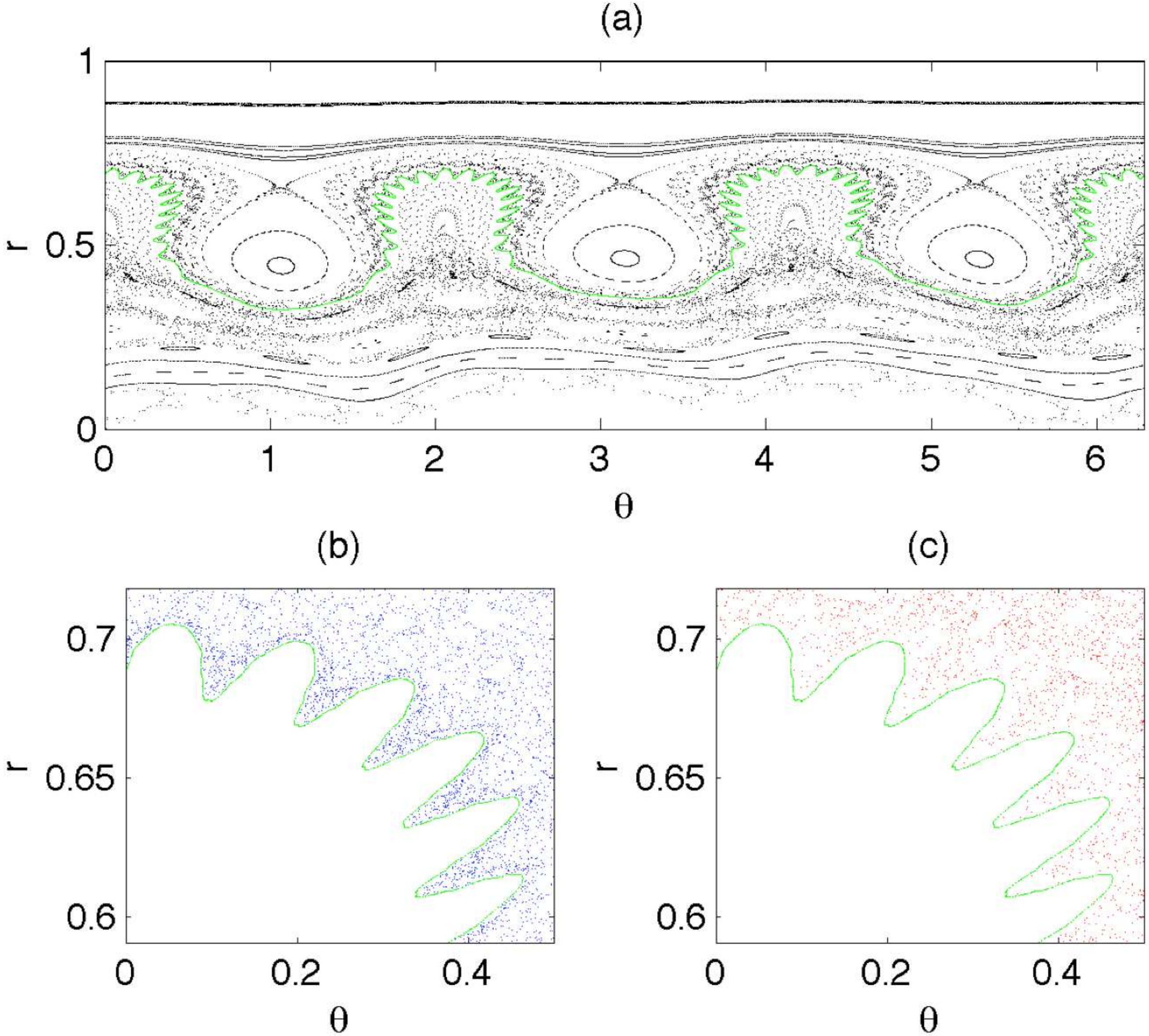


Map
*(No noise)*

Without noise

With noise

# Reconection

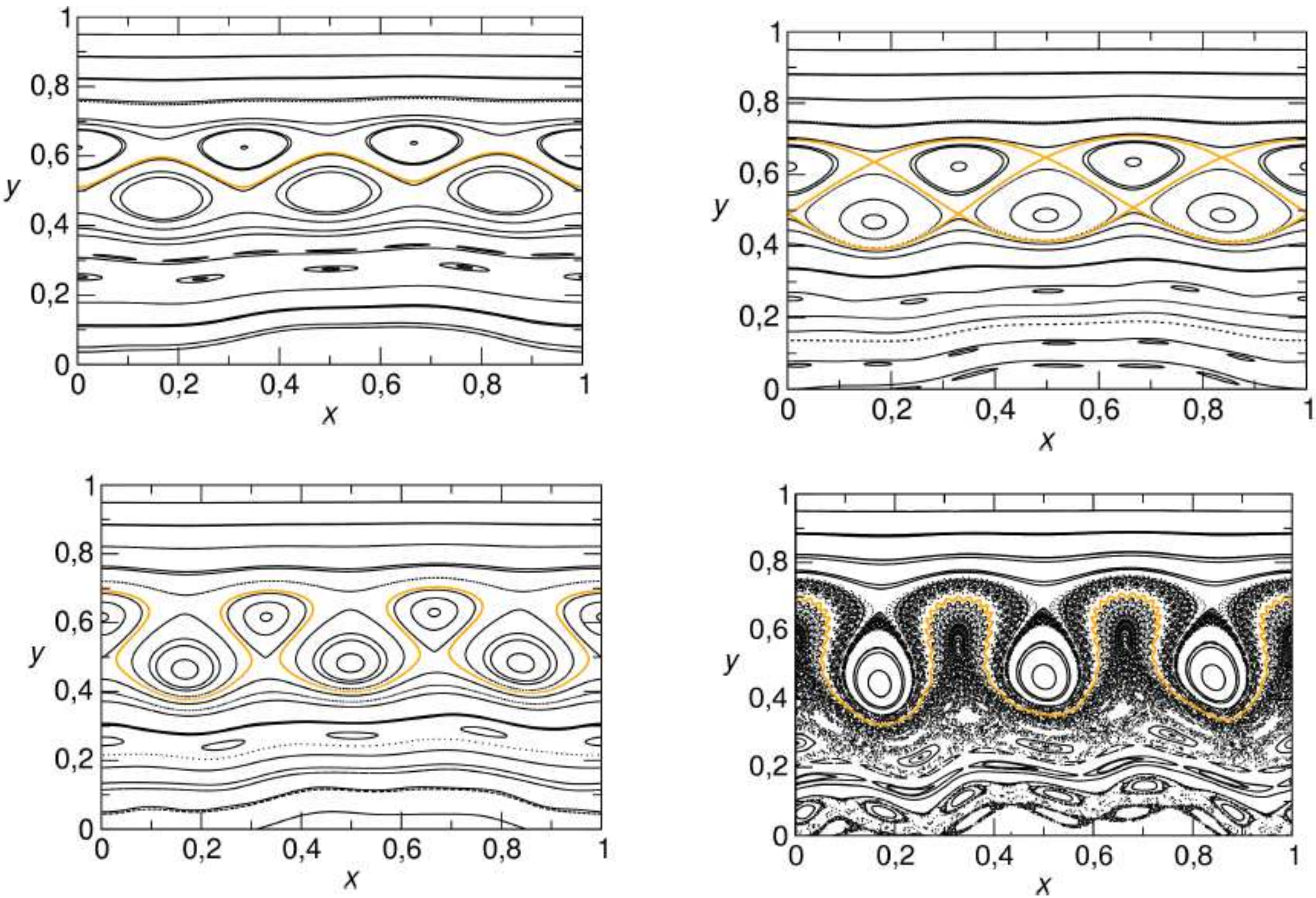

# Shearlees Barrier Break Up

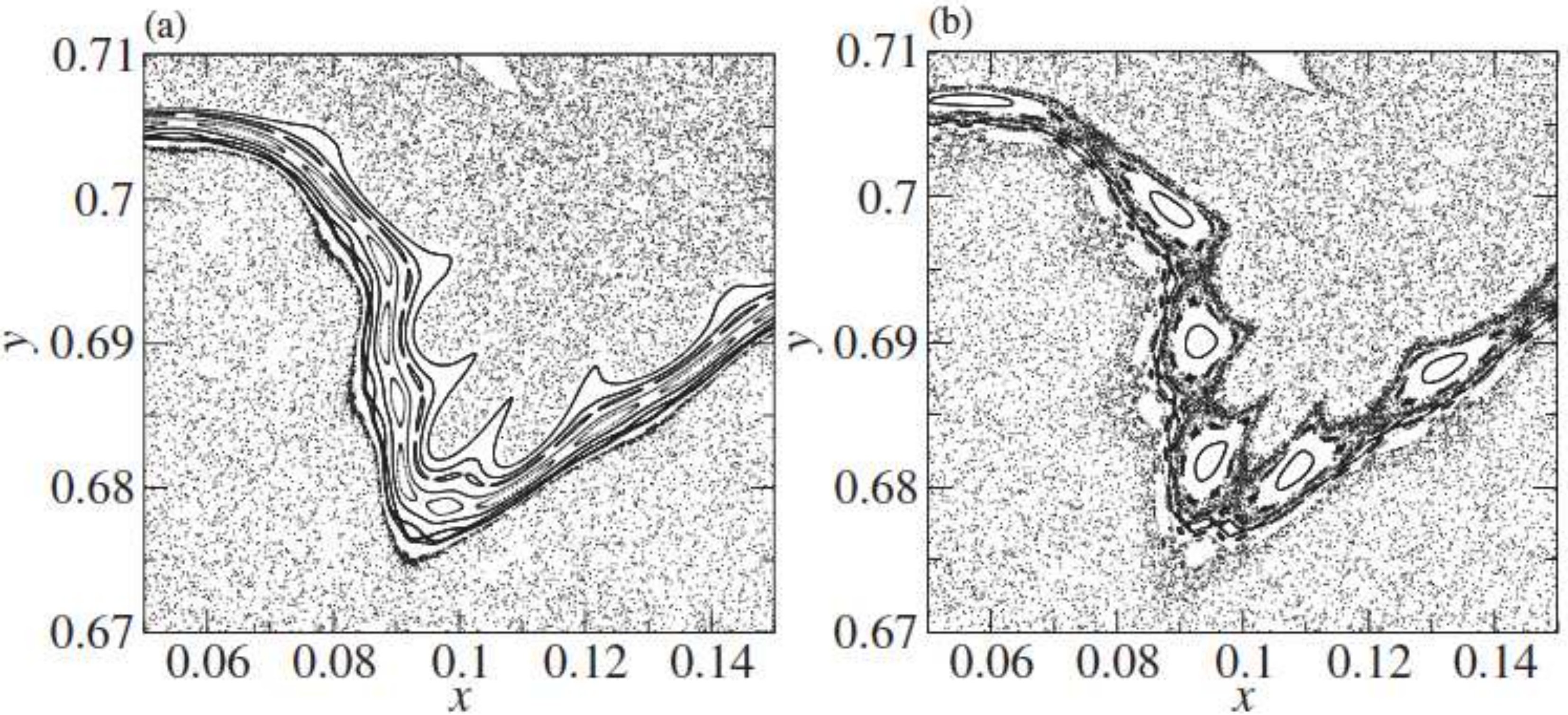


Zoom near the barrier for the non-twist Ullmann map for (a) $\epsilon = 0.3029$ and (b) $\epsilon = 0.3031$.

Shearless Bifurcation in the Twist Ullmann Map
Shearless barriers may also appear in twist maps!

Map

Zoom

Local frequency profile

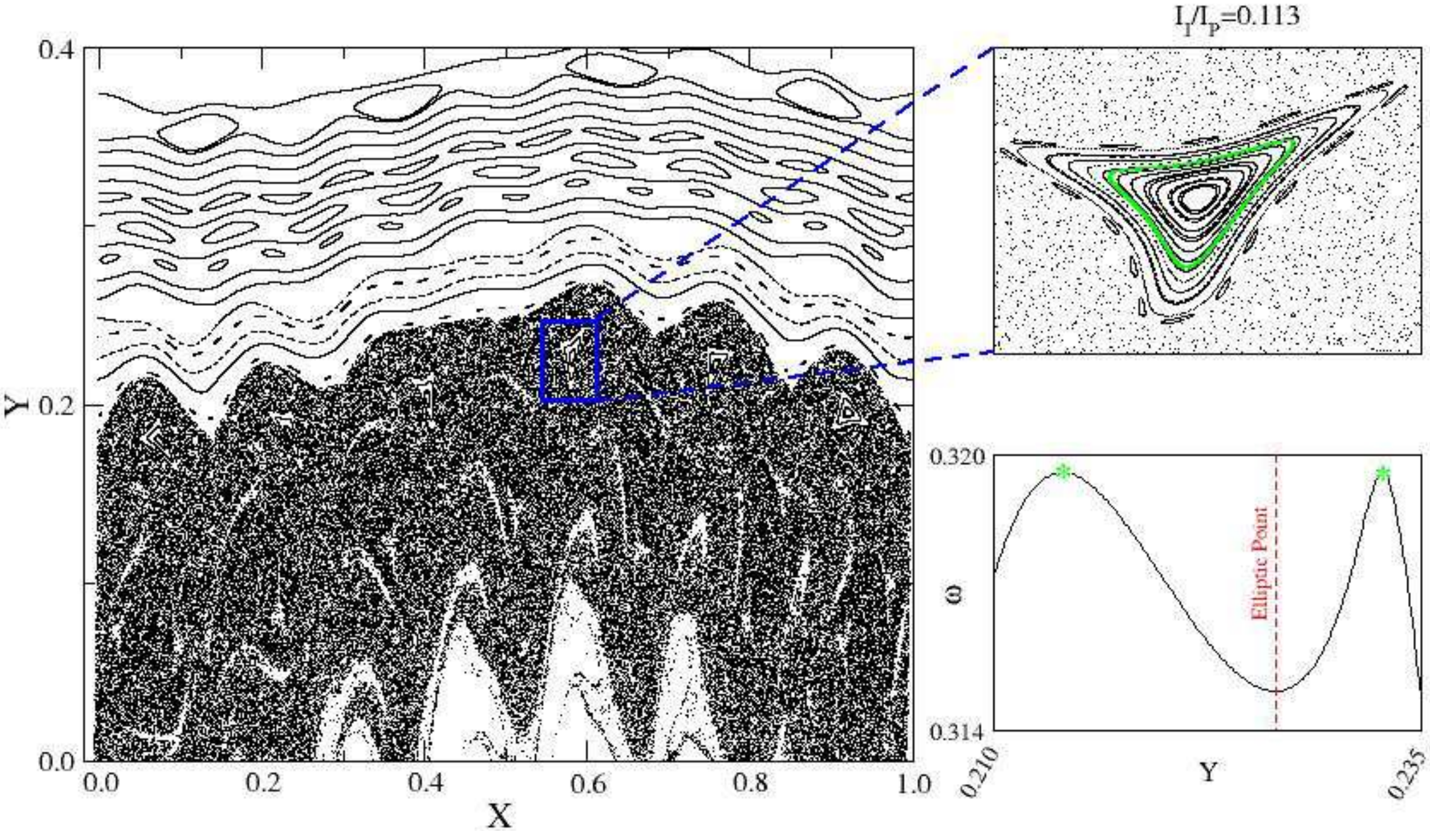

# Example in Tokamaks

## A symplectic mapping for the ergodic magnetic limiter

K. Ullmann, I.L. Caldas, CSF, 11 (2010)

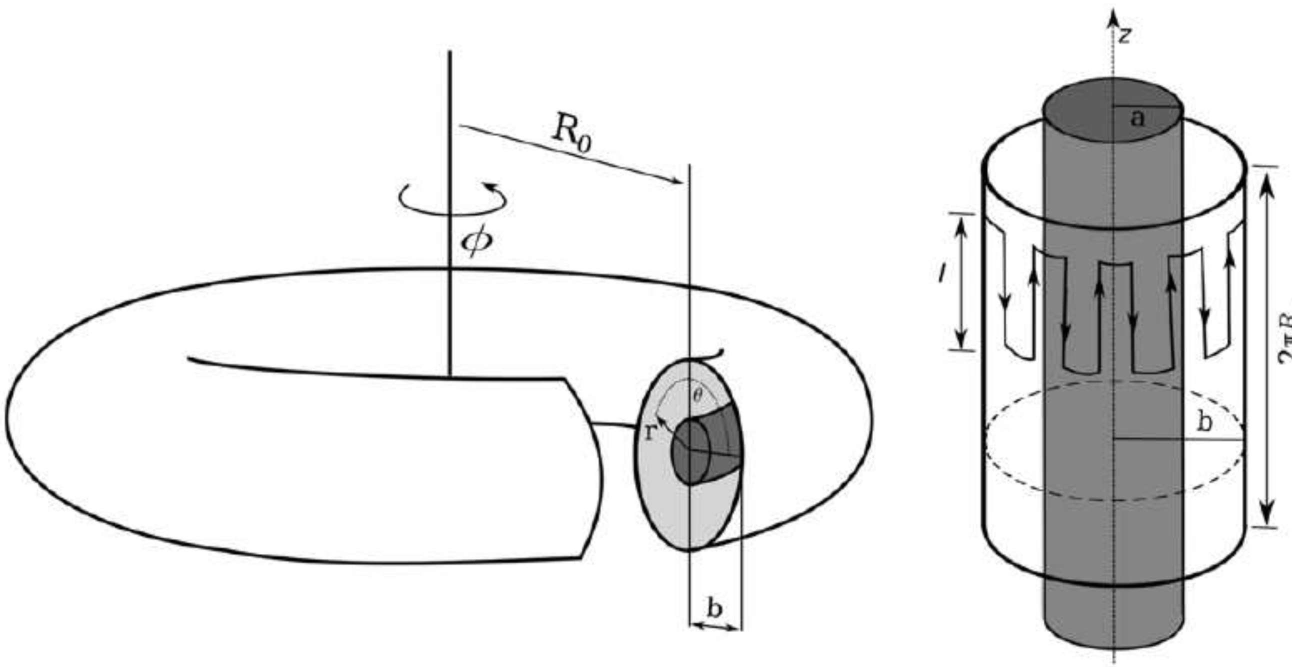


**Figure 1.** Tokamak scheme showing the main coordinate systems (left) and the $2\pi\,R_0$-periodic cylindrical approximation (right) where $l$ is the length of the wires of the EML.

# Ullmann Map

Ullmann, Caldas, CSF 11, 2000

$$F_1: \begin{cases} r_{n+1} = \dfrac{r_n}{1 - a_1 \sin\theta}, \\ \theta_{n+1} = \theta_n + \dfrac{2\pi}{q_{\mathrm{eq}}(r_{n+1})} + a_1 \cos\theta_n, \end{cases}$$

Equilibrium
Large aspect-ratio
$a_1$: toroidal correction

$$F_2: \begin{cases} r_{n+1} = r^*_{n+1} + \dfrac{mC\epsilon b}{m-1}\left(\dfrac{r^*_{n+1}}{b}\right)^{m-1} \sin(m\theta_{n+1}), \\ \theta^*_{n+1} = \theta_{n+1} - C\epsilon\left(\dfrac{r_{n+1}}{b}\right)^{m-2} \cos(m\theta_{n+1}), \end{cases}$$

Chaotic limiter
Control parameter $C \approx I/q_a$

I: limiter current
qa: safety factor at edge

# Onset of shearless magnetic surfaces in tokamaks

C. V. Abud, I.L. Caldas, Nucl. Fusion 54 (2014)

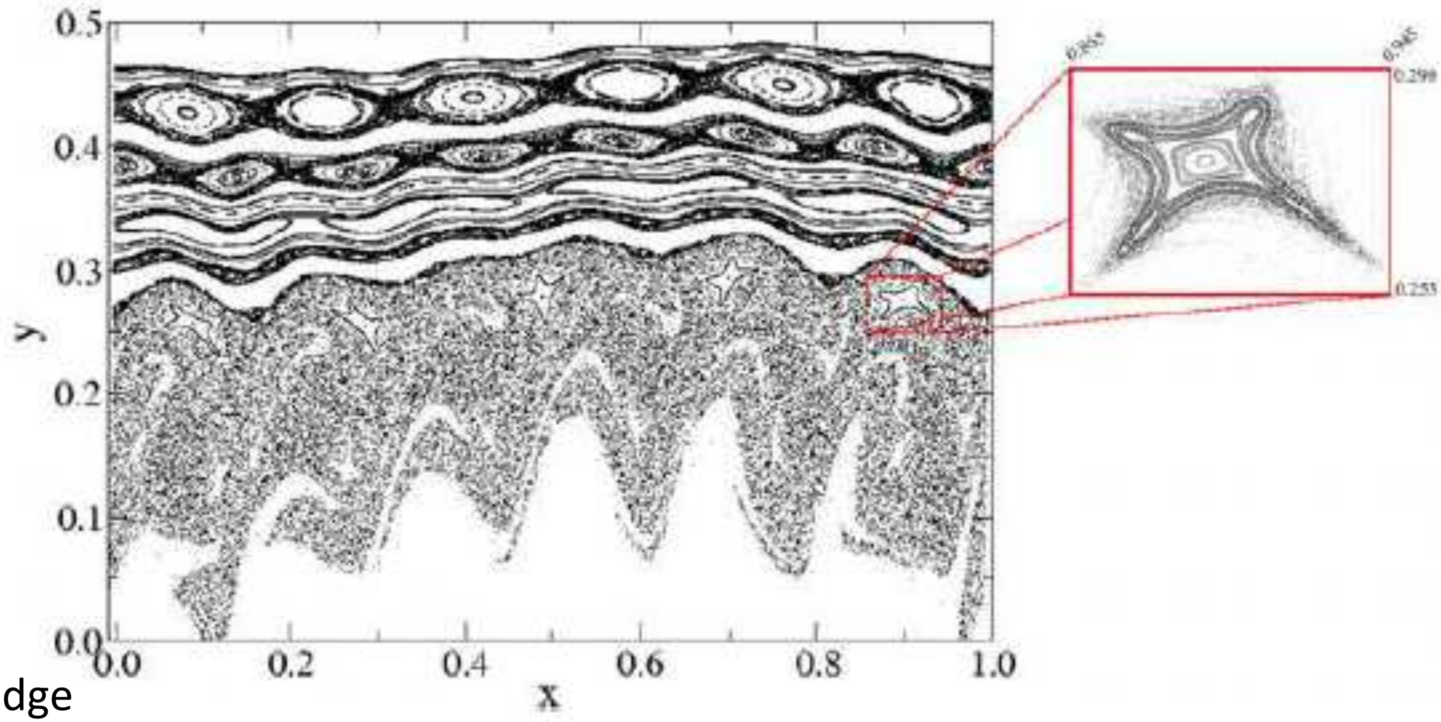


y = 0
plasma edge

**Figure 4.** Phase space of the Ullmann map with $\epsilon = 0.189$ and $m = 6$. The red box emphasizes the quadrupling bifurcation.

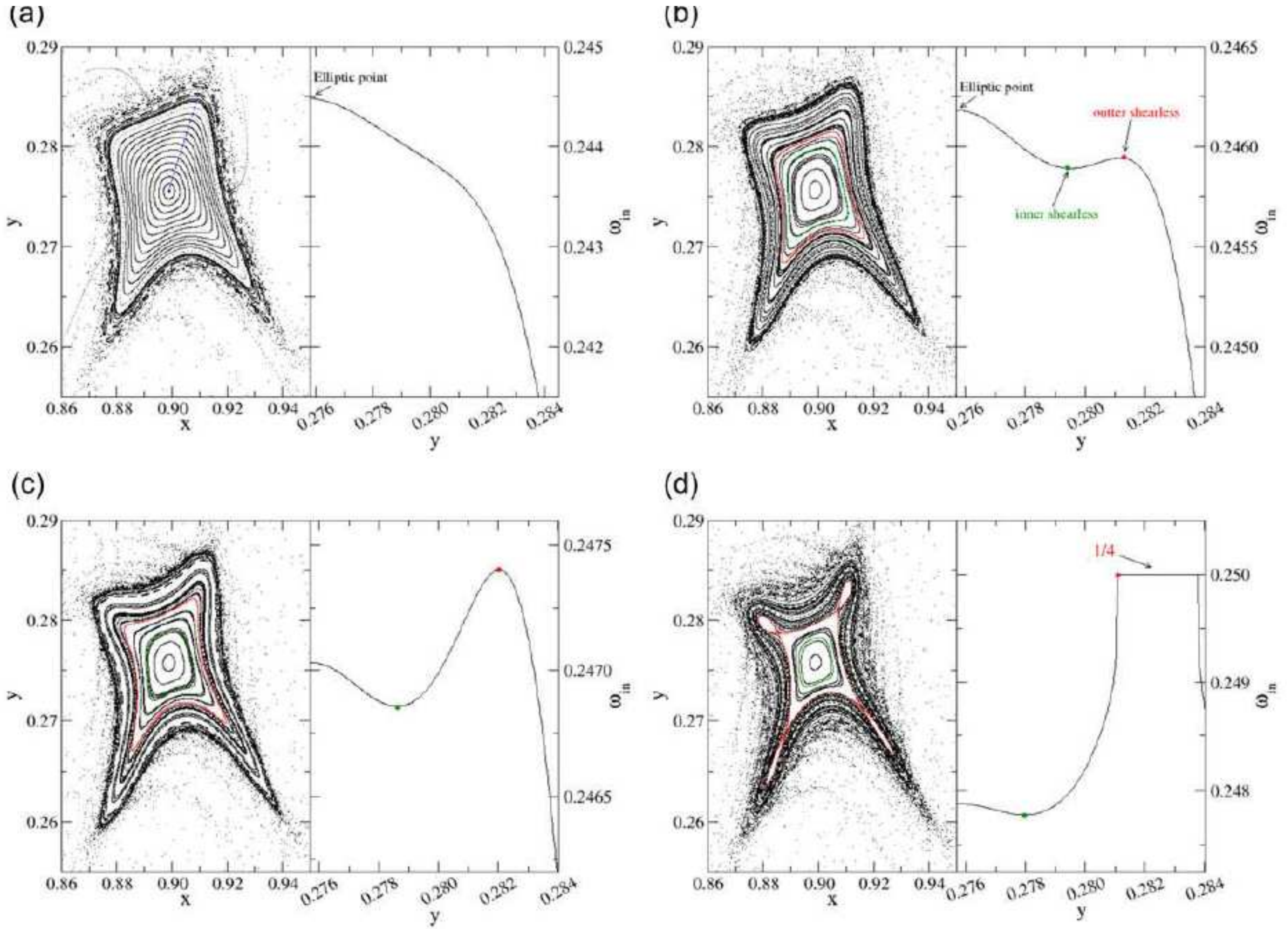


**Figure 5.** The quadrupling bifurcation in the Ullmann map. ($a$) $\epsilon = 0.185$; ($b$) $\epsilon = 0.187$; ($c$) $\epsilon = 0.188$ and ($d$) $\epsilon = 0.189$. Note
onset of two s-shearless tori arose for some value of $\epsilon$ between ($a$) and ($b$).

# Conclusion

Shearless invariant curves can also be created by changing the control parameters.

# III – Particle Transport in Tokamaks

Model

W. Horton, P. Hyoung-Bin, K. Jae-Min, D. Strozzi, P. J. Morrison, and C. Duk-In. Drift wave test particle transport in reversed shear profile. *Physics of Plasmas*, 5(11):3910–3917, 1998.

Results

Rosalem et al. NF (2014), PoP (2016),

Marcus et al. submitted to PoP

# Summary

Drift Wave Transport Model

Modeling E, B and v Profiles

Resonant modes

Rotation Number and Shearless Barrier

Effect of non resonant mode

Change on Electric field and resonant modes

Some remarks

# Large Aspect Ratio Tokamak, R/r >> 1

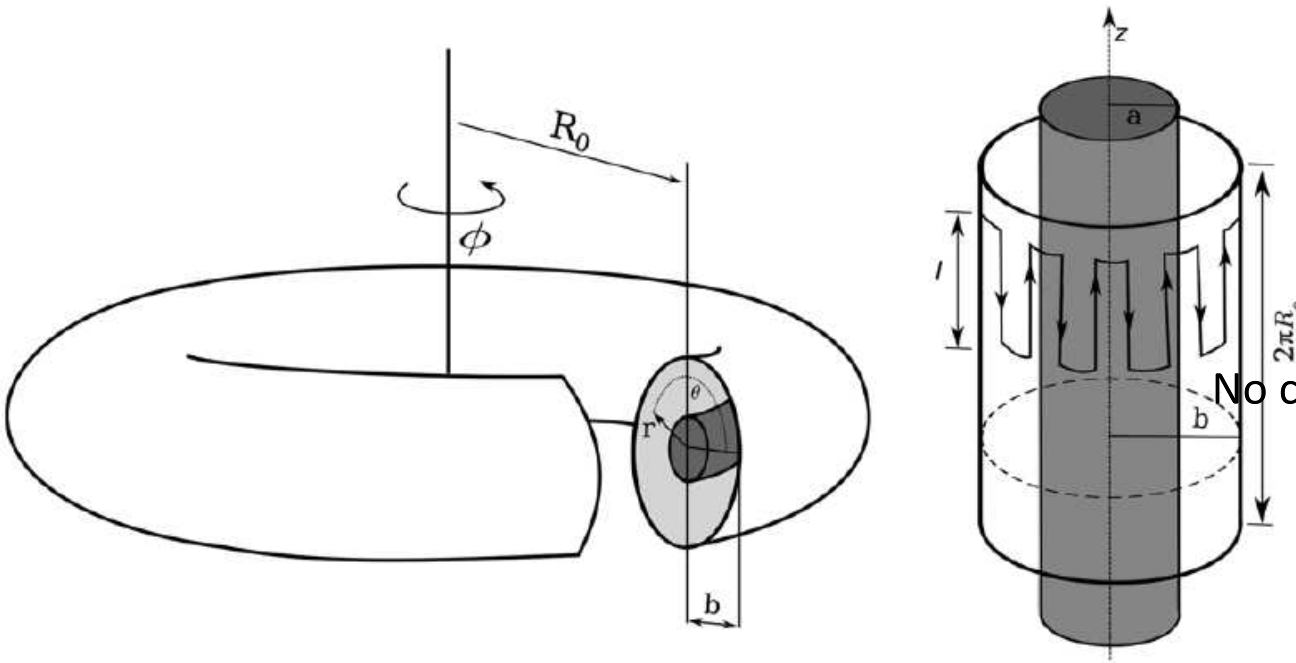


No chaotic limiter

Coordinates: r, θ $\qquad I = (r/a)^2$ and $\Psi = (M\vartheta - L\varphi)$.

Action, helical angle

# Drift Wave Transport Model

Horton, PoP 1998

## Guiding-center equation of motion

$$\frac{d\mathbf{x}}{dt} = v_\parallel \frac{\mathbf{B}}{B} + \frac{\mathbf{E}\times\mathbf{B}}{B^2}$$

$$\begin{cases} \dfrac{dr}{dt} = -\dfrac{1}{rB}\dfrac{\partial\tilde{\phi}}{\partial\theta} \\ \dfrac{d\theta}{dt} = \dfrac{v_\parallel}{r}\dfrac{B_\theta}{B} + \dfrac{1}{rB}\dfrac{\partial\tilde{\phi}}{\partial r} - \dfrac{E_r}{rB} \\ \dfrac{d\varphi}{dt} = \dfrac{v_\parallel}{R} \end{cases}$$

where $\mathbf{x} = (r, \theta, \varphi)$ is written in local polar coordinates standing $r$ as the radial position, $\theta$ and $\varphi$ as poloidal and toroidal angles, $R$ is the major plasma radius, $v_\parallel$ is the toroidal velocity of the guiding centers and $E_r$ (r) is the radial electric field profile in equilibrium.

### Fluctuating electrostatic potential

$$\tilde{\phi}(\mathbf{r}, t) = \sum_{L,M,n} \phi_{LMn} \cos(M\theta - L\varphi - n\omega_0 t)$$

Spatial electrostatic modes $L$ and $M$ are respectively poloidal and toroidal and assumed to be constant.

# Action-angle coordinates $(I, \psi)$

$$I \equiv (r/a)^2$$

$$\psi_{LM} \equiv M\theta - L\varphi$$

$$\begin{cases} \dfrac{dr}{dt} = -\dfrac{1}{rB}\dfrac{\partial\tilde{\phi}}{\partial\theta} \\ \dfrac{d\theta}{dt} = \dfrac{v_\parallel}{r}\dfrac{B_\theta}{B} + \dfrac{1}{rB}\dfrac{\partial\tilde{\phi}}{\partial r} - \dfrac{E_r}{rB} \\ \dfrac{d\varphi}{dt} = \dfrac{v_\parallel}{R} \end{cases}$$

$$\tilde{\phi}(\mathbf{r}, t) = \sum_{L,M,n} \phi_{LMn} \cos(M\theta - L\varphi - n\omega_0 t)$$

$$\boxed{\begin{aligned} \frac{dI}{dt} &= 2M \sum \phi_n \sin(\psi - n\omega_0 t) \\ \frac{d\psi}{dt} &= \frac{v_\parallel(I)}{R}\frac{1}{q(I)}[M - Lq(I)] - \frac{M}{\sqrt{I}}E_r(I) \end{aligned}}$$

# Resonant modes

Resonance conditions: Islands in Poincaré maps

$$\begin{aligned}\frac{dI}{dt} &= 2M\sum \phi_n \sin(\psi - n\omega_0 t)\\ \frac{d\psi}{dt} &= \frac{v_\parallel(I)}{R}\frac{1}{q(I)}[M - Lq(I)] - \frac{M}{\sqrt{I}}E_r(I)\end{aligned}$$

Time invariance of the action variable *I*

$$\frac{d}{dt}(\psi - n\omega_0 t) = 0 \rightarrow \frac{d\psi}{dt} = n\omega_0$$

$$\boxed{n\omega_0 = \frac{v_\parallel(r)}{R}\frac{1}{q(I)}[M - Lq(I)] - \frac{M}{\sqrt{I}}E_r(I)}$$

# Resonant modes

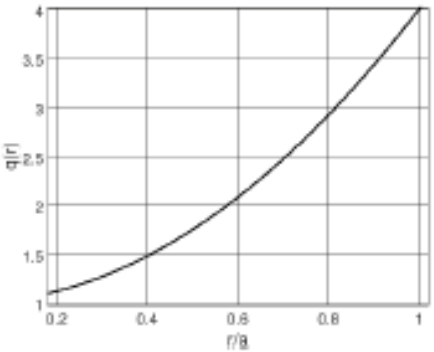


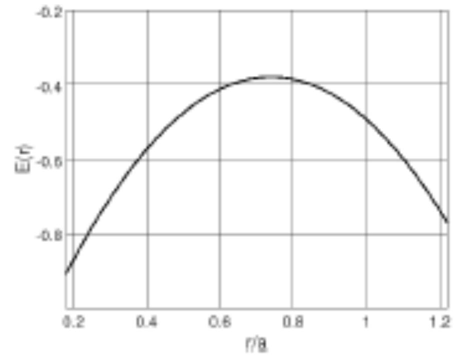


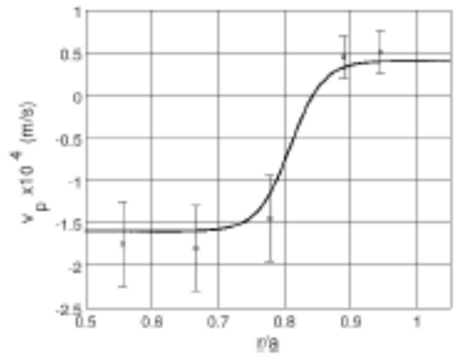


$$n\omega_0 \quad = \quad \frac{v_\parallel(r)}{R}\frac{1}{q(I)}[M - Lq(I)] - \frac{M}{\sqrt{I}}E_r(I)$$

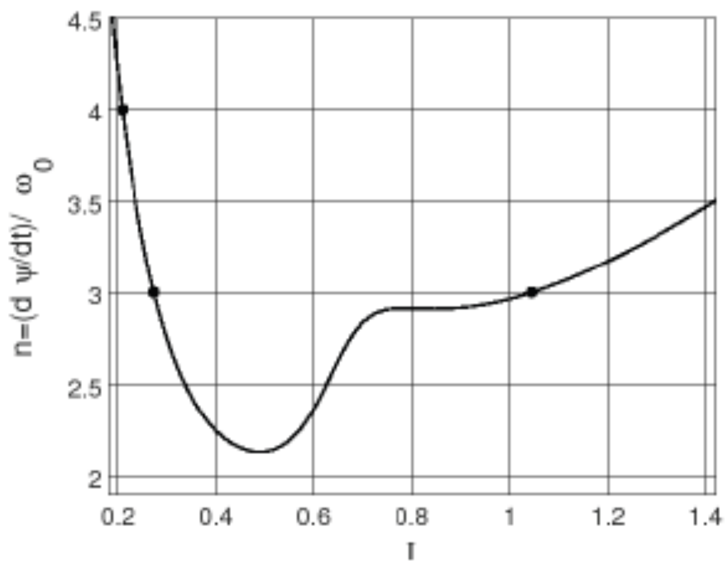

# Resonant modes

$$n\omega_0 = \frac{v_\parallel(r)}{R}\frac{1}{q(I)}[M - Lq(I)] - \frac{M}{\sqrt{I}}E_r(I)$$

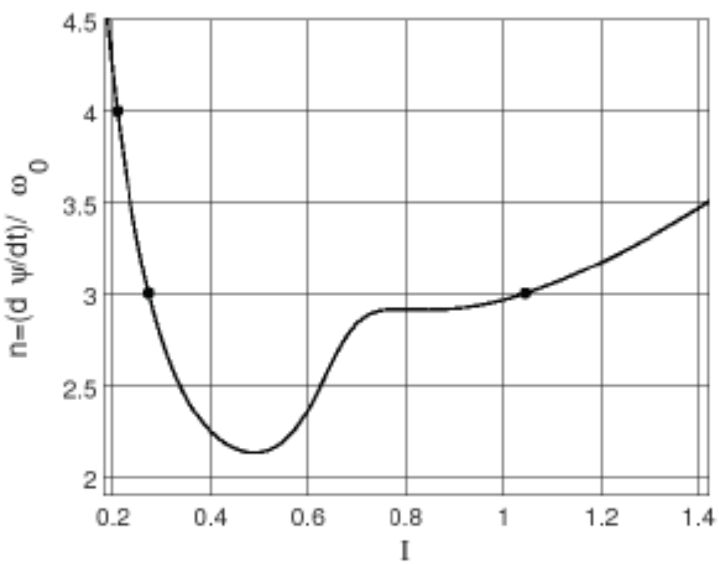


$n = (2, 3, 4) \to \phi_n = (0, 0.85, 0)$

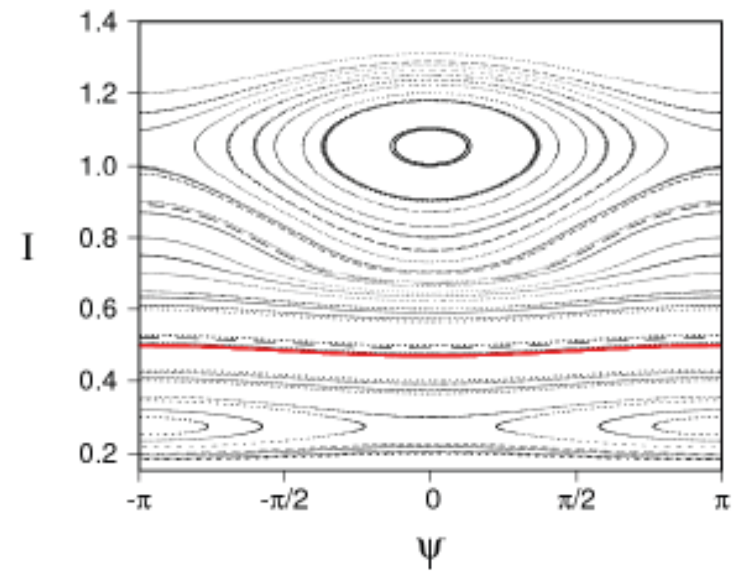

# Rotation Number and Shearless Barrier

Consider a two-dimensional dynamical system with a family of invariant closed curves that are formed by periodic or quasi-periodic trajectories. The trajectories trace the invariant curves at specific frequencies. A shearless transport barrier then is generally defined as the invariant curve whose frequency admits a local extremum within the family.

$$\phi_n = 0 \rightarrow I_0 = constant\ of\ motion \rightarrow \Omega_0 = \Delta\psi$$

For the non-integrable case and a given initial condition $\psi_0 \ \rightarrow \Omega = \lim_{l\rightarrow\infty} \Delta\psi_l / l$

$$n = (2, 3, 4) \rightarrow \phi_n = (0, 0.85, 0)$$

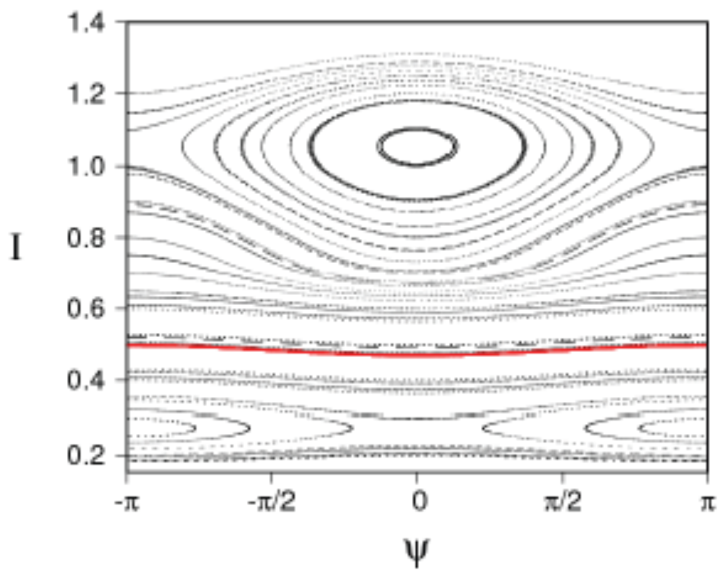


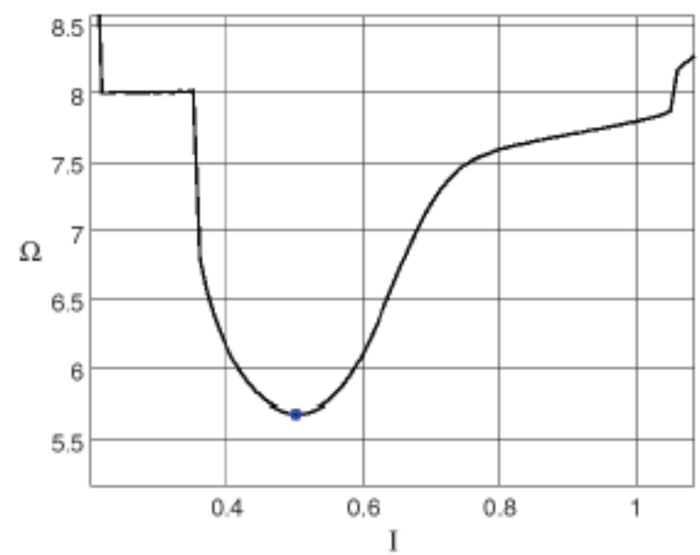

# Effect of non resonant mode

Resonance profile

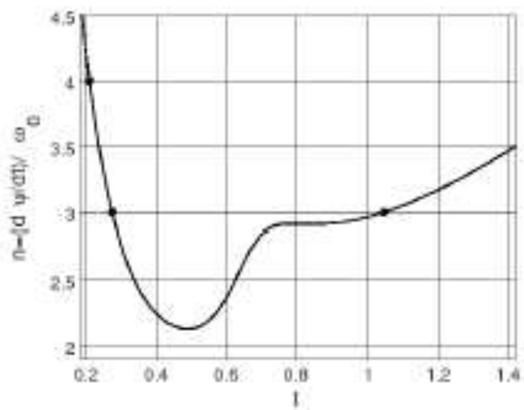


$$n = (2,3,4) \rightarrow \phi_n = (0.0, 0.85, 0.1)$$

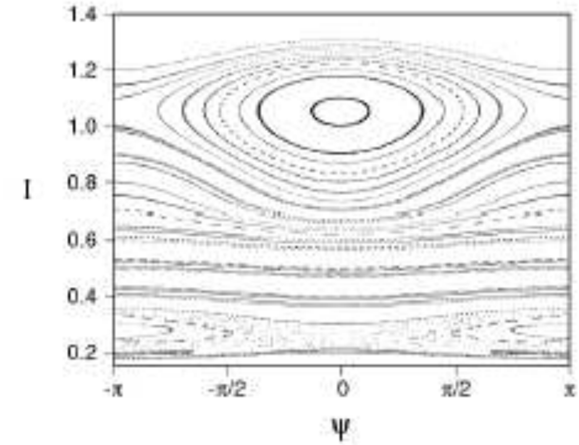


$$n = (2,3,4) \rightarrow \phi_n = (3.0, 0.85, 0.1)$$

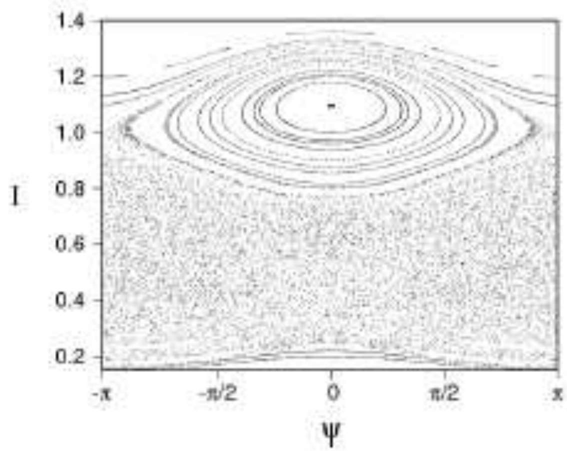


$$n = (2,3,4) \rightarrow \phi_n = (15.0, 0.85, 0.1)$$

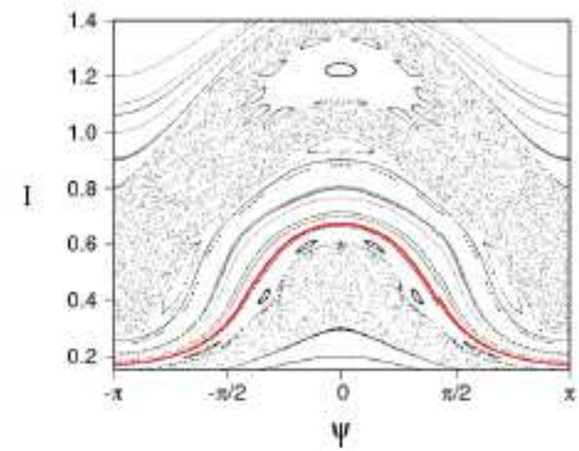

# Change on Electric field and resonant modes

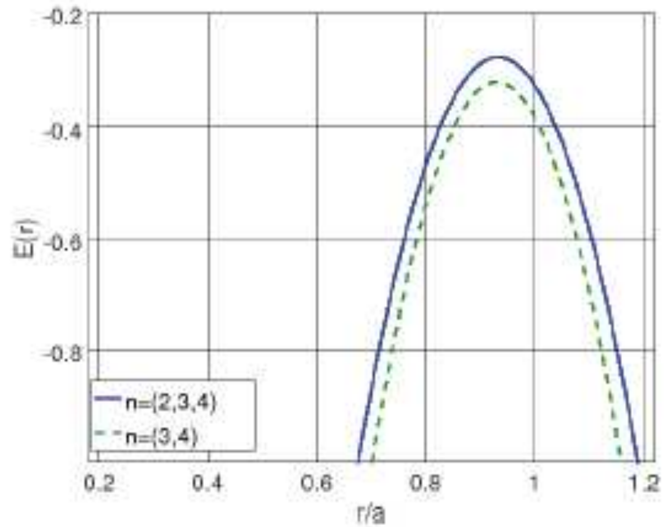


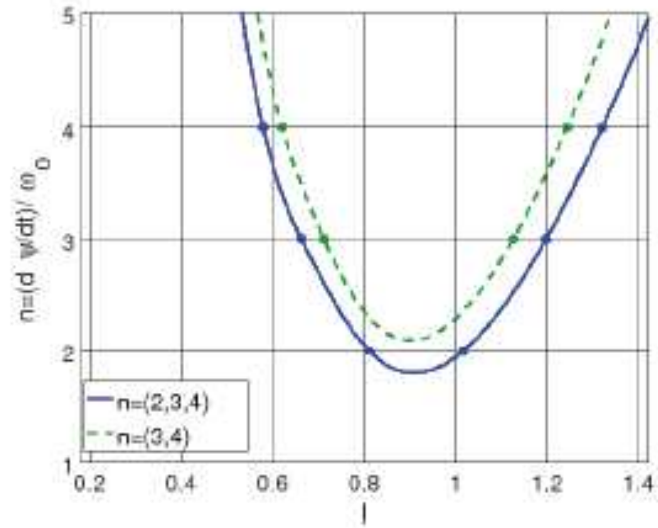


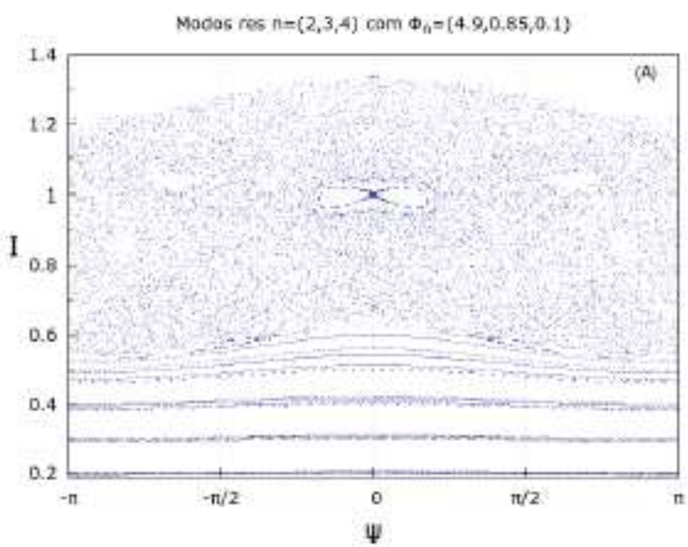


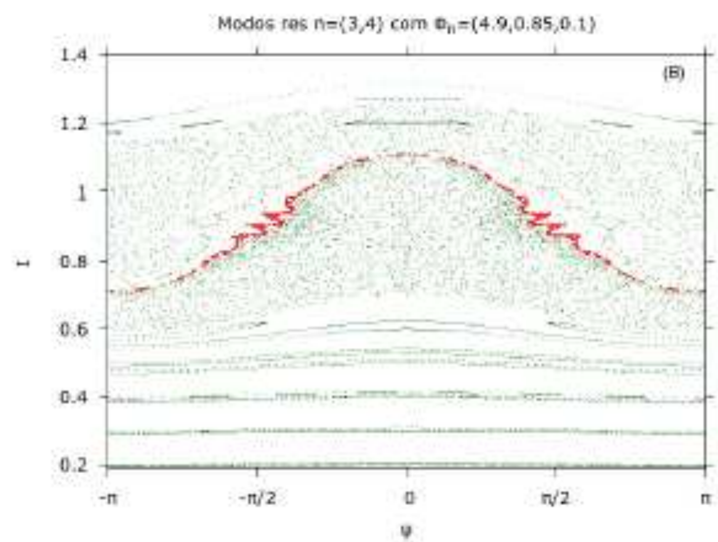

# Remarks

Non resonant waves are related to the invariant closed curves, which are connected to the shearless barrier, therefore to chaos reduction.

A change on the equilibrium radial electric field profile can shift a resonant mode to a non resonant and consequently reduce the chaos through the shearless barrier.

# Evidences of Shearlee Barrier in Helimaks

Collaboration with Prof. K. Gentle,  Texas University at Austin

Data Analyses
Toufen et al. PoP (2012, 2013, 2014)
Pereira et al. PPCF (2016)

Shearless Barriers (Theory)
Ferro, Caldas, PL A (2018).

# Texas Helimak

- Toroidal machine with simplified magnetic field lines configuration ➔ basically one dimensional equilibrium (dependence on the radial coordinate).

- Waves propagate on the vertical (z) direction, like waves propagating in the poloidal direction in tokamaks.

- Influence of the radial electric field profile on the plasma turbulence.

# Magnetic Field Lines Geometry

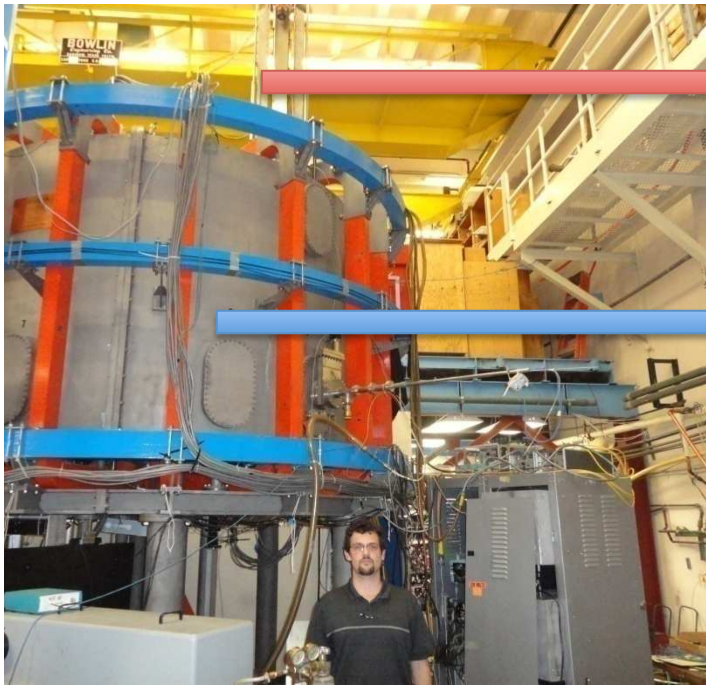

16 toroidal
Coils

+

3 vertical
coils

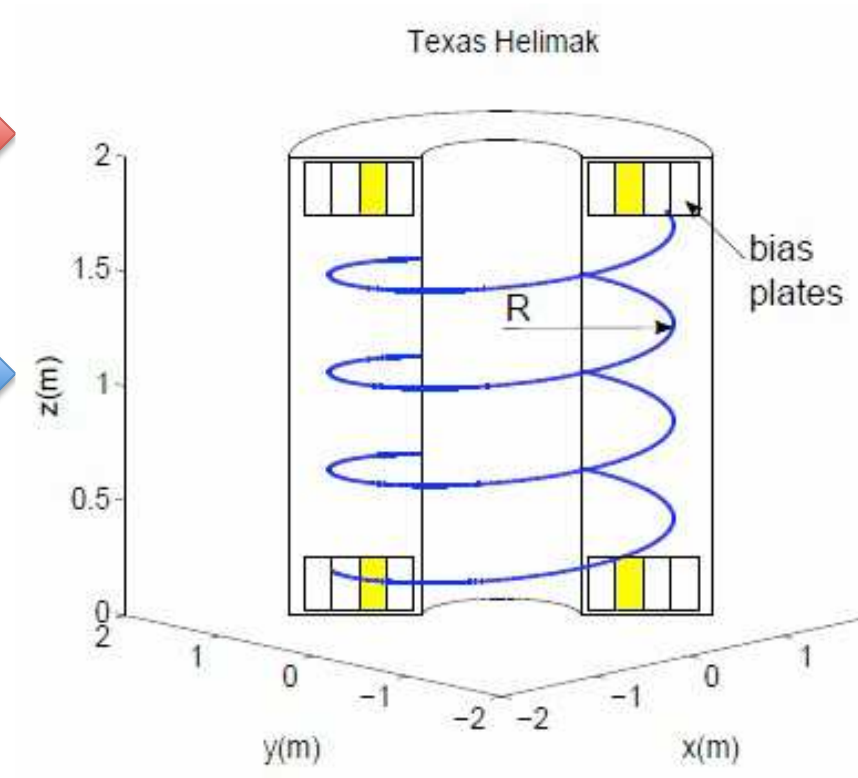


More than 700 probes

Spectrometer for vertical plasma flow ( velocity $V_z$)

# Texas Helimak

Vessel, Bias Plates, Probes

Magnetic Field Lines Geometry

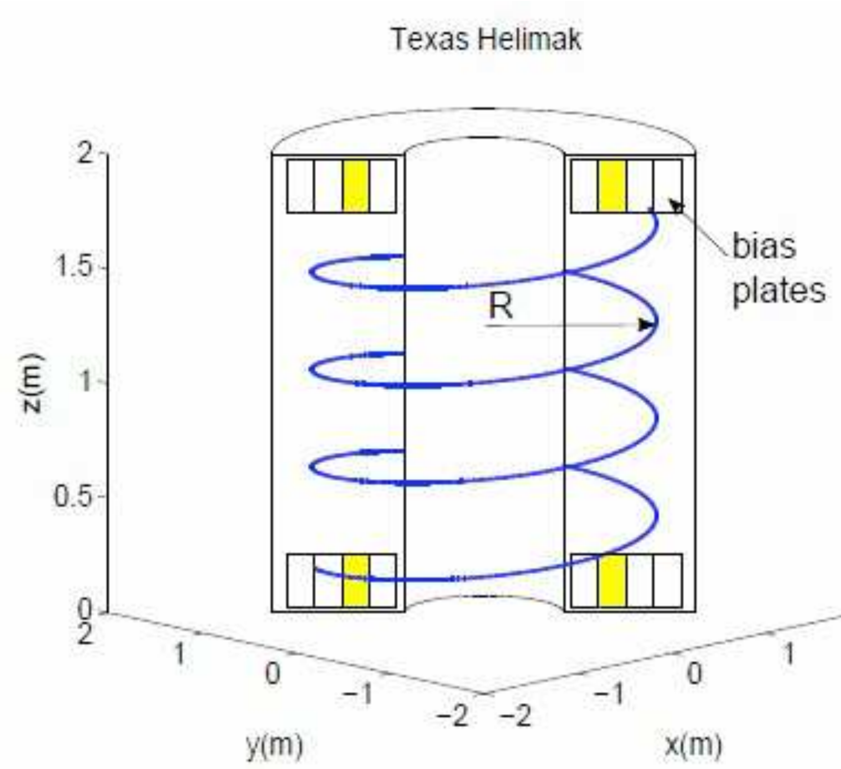


Fluctuation Amplitude

Independent of the vertical direction z

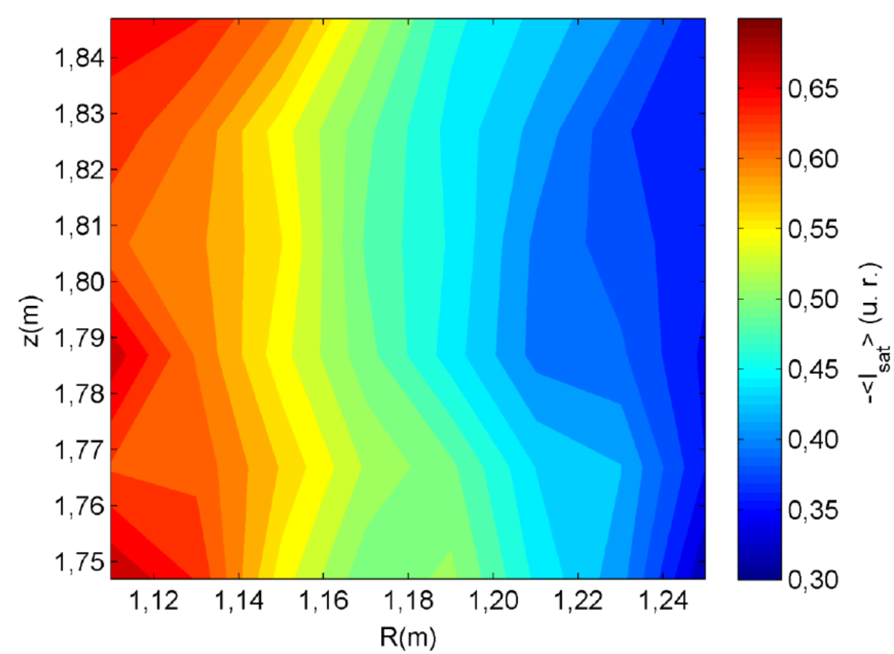


Waves propagate on the vertical (z) direction

# Radial Profile of Plasma Velocity in the Vertical Direction

(Spectrometer)

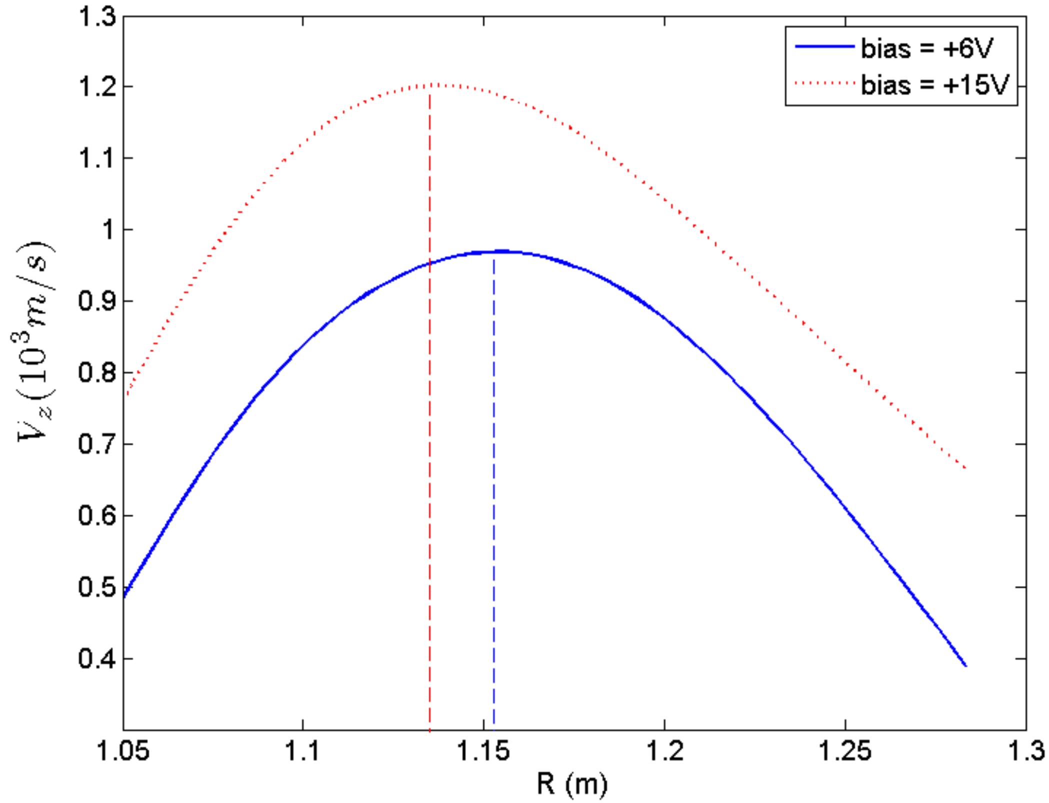


Radial position where the flow is shearless

# Evidence of Shearless (Radial) Transport Barriers

Turbulence Driven
Particle Transport Profile
(changing Bias)

Plasma Flow Shear Profile
(changing bias)

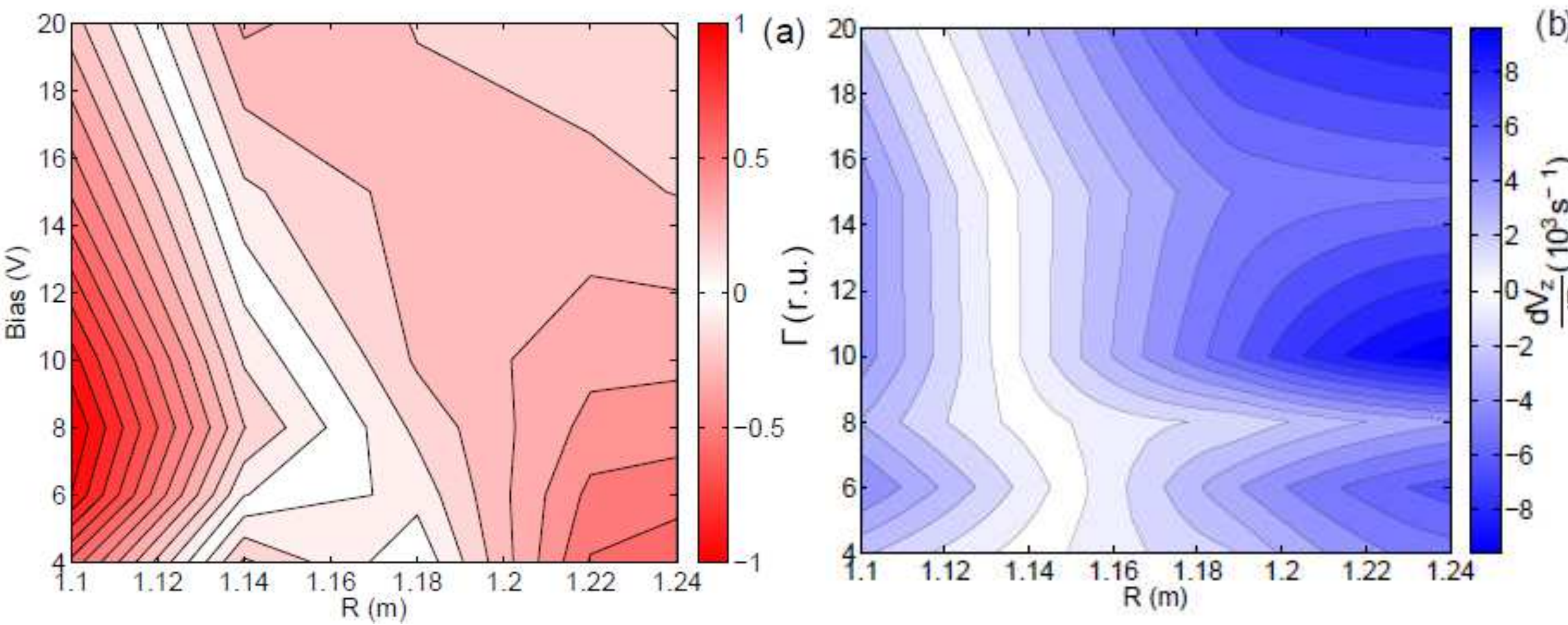


Toufen et al. PoP (2012)

# Conclusions

- Shearless  Invariants act as transport barriers in plasmas.
- Models of barriers in magnetic field line transport.
- Models of barriers in plasma particle transport.
- Experimental evidences in tokamaks and Texas Helimak.

Chaos, 2018

# Recurrence-based analysis of barrier breakup in the standard nontwist map

Moises S. Santos,[1] Michele Mugnaine,[1] José D. Szezech Jr,[2] Antonio M. Batista[a],[2] Iberê L. Caldas,[3] Murilo S. Baptista,[4] and Ricardo L. Viana[5]

[1] *Pós-Graduação em Ciências, Universidade Estadual de Ponta Grossa, 84030-900, Ponta Grossa, PR, Brazil.*

[2] *Departamento de Matemática e Estatística, Universidade Estadual de Ponta Grossa, 84030-900, Ponta Grossa, PR, Brazil.*[a)]

[3] *Instituto de Física, Universidade de São Paulo, 05508-900 São Paulo, SP, Brazil.*

[4] *Institute for Complex Systems and Mathematical Biology, University of Aberdeen, SUPA, AB24 3UE, UK.*

[5] *Departamento de Física, Universidade Federal do Paraná, 80060-000, Curitiba, PR, Brazil.*

(Dated: 22 March 2018)

We study the standard nontwist map that describes the dynamic behaviour of magnetic field lines near a local minimum or maximum of frequency. The standard nontwist map has a shearless invariant curve that acts like a barrier in phase space. Critical parameters for the breakup of the shearless curve have been determined by procedures based on the indicator points and bifurcations of periodical orbits, a methodology that demands high computational cost. To determine the breakup critical parameters, we propose a new simpler and general procedure based on the determinism analysis performed on the recurrence plot of orbits near the critical transition. We also show that the coexistence of islands and chaotic sea in phase space can be analysed by using the recurrence plot. In particular, the measurement of determinism from the recurrence plot provides us with a simple procedure to distinguish periodic from chaotic structures in the parameter space. We identify an invariant shearless breakup scenario, as well as we show that recurrence plots are useful tools to determine the presence of periodic orbit collisions and bifurcation curves.

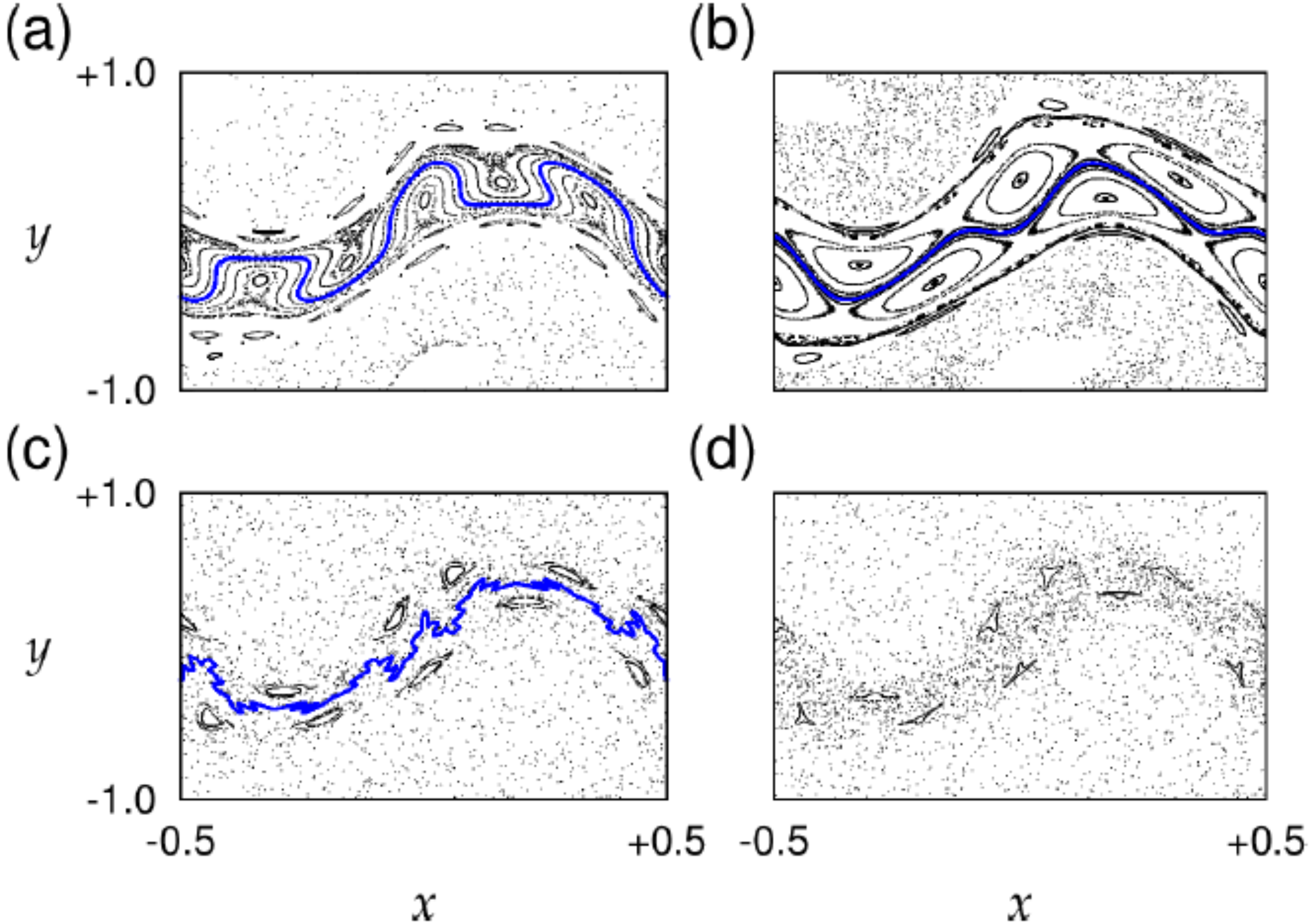


FIG. 1. Phase space of the SNM for (a) $a = 0.354$ and $b = 0.6$, (b) $a = 0.364$ and $b = 0.6$, (c) $a = 0.455$ and $b = 0.8$, and (d) $a = 0.455$ and $b = 0.847$. The blue line represents the shearless curve obtained by the evolution of the IP (1/4,b/2) as the initial condition in Eqs. (1).

The recurrence plot (RP) is a visualisation of a square matrix where a dot is placed at $(i,j)$ whenever $\vec{x}_i$ is nearby to $\vec{x}_j$[23–25]. The RP can be mathematically expressed as

$$RP_{i,j} = \Theta(\varepsilon - ||\vec{x}_i - \vec{x}_j||), \tag{2}$$

where $\vec{x}_i \in \mathbb{R}^m$ $(i,j = 1 \ldots k)$, $k$ is the number of possible states $\vec{x}_i$ in $m$-dimensional space, $\varepsilon$ is the return radius ($\varepsilon = 0.05$), $||.||$ indicates the Euclidean norm and $\Theta(.)$ is the Heaviside function. The interesting patterns observed in RPs led the authors in Ref.[8] to develop recurrence quantification analysis (RQA) to quantify the structures presents in the RPs. Thus, several diagnostics[26,27] can be obtained from Eq. (2), for example recurrence rate, laminarity, determinism, etc. Following[27], determinism is quantified by

$$\mathrm{DET} = \frac{\sum_{l=l_{\min}}^{k} lP(l)}{\sum_{l=1}^{k} lP(l)}, \tag{3}$$

where $P(l)$ represents the probability distribution of diagonal lines of length $l$ ($l_{\min} = 2$) present in the recurrence plot. A diagonal line of length $l$ indicates whether there are two timely separated pieces of the time-series that remain $\varepsilon$-close by a time of $l$. The more deterministic a system is, the longer the diagonal lines will be. Stochastic systems have very short or no diagonal lines

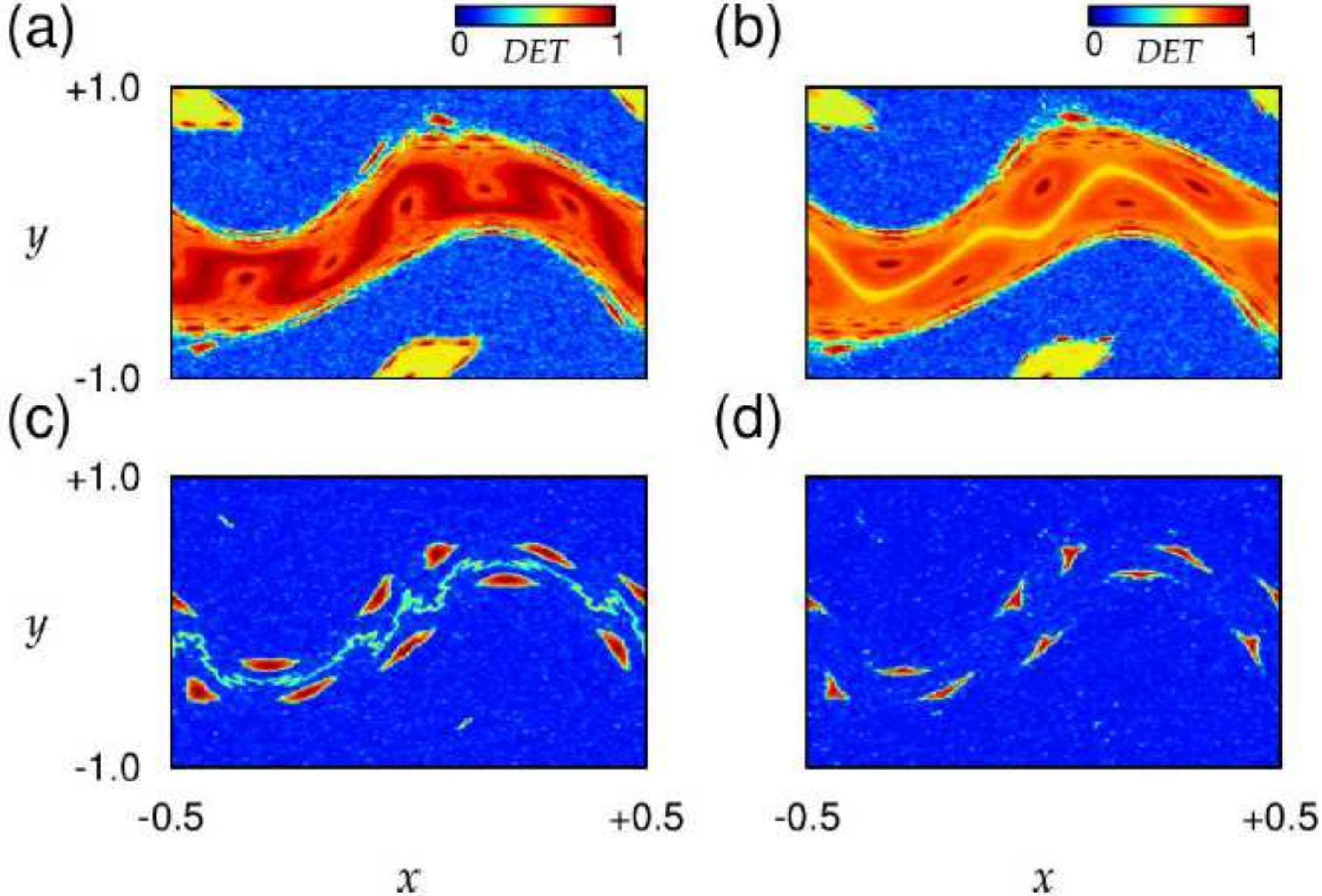


FIG. 3. Determinism phase space of the SNM for (a) $a = 0.354$ and $b = 0.6$, (b) $a = 0.364$ and $b = 0.6$, (c) $a = 0.455$ and $b = 0.8$, and (d) $a = 0.455$ and $b = 0.847$.

# Critical Curve in Parameter Space
# Fractal Border

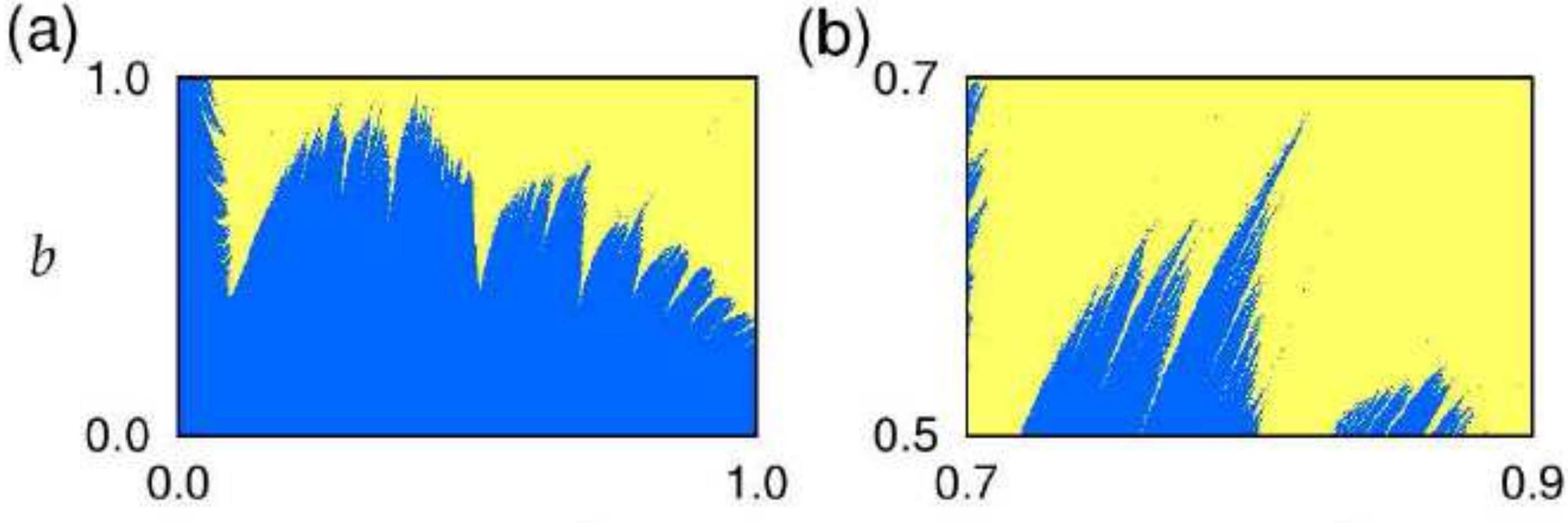


FIG. 4. Barrier breakup of the SNM using two methods. Figures (a) and (b) are calculated through the IP according to Ref.[17], where the blue (yellow) region represents the existence (breakup) of the shearless curves. Figures (c) and (d) are

# SHEARLESS INVARIANT CURVES IN CONFINED PLASMAS

IBERÊ CALDAS — Notes by Jeffrey Heninger

## Standard Nontwist Map

$$y_{n+1} = y_n \; a(1 - x_{n+1}^2) \qquad \text{mod } 1$$
$$x_{n+1} = x_n - b \sin(2\pi y_n)$$

Rotation Number: $\omega = \lim_{n \to \infty} \frac{x_{n+1} - x_0}{n}$

- To find the shearless curve, compute this for each $y$ along $x = 0$.
- The maximum marks where the shearless curve crosses $x = 0$.

Shearless curve is often the last to break.

- Before this, there can be reconnection events.
- Even after it breaks, the location where it was is sticky.
  - Stickiness can vary dramatically with small parameter changes.

Look at islands near where the invariant curve was to understand stickiness

- High transmissivity if the islands' manifolds cross with the other islands' manifolds.

Location of shearless curve in $(a,b)$ parameter space – very irregular.

- Calculated using John Greene's method.
  - Sudden change in stability of scads of nearby periodic orbits $\Rightarrow$ invariant has broken.
- Alternatively, use Slater's Criterion.
  - Slater's Theorem, applied along the invariant curve
  - Choose a small segment along the invariant curve
  - If only 3 recurrance times $\Rightarrow$ not broken, more than 3 $\Rightarrow$ broken.
  - Faster, but not as precise as Greene's method

## NonTwist Bifurcations

when do maps have shearless invariants?

there is a shearless curve around islands in the standard map

- bifurcation that creates 3 new islands

## Magnetic Surfaces in Tokamaks

Tokamak - confines a plasma in a torus
  toroid & poloidal magnetic field lines
  field line equations are a Hamiltonian system
    time = toroidal angle
    if integrable, find action-angle variables
  take Poincaré section
  perturb the Hamiltonian by an external coil
    depends on toroidal angle (⇒ Hamiltonian time)

can get shearless curves as invariants in these magnetic fields
  these barriers ⇒ improve confinement

**Ulmann Map**
  symplectic map to model the magnetic field lines in tokamaks
    $(r, \theta)$ in torus $\rightarrow$ $(x, y)$ for map

  Equilibrium described by map - with control parameters $a_1$
  Perturbative map due to external current - with amplitude parameter $C$
    have to work with both

  In this map, we can see:
    shearless curve
    reconnection & meanders
    breakup of shearless curve & stickiness
    within islands, there are shearless curves associated with a triple bifurcation
      also bifurcation that creates 4 islands
      these affect transport across the sticky region

## Particle Transport in Tokamaks

model includes both motion along the magnetic fields & drifts $(\vec{E} \times \vec{B})$
  need to know equilibrium $\vec{B}$ & $\vec{E}$ and the fluctuating $\vec{E}$ due to turbulence

look for resonant modes
  shearless curve is the minimum between 2 resonances
  a non resonant mode can also create/destroy shearless curve
    could decrease transport by increasing turbulence if you make a shearless curve
  small changes in electric field can also create/destroy shearless curve

B3

## Texas Helimak

Simplified magnetic field geometry - cylinder containing helitical magnetic field lines
can control radial electric field using plates at top & bottom
perturbations typically only depend on r - not z

experimental evidence that transport is low when the velocity shear is small.